

ATAS 2022

5th International Workshop on Advanced Techniques in Actinide Spectroscopy

&

AnXAS 2022

9th Workshop on Speciation, Techniques and Facilities for Radioactive Materials at
Synchrotron Light Sources



Organizing committees

Local:

- *ROBL/HZDR*
 - **Andreas Scheinost**
 - **Kristina Kvashnina**
 - **Damien Prieur**
 - **Christoph Hennig**
 - **Jan Pieter Glatzel** (*ESRF*)
- *ESRF – Administrative coordinators:*
 - **Valérie Clément**
 - **Eva Jahn**
 - **Sabine Schreiber**
 - **Ewa Wyszynska**

Scientific:

- **Robert J. Baker**, [Trinity College Dublin](#) (Ireland)
- **Rainer Dähn**, [PSI](#) (Paul Scherrer Institut, Switzerland)
- **Christophe Den Auwer**, [Université de Nice](#) (France)
- **Harald Foerstendorf**, [HZDR](#) (Helmholtz-Zentrum Dresden-Rossendorf, Germany)
- **Ken Kemner**, [ANL](#) (Argonne National Laboratory, USA)
- **Katherine Morris**, [The University of Manchester](#) (UK)
- **Katharina Mueller**, [HZDR](#) (Helmholtz-Zentrum Dresden-Rossendorf, Germany)
- **Tobias Reich**, [University of Mainz](#) (Germany)
- **Joerg Rothe**, [KIT](#) (Karlsruhe Institute of Technology, Germany)
- **David Shuh**, [LBL](#) (Lawrence Berkeley Laboratory, USA)
- **Jim Tobin**, [University of Wisconsin](#) (USA)
- **Satoru Tsushima**, [Tokyo Institute of Technology](#) (Japan)
- **Tsuyoshi Yaita**, [JAEA](#) (Japan Atomic Energy Agency, Japan)
- **Ping Yang**, [LANL](#) (Los Alamos National Laboratory, USA)

WORKSHOP SPONSORS



Instruments That Advance The Art



MIRION
TECHNOLOGIES



FMB
OXFORD



ROYAL SOCIETY
OF **CHEMISTRY**

DECTRIS
detecting the future

Monday 17th October

11:30 - 14:00 **Registration** - *ESRF Main Hall*

12:30 - 13:50

Lunch - *EPN Campus Restaurant*

14:00 - 14h15 **Welcome** - *ESRF Auditorium*

Radioactive Waste Disposal : D. Shuh and K. Mueller

- | | | |
|---------------|---|---|
| 14:15 - 14:55 | Claire CORKHILL
University of Sheffield, UK | Application of micro-focused x-ray techniques to simulant Chernobyl and Fukushima nuclear fuel debris |
| 14:55 -15:15 | Thomas NEILL
University of Manchester, UK | Colloidal particulates in spent nuclear fuel storage: from fundamental properties to effluent treatment |
| 15:15 - 15:35 | Isabelle JESSAT
HZDR, Germany | Np(V) sorption onto zirconia: a combined spectroscopy, batch and modeling study |
| 15:35 - 15:55 | Anita KATHERAS
Institute of Geological Sciences,
Switzerland | Ab initio modelling of magnetite surfaces for Pu retention |

Coffee Break

Bio-Geochemistry : R. Bernier-Latmani and C. DenAuwer

- | | | |
|---------------|--|---|
| 16:10 - 16:50 | Maxim BOYANOV
Institute of Chemical Engineering,
Bulgaria | Speciation of oxidized and reduced uranium in wetland sediments |
| 16:50 - 17:10 | Callum ROBINSON
University of Manchester, UK | Approaches to groundwater radionuclide remediation at Sellafield - in situ phosphate mineralisation |
| 17:10 - 17:30 | Sebastian FRIEDRICH
HZDR, Germany | Complexation of Eu(III) and Cm(III) by EGTA related aminopolycarboxylic acids |
| 17:30 - 17:50 | Romain STEFANELLI
University of Nice-Sophia
Antipolis, France | Speciation and accumulation of uranium in mussels <i>Mytilus Gallo-provincialis</i> |

18:00 - 21:00

Cheese and Wine Reception - *Cafeteria EPN Campus*

Tuesday 18th October

Aqueous & Coordination Chemistry : T. Yaita and A. Scheinost

- | | | |
|---------------|---|---|
| 9:00 - 9:40 | Thomas DUMAS
CEA Marcoule, France | Spectroscopy for plutonium hydrolysed species in solution and application of model structures in data analysis. |
| 9:40 - 10:00 | Enrique SANCHEZ MARCOS
University of Sevilla, Spain | Describing Radioactive Actinyl Cations in Water by Combining EXAFS + Molecular Dynamics |
| 10:00 - 10h40 | Koichiro TAKAO
Tokyo Institute of Technology, Japan | Molecular Design of Pentadentate Planar Ligand and Its Coordination with UO ₂ ²⁺ towards Uranium Recovery from Seawater |

Coffee Break

Synchrotron Facility Reports : K. Kvashnina and S. Minasian

- | | | |
|---------------|---|--|
| 11:00 - 11:30 | Myrtille HUNAULT
Synchrotron Soleil, France | Characterisation of actinide materials at the MARS beamline |
| 11:30 - 12:00 | Dimosthenis SOKARAS
SLAC National Accelerator Laboratory, USA | High-energy-resolution X-ray spectroscopy and actinides research at SLAC |
| 12:00 - 12h30 | Damien PRIEUR
HZDR, ROBL-CRG, France | ROBL-II at ESRF: a synchrotron toolbox for actinide research |

Lunch - EPN Campus Restaurant

Nuclear Materials : V. Svitlyk and D. Prieur

- | | | |
|---------------|--|---|
| 14:00 - 14:40 | Olaf WALTER
European Commission, Germany | Actinide oxalates as key intermediates in actinide chemistry |
| 14:40 - 15:00 | Shannon K. POTTS
Forschungszentrum Jülich, Germany | Investigation on the Structural Incorporation of Dopants into the Uranium Oxide Structure |
| 15:00 - 15:20 | Philippe MARTIN
CEA Marcoule, France | Extreme multi-valence states in mixed actinide oxides U _{1-y} MyO _{2±x} |
| 15:20 - 15:40 | Luke TOWNSEND
University of Sheffield, UK | Structural characterisation of advanced Cr & Mn doped UO ₂ fuels using X-ray Absorption Spectroscopy |
| 15:40 - 16:00 | Rafael CAPRANI
CEA Marcoule, France | Fission products speciation in high burnup MOx fuel: fabrication and experimental characterization of Pu-bearing simulated fuel |

Coffee Break

Electronic Structure : R. Polly and V. Vallet

- | | | |
|---------------|--|---|
| 16:20 - 17:00 | Stefan MINASIAN
Lawrence Berkeley National Laboratory, USA | Report from the ALS: Pinpointing Actinide Bonding with Soft X-rays |
| 17:00 - 17:20 | Tonya VITOVA
Karlsruhe Institute of Technology, Germany | Actinide bonding properties – stability relations probed by high resolution X-ray spectroscopy |
| 17:20 - 17:40 | Harry RAMANANTOANINA
University of Karlsruhe, Germany | Electronic structure and bonding properties of U ⁶⁺ by high-resolution X-ray spectroscopy and computations |
| 17:40 - 18:00 | Kutis STANISTREET-WELSH
Lancaster University, UK | Simulating Uranyl Oxygen K-edge XANES using Multiconfigurational RASSCF Methods |

18:00 - 21:00

Poster Session / Cocktail - *Main Hall and Mezzanine*

Wednesday 19th October

Emerging Techniques : M. Hunault and J. Rothe

9:00 - 9:40	Sergei BUTORIN Uppsala University, Sweden	Electronic Structure of Actinide Compounds as Probed by Advanced X-ray Spectroscopy: Experiment and Theory
9:40 - 10:00	Alexander DITTER Lawrence Berkeley National Laboratory, USA	Tender X-ray Spectromicroscopy of Actinide Particles at the Advanced Light Source
10:00 - 10h20	David SHUH Lawrence Berkeley National Laboratory, USA	Soft X-ray Chemical Speciation Mapping of Uranium Oxide Focused Ion Beam Sections
10:20 - 10h40	Rene BES University of Helsinki, Finland	What can we learn from U L1-edge HERFD-XAS?

Coffee Break

Synchrotron Facility Reports : L. Solari and J.P. Glatzel

11:00 - 11:30	Frederick MOSSELMANS Diamond Light Source Ltd, UK	The Active Materials Laboratory and actinide research opportunities at Diamond Light Source - ZOOM SESSION
11:30 - 12:00	Tetsuo OKANE Japan Atomic Energy Agency, Japan	Actinide science of JAEA Beamline in SPring-8
12:00 - 12h20	Volodymyr SVITLYK HZDR, ROBL-CRG, France	Revealing long-range and long-term properties of actinides with diffraction at the Rossendorf Beamline

Lunch - EPN Campus Restaurant

Electronic Structure : S. Tsushima and A. Severing

14:00 - 14:40	Valérie VALLET University of Lille, CNRS, France	Exploring luminescence properties of uranyl-based complexes by TR-LFS and ab initio method
14:40 - 15:00	Andre SEVERO PEREIRA GOMES University of Lille, CNRS, France	Relativistic correlated electronic structure and the calculation of accurate ground-state, core and valence properties of heavy element species
15:00 - 15:20	Michael BAKER University of Manchester, UK	M4-edge resonant inelastic X-ray scattering as a quantitative probe of actinide electronic structure and bonding
15:20 - 15:40	Robert POLLY Karlsruhe Institute of Technology, Germany	Relativistic Multiconfigurational Ab Initio Calculation of XANES spectra and RIXS maps of radionuclide compounds

Coffee Break

Electronic Structure : S. Butorin

16:00 - 16:20	Lucia AMIDANI HZDR, ROBL-CRG, France	XANES calculations of actinide-based materials
16:20 - 17:00	Andrea SEVERING University of Karlsruhe, Germany	Seeing multiplets in UO ₂ and UGa ₂ with NIXS and tender RIXS

17:00

End of the day

Thursday 20th October

Bio-Geochemistry : M. Boyanov and tbc

9:00 - 9:40	Rizlan BERNIER-LATMANI EPFL ENAC ISTE, Switzerland	Nanoscale mechanism of hexavalent uranium reduction by magnetite
9:40 - 10:00	Markus BRECKHEIMER Johannes Gutenberg-Universität Mainz, Germany	Chemical tomography of pyrite composites extracted from Opalinus Clay and reacted with Np and Pu
10:00 - 10h20	Daniel BUTSCHER HZDR, Germany	Investigation of the interaction of uranium(VI) with the biofluids of the human digestive system
10:20 - 10h40	Satoru TSUSHIMA HZDR, Germany	Selective binding of uranyl(VI) by protein through polar and hydrophobic interactions

Coffee Break

Synchrotron Facility Reports : D. Sokaras and C. Hennig

11:00 - 11:30	Bianca SCHACHERL Karlsruhe Institute of Technology, Germany	Radionuclide research at the KIT synchrotron source – the INE and ACT experimental stations
11:30 - 12:00	Yuying HUANG Shanghai Advanced Research Institute, CAS, China	Study of actinide compounds using X-ray spectroscopy with high resolution X-ray spectrometer at Shanghai Synchrotron Radiation Facility - ZOOM SESSION
12:00 - 12h30	Malgorzata MAKOWSKA Paul Scherrer Institute, Switzerland	Multimodal multidimensional chemical imaging at the microXAS beamline of the Swiss Light Source

Lunch - EPN Campus Restaurant

Aqueous & Coordination Chemistry : K. Takao and T. Dumas

14:00 - 14:20	Tsuyoshi YAITA Japan Atomic Energy Agency - JAEA/SPring-8, Japan	Selective Am(III)-(V) oxidation by multiphoton excitation
14:20 - 14:40	Tobias REICH Johannes Gutenberg-Universität Mainz, Germany	Investigation of complexation and redox reactions of actinides using CE-ICP-MS - ZOOM SESSION
14:40 - 15:00	Dominique GUILLAUMONT CEA, France	Structure and Stability of plutonium hexanuclear cluster in the gas phase and in solution
15:00 - 15:20	Anne HELLER TU Dresden, Germany	Multi-method investigation of the Eu/La complexation with HEDP

Radioactive Waste Disposal : C. Corkhill and H. Foerstendorf

15:20 - 16:00	Sam SHAW University of Manchester, UK	Fe(II) Induced Reduction and Sulfidation of U(VI)-incorporated Goethite
---------------	---	---

Coffee Break

16:20 - 16:40	Alexander TALYZIN Umea University, Sweden	Sorption of radionuclides by oxidized carbons: from graphene oxide to super-oxidized high surface area carbons - ZOOM SESSION
16:40 - 17:00	Augusto FARIA OLIVEIRA HZDR, Germany	Insights into the Enigmatic TcO ₂ ·xH ₂ O Structure via Atomistic Simulations and EXAFS
17:00 - 17:20	Yanting QIAN Paul Scherrer Institute, Switzerland	Retention of Tc and Se on Fe-bearing clay minerals
17:20 - 17:40	Natalia MAYORDOMO HERRANZ HZDR, Germany	Tc(VII) reductive immobilization by Sn(II) pre-sorbed on alumina nanoparticles

19:30

Young Scientist and Poster Award - Restaurant Madam, Grenoble
(Meeting point at the site entrance 19:00)



Friday 21st October

Visitor Center

09:30 - 10:00 **ESRF presentation**
ESRF/EBS new accelerator presentation

10:00 - 10:20 **Coffee Break**

Beamlines visits :

10:20 - 12:30 **ID12 - BM20 - ID20 - BM23 - ID26 - ID27 - ID28 - ID32**

Registration: please put your name on the lists for one of the 5 groups

12:30 - 14:00 **Lunch - EPN Campus Restaurant**

14:00 **End of ATAS-AnXAS 2022**

5th International
Workshop on Advanced
Techniques in Actinide
Spectroscopy



9th Workshop on
Speciation, Techniques
and Facilities for
Synchrotron Radiation

Speakers' Abstracts

XANES calculations of actinide-based materials

L. Amidani^{1,2} and K. O. Kvashnina^{1,2}

¹ The ROBL beamline at the ESRF, 71 avenue des Martyrs, 38000 Grenoble, France.

² Institute of Resource Ecology, HZDR, Bautzner Landstraße 400, 01328 Dresden, Germany.

XANES, with its high sensitivity to the oxidation state and the local structure, is a very powerful tool to investigate actinide-based materials. The use of the High-Energy-Resolution Fluorescence-Detected (HERFD) mode opened new perspective in this field. By reducing the core-hole lifetime broadening, HERFD allows a relevant gain in resolution at the L_3 edge and a major improvement for $M_{4,5}$ edges.

The information contained in a XANES spectrum are often hard to extract and therefore need the support of theory. However, calculations of actinide materials made complex by the comparable strength of intra-electronic interactions, spin-orbit and influence of the local environment. Efforts are ongoing to take all the relevant physics into account, however today none of the theoretical framework used in XANES calculations can account for all relevant interactions over a large cluster of atoms.

If we do not yet have a unique theoretical framework that can be applied to all actinide systems, we can still select the theory that is more adapted to specific cases. In this contribution we will present progresses in the interpretation of XANES of actinide systems obtained by using the DFT-based code FDMNES [1]. Results at the L_3 and $M_{4,5}$ edges on Th^{4+} and U^{6+} systems will be presented [2-4]. These systems, where the intra-electronic interactions are less relevant due to the absence of 5f valence electrons, are particularly suited to investigate the importance of the local environment on the spectral shape. Our results endorse the use of HERFD XANES coupled with DFT-based calculations to investigate complex actinide-containing systems.

[1] Joly, Y. et al. (2009) *J. of Physics: Conf. Series* 190, 012007.

[2] Amidani, L. et al. (2019) *Phys. Chem. Chem. Phys.* 21, 10635–10643.

[3] Amidani, L. et al. (2021) *Chem. Eur. J.* 27, 252–263.

[4] Amidani, L. et al. (2021) *Inorg. Chem.* 60, 16286–16293.

M₄-edge resonant inelastic X-ray scattering as a quantitative probe of actinide electronic structure and bonding

Timothy G. Burrow and Michael L. Baker

Department of Chemistry, The University of Manchester, Manchester, M13 9PL, UK. The University of Manchester at Harwell, Diamond Light Source, Harwell Campus, OX110DE, UK.

michael.baker@manchester.ac.uk

M₄-edge high energy resolution fluorescence detected X-ray spectroscopy is an accurate probe of actinide oxidation state and coordination symmetry. To take greater advantage of the electronic structure information present at the M₄-edge, an alternative analysis protocol will be proposed. This method involves consideration of all scattering intensities present at the M β emission line that are analysed within a multiplet theory framework that considers the photon-in photon-out inelastic scattering process. A detailed resonant inelastic X-ray scattering study on a series of highly air-sensitive U(VI) molecules will be presented. The selection of molecules studied include both novel organometallics as well as chlorides. The resonant inelastic x-ray scattering derived electronic structure are compared against complementary methods, including Cl K-edge X-ray absorption near edge structure and density functional theory. It is concluded that M₄-edge resonant inelastic X-ray scattering carries untapped information pertinent to answering fundamental questions concerning the role of the 5f orbitals to actinide-ligand bonding.

Nanoscale mechanism of hexavalent uranium reduction by magnetite

Barbora Bártořová¹, Zezhen Pan², Thomas LaGrange¹, *Rizlan Bernier-Latmani¹

¹EPFL, Lausanne, Switzerland, correspondence *rizlan.bernier-latmani@epfl.ch

²Fudan University, Shanghai, China

Uranium (U) is a ubiquitous element in the Earth's crust and in nuclear waste and its biogeochemical behavior is largely constrained by its redox transformation from soluble uranium hexavalent species (U(VI)) to sparingly soluble tetravalent species (U(IV)) under anoxic conditions. U(VI) reduction by mineral phases, most commonly ferrous iron-bearing minerals, has been shown to produce crystalline U in the form of U(IV)O₂ as the end product, but also to form persistent pentavalent U (U(V)). Magnetite (Fe₃O₄) is an Fe(II)-bearing iron oxide that is relevant both to natural environments and to nuclear waste repositories, in the latter as a result of the corrosion of steel waste canisters. Theoretical calculations reported the reduction from U(VI) to U(V) by aqueous Fe(II) to be facile and demonstrated that the incorporation of U in solid phases widens the stability field of U(V) species in the reduction by magnetite [1]. Experimental studies have shown that the co-precipitation of U(VI) and magnetite resulted in the formation of a stable uranate(V) coordination in the iron oxide mineral phases [2]. Furthermore, our recent study [3] showed the presence of U(V) as a result of U(VI) reduction by preformed magnetite and its persistence prior to further reduction to UO₂ nanoparticles.

Most interestingly, we reported the formation of single U oxide nanocrystals (1-5 nm) followed by the formation of nanowires that extended from the magnetite surface outward (Figure 1). Over time, the nanowires collapsed into ordered UO₂ nanoclusters, resembling those previously reported for the final product after U(VI) reduction by magnetite [4]. U(IV) was suggested as the dominant valence state in the nanowires based on both Fast Fourier Transform (FFT) on specific regions of High-Angle annular dark field- scanning transmission microscopy (HAADF-STEM) images of the nanowires and the branching ratios obtained from M4/M5 peaks from U TEM-EELS (electron energy loss spectroscopy) spectra. Due to the sensitivity of U(V) under the beam, reduction of U(V) species may occur, and the presence of mixed valence states may be overlooked by using the branching ratios acquired from U EELS spectra under high beam current. Besides the beam sensitivity issue, discriminating between UO₂ and UO_{2+x} (0 < x < 1, representing mixed valence uranium oxides, such as U₃O₈) robustly is challenging when using only FFT.

Based on recent microscopic evidence for a range of crystallinity and order in the nanoparticles, we acquired the O K-edge EELS spectra from individual nanoparticles within the nanowires and compared the edge feature to that of U oxide reference standards in order to characterize the valence state of individual nanocrystals within the nanowires.

The mechanism that emerges at the scale of individual nanoparticles (1-5 nm) is the initial reduction of U(VI) to U(V) at the magnetite surface, producing mixed valence oxides UO_{2+x} that self-assemble into nanowires (Fig. 1). These nanowires are stable as long as no further reduction occurs. However, if sufficient electrons are available from magnetite, they are delivered to the mixed valence U oxides, resulting in the formation of fully reduced UO₂. The nanowires are no longer thermodynamically stable at the stage and collapse into nanoclusters.

The reduction of U(VI) by magnetite represents an example of heterogeneous reductive precipitation that, due to the properties of uranium, can be resolved at the near atomic scale and reveal the complexity of electron transfer from mineral to metal.

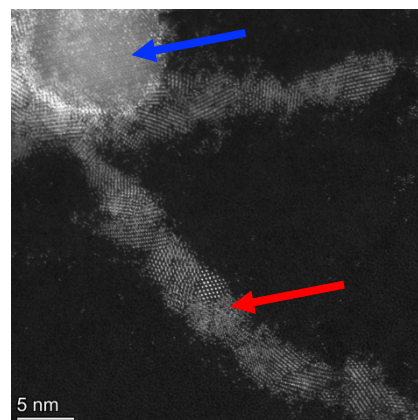


Fig. 1: Magnetite particle (blue arrow) with UO_{2+x} nanoparticles self-assembled into nanowires (red arrow).

[1] Collins et al., *J. Phys. Chem. A*, **121**, 6603–6613 (2017).

[2] Pidchenko et al. *Environ. Sci. Technol.*, **51**, 2217–2225 (2017).

[2] Pan et al., *Nat. Commun.*, **11**, 4001 (2020)

[3] Latta et al., *Environ. Sci. Technol.*, **48**, 3, 1683–1691 (2014)

What can we learn from U L₁-edge HERFD-XAS?

R. Bes^(1,2), G. Leinders⁽³⁾, and K. Kvashnina^(4,5)

¹ Department of Physics, University of Helsinki, P.O. Box 64, FI-00014 Helsinki, Finland

² Helsinki Institute of Physics, Department of Physics, University of Helsinki, P.O. Box 43, FI-00014 University of Helsinki, Finland

³ Belgian Nuclear Research Centre (SCK CEN), Institute for Nuclear Materials Science, Boeretang 200, B-2400 Mol, Belgium.

⁴ The Rossendorf Beamline at ESRF, The European Synchrotron, CS40220, 38043 Grenoble Cedex 9, France

⁵ Institute of Resource Ecology, Helmholtz Zentrum Dresden-Rossendorf (HZDR), PO Box 510119, 01314 Dresden, Germany

X-ray absorption spectroscopy experiments on Uranium compounds are often performed at the U L₃- and L₂-edges (at 17.166 keV and 20.948 keV). Indeed, the high penetration depth of X-rays in the hard regime allows to perform the experiments through the confinement barriers usually required at synchrotron when dealing with radioactive materials. At the same time, the core-hole broadening is kept to reasonable values of 8.2 eV and 9.5 eV respectively. However, the L₁-edge (at 21.758 keV) is not often performed due to the very large core-hole lifetime broadening of about 17 eV, which hinders resolving useful features.

By applying High Energy Resolution Fluorescence Detected-XAS (HERFD- XAS), several features can become visible thanks to the tremendous gain in energy resolution offered by the virtual reduction of the core-hole broadening in the RIXS regime [1]. Unprecedented details on the electronic and local structure of actinides' materials are therefore now reachable thanks to the recent development of emission spectrometers [2-4]. Successful examples of applications are a direct evaluation of valence state mixture [5-6], crystal field splitting of the 6d shells [7-8] and 5f electrons localization [9] to name a few. In particular, the U M_{4,5}-edge demonstrated itself a very valuable tool for determining the valence state mixture of actinides and it cannot be overlooked nowadays thanks to its high sensitivity. Nevertheless, the tender X-ray regime of M-edges is not well adapted to cases where confinement barriers or sample environment are precluding experiments to be performed. Therefore, one should search for an alternative in the hard X-ray regime, if any, i.e. at the L-edges. Starting with the L₃-edge, the occurrence of a quadrupolar transition at the low energy side of the white-line is increasing the uncertainty associated to valence state determination, making quantitative analysis less precise. One may obviously expect similar behavior at the L₂-edge, leading to consider what we can learn from L₁-edge. In this presentation, we will discuss the opportunity of using U L₁-edge for valence state quantitative analysis.

[1] K. Hamalainen, et al., Phys. Rev. Lett. 67 (1991) 2850.

[2] I. Llorens, et al., Radiochim. Acta 102 (2014) 957.

[3] A. Zimina et al., Rev. Sci. Instrum. 88 (2017) 113113.

[4] Kvashnina et al., J. Synchrotron Rad. 23 (2016) 836.

[5] K.O. Kvashnina, et al., Phys. Rev. Lett. 111 (2013) 253002.

[6] G. Leinders, et al., Inorg. Chem. 56 (2017) 6784.

[7] S. Butorin, et al., Chem. Eur. J. 22 (2016) 9693.

[8] R. Bes, et al., J. Synchrotron Rad. 29 (2022) 21.

[9] T. Vitova, et al., Nature communications 8 (2017) 16053.

Speciation of oxidized and reduced uranium in wetland sediments

Maxim Boyanov,^{1,2*} Edward O'Loughlin,² Daniel Kaplan,³ Limin Zhang,^{4,5} Hailiang Dong,^{4,5} Ken Kemner²

¹ Institute of Chemical Engineering, Bulgarian Academy of Sciences, Sofia, Bulgaria

² Biosciences Division, Argonne National Laboratory, Argonne, IL 60439, USA

³ Savannah River National Laboratory, Aiken, SC, USA

⁴ State Key Laboratory of Microbial Resources, Chinese Academy of Sciences, Beijing

⁵ State Key Laboratory of Biology and Environmental Geology, China University of Geosciences, Beijing

Uranium mining and production activities have resulted in significant accumulation of depleted uranium (²³⁸U) at contaminated sites around the world. Predicting the dispersal and transport of these stocks is of paramount importance to public safety. In order to inform policy decisions reactive transport models must adequately account for U transformations in complex natural systems, which necessitates a molecular-level understanding of the interfacial and redox chemistry of U in the presence of minerals, bacteria, and dissolved ligands. Although much is known about U mineralogy, adsorption/complexation mechanisms, and redox transformations in laboratory systems [1], significant uncertainties remain in natural sediments where several of the above factors influence U speciation.

Wetlands are landscape features where standing water is present all or part of the time. The abundance of organic matter drives microbial activity and anoxia, resulting in redox fluctuations and significant cycling of the major and minor elements. To understand the long-term transformations of U under such conditions we are studying a contaminated site at the Savannah River National Laboratory (USA), where nuclear target assemblies production in the 1960s resulted in significant U discharges in the nearby Tims Branch wetland. Multiple sediment cores were analyzed for elemental distribution and U/Fe speciation using synchrotron x-ray spectroscopy techniques. Results show that U was present in the top 5-10 cm of the sediment. Cores taken from water-saturated areas had 13% - 30% Fe^{II}/Fe^{total}, indicating the establishment of reducing conditions. U L_{III}-edge XANES and EXAFS spectroscopy indicated that >95% of U associated with the reduced sediment was non-uraninite U^{IV}. Alternating oxic/anoxic incubations of the sediments amended with glucose demonstrated a facile and reversible transition between adsorbed U^{VI} and the mononuclear U^{IV} species. The valence transitions of sediment-associated U in response to redox variations that are typical of wetland environments suggest that the lability of both U^{VI} and U^{IV} species must be considered when modeling U transport in wetlands.

The observed non-uraninite U^{IV} species present a particular challenge in that respect, as very limited information is available for inclusion of such species in transport models. Both minerals and organic ligands can affect U^{IV} speciation in wetlands, so we conducted controlled bioreduction experiments with *Shewanella putrefaciens* strain CN32 in the presence of clay minerals and organic ligands (citrate, EDTA, or DFOB). In the presence of citrate, bioreduced U^{IV} formed a soluble U^{IV}-citrate complex in experiments with either Fe-rich or Fe-poor clay mineral. In the presence of EDTA, U^{IV} occurred as a soluble U^{IV}-ligand complex in experiments with Fe-poor montmorillonite. However, U^{IV} remained associated with the solid phase in Fe-rich nontronite experiments through the formation of a ternary U^{IV}-EDTA-surface complexes, as suggested by the EXAFS analysis [2]. Similarly, a U^{IV}-DFOB complex was sequestered in the interlayer of NAu-2 clay, as indicated by EXAFS, XRD, and TEM analyses [3]. These studies indicate that the interaction between organic ligands and clay minerals significantly affect both U^{VI} and U^{IV} speciation and stability. The results also highlight the need for inclusion of additional reactions in reactive transport models to represent the influence of mineral and organic matter components in natural systems, in order to improve the accuracy of model predictions.

[1] O'Loughlin, E., Boyanov, M., Antonopoulos, D., Kemner, K. Chapter 22 in: Aquatic Redox Processes; P.G. Tratnyek, T. J. Grundl, and S. Haderlein, Eds. American Chemical Society, Washington DC, pp. 477-517

[2] L. Zhang, Y. Chen, Q. Xia, K.M. Kemner, Y. Shen, E.J. O'Loughlin, Z. Pan, Q. Wang, Z. Wang, Y. Huang, H. Dong, M.I. Boyanov. *Environ.Sci.Technol.* 55, 9, 5929–5938 (2021).

[3] L. Zhang, H. Dong, R. Li, D. Liu, L. Bian, Y. Chen, Z. Pan, M.I. Boyanov, K.M. Kemner, J. Wen, Q. Xia, H. Chen, E.J. O'Loughlin, Y. Huang, "The effect of desferrioxamine B on adsorption and bioreduction of U(VI) by iron-reducing bacteria". In revision at ES&T (2022).

Chemical tomography of pyrite composites extracted from Opalinus Clay and reacted with Np and Pu

M. Breckheimer,¹ S. Amayri,¹ D. Ferreira Sanchez,² D. Grolimund,² T. Reich¹

¹ Johannes Gutenberg University Mainz, Department of Chemistry, TRIGA Site, 55128 Mainz, Germany

² Paul Scherrer Institute, Swiss Light Source, microXAS Beamline Project, 5232 Villigen PSI, Switzerland

Argillaceous rock is considered as a potential host rock for the final disposal of high-level radioactive waste (HLW) in a deep geological repository. Opalinus Clay (OPA) from the Mont Terri rock laboratory (St-Ursanne, Switzerland) serves as a reference material for natural clay rock exhibiting structural and mineralogical heterogeneities in a range of length scales [1]. Retention and transport parameters necessary for the safety case of a HLW repository are accessible through batch sorption studies with dispersed OPA [2] as well as diffusion experiments, obtaining diffusion profiles through abrasive peeling [3]. In both cases, however, the micro-scaled and potentially reactive heterogeneities are not accounted for, resulting in spatially and compositionally averaged information.

Complementing these methods, spatially resolved measurements on OPA samples were performed in previous studies by synchrotron-based multimodal chemical imaging at the microXAS beamline (Swiss Light Source), combining the micro-beam modalities of micro-X-ray absorption (μ XAS), micro-X-ray fluorescence (μ XRF), and micro-X-ray diffraction (μ XRD). In these experiments with Np(V) and Pu(V,VI) a significant role of pyrite (FeS_2), contained in OPA to about 4 wt. %, could be identified concerning the observed redox transformations to reduced tetravalent, less mobile species and retention. The latter, however, was observed with varying degrees of spatial correlation to this Fe(II)-bearing mineral, indicating a possibly decoupled mechanism of redox and sorption processes [4-6].

To further elucidate this relevant reactive transport mechanism, the interaction of Np and Pu with preferably pristine pyrite composites, extracted as sub-mm-sized particles from OPA, was investigated in this study by means of multimodal chemical tomography at the microXAS beamline. Two representative composite morphologies could be identified by SEM/EDX: micro-crystalline and (poly)framboidal aggregates of pyrite crystallites, distinguished by crystallite size and ordering, predominantly cemented by calcite. All processes involving wet chemistry were performed under anaerobic conditions and calcite saturation, preventing a potential pyrite oxidation and dissolution of the cementing phase. A selection of sub-100 μm sized particles was subjected to sorption experiments with solutions of either 7.4 μM $^{237}\text{Np(V)}$ or 13-14 μM $^{242}\text{Pu(VI)}$ in OPA pore water (pH 7.7-7.9, $I=0.4$ M) and subsequently prepared into capillaries. Selected particles of both morphologies were measured by chemical tomography, gaining volume information in the form of tomograms with voxel sizes of 1-1.5 μm^3 . Inner structure, chemical composition and elemental and mineral phase correlations of these pyrite composites were derived by means of absorption contrast (μ CT), μ XRF-CT, and μ XRD-CT. Spatial distributions of Np and Pu were obtained by L_{III} absorption edge contrast and deconvolution of full XRF spectra.

Despite the necessary selection of a limited number of particles in this study, the results so far indicate an enhanced retention reactivity of the framboidal morphology. The spatial distributions of both Np and Pu are correlated with the interspace of the pyrite aggregates, predominantly cemented by calcite.

In conclusion, this study presents a contribution in extending the understanding of the reactive transport in Opalinus Clay as a natural heterogeneous host rock, relevant for the safety case of a HLW repository.

Acknowledgements

Funding from the German Federal Ministry of Education and Research (BMBF) under contract number 02NUK044B, from the Federal Ministry for Economic Affairs and Energy (BMWi) under contract numbers 02E11415A and 02E11860A, and from the European Union's Horizon 2020 project EURAD (WP FUTuRE), EC Grant agreement no. 847593, is acknowledged.

[1] Nagra (2002) Tech. Ber. 02-03, Projekt Opalinuston, Wetingen, Switzerland.

[2] Amayri, S., Fröhlich, D.R., Kaplan, U., Trautmann, N. and Reich, T. (2016) *Radiochim. Acta* 104(1), 33-40.

[3] Wu, T., Amayri, S., Drebert, J., Van Loon, L.R. and Reich, T. (2009) *Environ. Sci. Technol.* 43, 6567-6571.

[4] Fröhlich, D.R., Amayri, S., Drebert, J., Grolimund, D., Huth, J., Kaplan, U., Krause, J. and Reich T. (2012) *Anal. Bioanal. Chem.* 404, 2151-2162.

[5] Kaplan, U., Amayri, S., Drebert, J., Rossberg, A., Grolimund, D. and Reich T. (2017) *Environ. Sci. Technol.* 51, 7892-7902.

[6] Börner, P.J.B. (2017) PhD thesis, Johannes Gutenberg University Mainz, Mainz, Germany.

Electronic Structure of Actinide Compounds as Probed by Advanced X-ray Spectroscopy: Experiment and Theory

Sergei M. Butorin

Department of Physics and Astronomy, Uppsala University, Sweden

A theoretical overview of the core-to-core (3d-4f) resonant inelastic x-ray scattering (RIXS) spectra of compounds of tetravalent and trivalent actinides (An=Th, U, Np, Pu, Am, Cm, Bk, Cf) will be provided [1,2]. The 3d-4f RIXS maps were calculated using crystal-field multiplet theory and the Anderson impurity model and turned out to be significantly different at the An M_5 versus M_4 edges due to selection rules and final state effects.

The results of the calculations allowed for a general analysis of so-called high-energy-resolution fluorescence-detected x-ray absorption (HERFD-XAS) spectra. The cuts of the calculated RIXS maps along the incident energy axis at the constant emitted energy, corresponding to the maximum of the RIXS intensity, represented the HERFD spectra and provided their comparison with calculated conventional x-ray absorption (XAS) spectra with a reduced core-hole lifetime broadening at the An M_5 and M_4 edges.

Whereas, the An M_5 HERFD profiles were found to depart from the x-ray absorption cross-section in terms of appearing additional transitions, the results of calculations for the An M_4 edges demonstrate overall better agreement between the HERFD and XAS spectra for most dioxides, keeping in mind a restricted HERFD resolution due to the core-hole lifetime broadening in the final state. The results confirm the utility of HERFD for the An chemical state determination and indicate the importance of calculating the entire RIXS process in order to interpret the HERFD data correctly.

The 3d-4f RIXS and HERFD-XAS measurements were performed for a number of actinide compounds to provide a comparison with calculated results.

[1] Butorin, S.M. (2020) *Inorg. Chem.* 59, 16251-16264.

[2] Butorin, S.M. (2021) *J. Chem. Phys.* 155, 164103.

Investigation of the interaction of uranium(VI) with the biofluids of the human digestive system

D. Butscher,¹ R. Steudtner,¹ T. Stumpf,¹ A. Barkleit¹

¹ Helmholtz-Zentrum Dresden-Rossendorf, Institute of Resource Ecology, Bautzner Landstraße 400, 01328 Dresden, Germany

When radionuclides (RNs) enter the food chain and are ingested by humans, they pose a potential health risk due to their radio- and chemotoxicity. After oral ingestion, RNs first come into contact and interact with the biofluids of the digestive system. For the development of a rapid as well as efficient method for the decorporation of RNs, it is necessary to know the biokinetic processes as well as the speciation in the digestive system. Therefore, the aim of this work was to investigate the interactions of uranium(VI) with the biofluids of the human digestive system, with the gastrointestinal digestive segments stomach and small intestine as well as the whole digestive system at the molecular level. To simulate the biofluids, saliva, gastric juice, pancreatic juice and bile, and the digestive segments were synthesized based on human physiology.[1] For the determination of chemical speciation, luminescence spectra were measured using time-resolved laser-induced fluorescence spectroscopy under cryogenic conditions (cryo-TRLFS) at 153 K. Species distribution was then determined by parallel factor analysis (parafac), where the resulting species were assigned using the spectra of the individual complexes. These results were compared with thermodynamic modeling.

Based on the TRLFS experiments, it can be shown that the speciation of uranium is predominantly dominated by the inorganic components, mainly carbonate and to a smaller extent phosphate. Among the organic components, only the protein mucin is involved in speciation at acidic pH values, such as in the stomach. Therefore, the complexation of mucin with uranium(VI) was investigated in more detail.

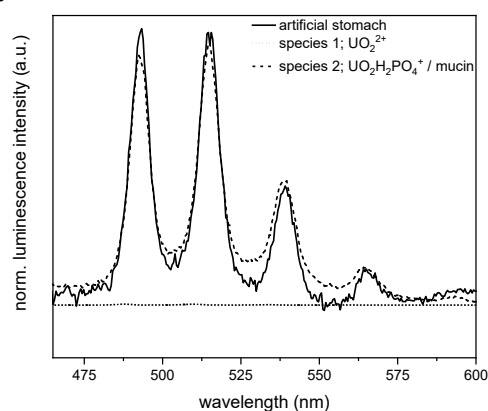


Fig. 1: Luminescence spectrum of uranium(VI) in artificial stomach at pH 1.3.

This work is funded by the German Federal Ministry of Education and Research (BMBF) under grant number 02NUK057A and is part of the joint project RADEKOR.

[1] Wilke, C. et al. (2017) J. Inorg. Biochem. 175, 248-258.

Fission products speciation in high burnup MOx fuel: fabrication and experimental characterization of Pu-bearing simulated fuel

R. Caprani^{1,2}, P. Martin¹, D. Prieur², J. Martinez¹, F. Lebreton¹, N. Clavier³

¹ CEA, DES, ISEC, DMRC, Univ Montpellier, Marcoule, France

² Helmholtz Zentrum Dresden Rossendorf (HZDR), Dresden, Germany

³ Institut de Chimie Séparative de Marcoule, Univ Montpellier, CEA, CNRS, ENSCM, Marcoule, France

In the context of nuclear fuel recycling, $U_{1-y}Pu_yO_{2-x}$ Mixed Oxides (MOx) are currently considered as the most suitable fuel. After manufacturing, these materials have to fulfil precise microstructural and physico-chemical properties, which are known to change drastically during irradiation due to the formation of Fission Products (FP) [1,2]. Even if thermodynamic modelling of spent fuel is constantly improved [3], the main difficulty remains the lack of experimental data on spent fuel especially about FP speciation.

Considering both high radiotoxicity and complex chemical composition of the spent fuel, model materials called SIMfuel have been developed in the last decades [4-6]. Currently, SIMfuels are constituted by fresh UO_2 doped with non-radioactive FP isotopes. These materials have been shown to be fairly representative of real UO_2 spent fuel, but with several advantages, namely their reduced radiotoxicity, and the possibility to separate the effect of selected FP. Nevertheless, the impact of Pu on the fuel chemistry cannot be addressed by UO_2 SIMfuel. In this frame, we developed a fabrication route to synthesize three different batches of Pu-bearing SIMfuel (SIMMOx) samples, using FP content representative of real irradiated fuel with a burn up of 13 at. %:

- Batch “S”, containing only « soluble » FPs (Ce, La, Nd, Sr, Y, Zr),
- Batch “M”, adding FP known to form metallic precipitates (same as “S” + Mo, Pd, Rh, Ru),
- Batch “B”, adding Ba as precursor of typical oxide precipitates (same as “M” + Ba).

The evolution of the chemical behaviour of both actinides (U, Pu, Am) and fission products (Ba, Ce, La, Mo, Nd, Pd, Rh, Ru, Sr, Y, Zr) has been followed through several characterization techniques.

XRD showed a monophasic (U,Pu) O_2 matrix, while local analysis (μ -Raman and EPMA) highlighted the presence of various FP-based precipitates, similar to the ones characteristic of irradiated MOx fuel[7].

XAS experiments performed at ESRF-ROBL, allowed the study of the actinides L-edges and K-edge analysis on Sr, Y, Zr, Mo, Pd, Rh, and Ru. The determination of the oxidation state of U, Pu, and Am and oxygen stoichiometry (O/M ratio) are given Table 1. As shown, U and Pu are always present in multivalent form as suggested in previous works [8]. It is important to highlight how the totality of Am and a significant fraction of Pu are present in their trivalent state even though the material has an overall O/M>2.00.

Three thermal treatments were applied to simulate conditions of engineering interest in both regular and accidental scenarios such as: reducing environment, LOCA accidents, and failure of geological confinement.

The same characterization strategy was applied to the annealed samples.

Under the most oxidizing conditions, the matrix is shown to oxidize and become biphasic, even if the Pu(III)/Pu(IV) ratio remains unchanged. On the other hand, the average oxidation state of U is 4.886(5) suggesting the presence of a complex mix of oxidised phases.

Tab. 1: Mean oxidation state of actinides for the as-sintered samples determined through XANES at the L_3 edges. $M = U+Pu+Am$.

Batch	U	Pu	Am	O/M
S	4.076(5)	3.884(5)	3.000(5)	2.011(5)
M	4.122(5)	3.982(5)	3.008(5)	2.040(5)
B	4.071(5)	3.876(5)	3.121(5)	2.016(5)

[1] Y. Guerin, Compr. Nucl. Mater., Elsevier, Oxford, 2012.

[2] K. Samuelsson et al., J. Nucl. Mater., 532, 2020, 151969.

[3] C. Guéneau et al, Calphad, 72, 2021, 102212.

[4] C. Le Gall, PhD Thesis, Université Grenoble Alpes, 2018.

[5] E. Geiger, PhD Thesis, Université Paris-Saclay, 2016.

[6] P.G. Lucuta et al., J. Nucl. Mater., 168, 1991, 48-60.

[7] R. Parrish et al, J. Nucl. Mater. 510, 2018, 644–660.

[8] D. Prieur et al, Inorg Chem., 2018, 57, 3, 1535–1544.

Application of micro-focused x-ray techniques to simulant Chernobyl and Fukushima nuclear fuel debris

H. Ding,¹ M. C. Wilkins,¹ L. M. Mottram,¹ M. C. Stennett,¹ D. Grolimund,² R. Tappero,³ S. Nicholas,³ N. C. Hyatt,¹ C. L. Corkhill¹

¹ Department of Materials Science and Engineering, The University of Sheffield, UK

² Swiss Light Source, Paul Scherrer Institute, Villigen, Switzerland

³ Brookhaven National Laboratory, NSLS-II, Upton, NY 11973, USA

During the loss of coolant accidents at the Chernobyl Nuclear Power Plant (ChNPP) and the Fukushima Daiichi Nuclear Power Plant (1F) the temperature within the reactors rose in excess of 2000 °C. Overheating of the reactor cores led to melting of fuel pellets (UO_2 and $(\text{U,Pu})\text{O}_2$) and fuel cladding (zircaloy), as well as other core materials such as control rods (stainless steel and B_4C). In both accidents, a portion of the melted core materials penetrated through the bottom of the reactor pressure vessel, further reacting with concrete and steel pipe work. The resulting materials, once cooled, are known as Lava-like Fuel Containing Materials (LFCM) at ChNPP, and Molten Core-Concrete Interaction products (MCCI) at 1F. Understanding the chemical and physical properties of these materials is of importance for their retrieval, storage and disposal. Relatively few samples of meltdown materials are available for study, none of which are sourced from 1F, and their analysis is challenging due to the radiation hazard associated with their handling. We therefore developed low-radioactivity (i.e. depleted uranium only) simulants to expand the knowledge base of these materials [1].

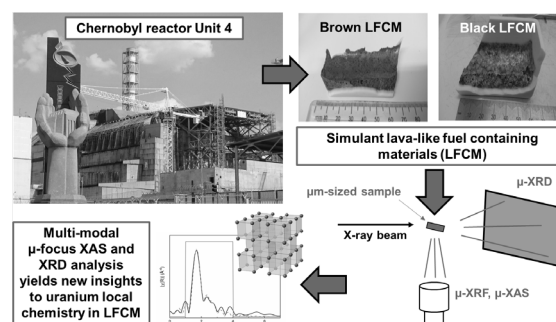


Fig. 1: Simulant and micro-focus X-ray analysis approach to understanding nuclear fuel debris chemistry.

Using element-specific chemical probes (micro-X-ray fluorescence and X-ray absorption spectroscopy), coupled with micro-diffraction analysis, the crystalline phase assemblage of these heterogeneous materials was established (Fig. 1). In LFCM, “chernobylite” and a range of compositions in the $(\text{U}_{1-x}\text{Zr}_x)\text{O}_2$ solid solution were observed [2]. Novel insight to nuclear accident fuel chemistry was obtained by establishing the oxidation state and local coordination of uranium not only in these crystalline phases, but uniquely in the amorphous fraction of the material, which varied depending on the history of the nuclear lava as it flowed through the reactor [2, 3]. For the MCCI materials, in which Ce was added as a surrogate for Pu, the expected suite of U-Zr-O containing minerals was observed, in addition to crystalline silicate phases CaSiO_3 , SiO_2 -cristobalite and Ce-bearing percleveite, $(\text{Ce,Nd})_2\text{Si}_2\text{O}_7$. The formation of percleveite resulted from reaction between the U-Zr-O-depleted Ce-Nd-O melt and the silicate (SiO_2) melt. It was determined that the majority of U was present as U^{4+} , whereas Ce was observed to be present as Ce^{3+} , consistent with the highly reducing synthesis conditions. A range of Fe-containing phases characterised by different average oxidation states were identified, and it is hypothesised that their formation induced heterogeneity in the local oxygen potential, influencing the oxidation state of Ce. It is concluded that the presence of Pu-bearing silicates in real MCCI seems plausible, should the redox environment be sufficient to promote reduction of Pu^{4+} to Pu^{3+} [4].

This study demonstrates that micro-focus X-ray analysis of very small fractions of material can yield rich chemical information, which could be applied to real nuclear-melt down materials in support of decommissioning and nuclear fuel debris management.

[1] Barlow, S. T. et al. (2020) npj Mater. Degrad. 4, 3.

[2] Ding, H. et al. (2021) J. Mater. Chem. A, 9, 12612 – 12622.

[3] Ding, H. et al. (2021) J. Synchrotron Rad., 28, 1672 – 1683.

[4] Ding H. et al. (2022) npj Mater. Degrad. 6, 10.

Tender X-ray Spectromicroscopy of Actinide Particles at the Advanced Light Source

A. Ditter¹, S. Fakra¹, J. Ward², A. Duffin², M. Miller², R. Coles³, J. Thieme³, B. Bowerman³, M. Schoonen³, D. Shuh¹.

¹ Lawrence Berkeley National Laboratory

² Pacific Northwest National Laboratory

³ Brookhaven National Laboratory

The study of particles has seen increasing importance in nuclear forensics and nuclear safeguards. Though isotopic measurement remains the primary priority, complementary techniques to determine elemental and chemical signatures give important clues to the provenance of a specimen. However, preparing particle samples for electron microscopy elemental analysis is challenging due to the vacuum and conductivity requirements of the instruments. On the other hand, microfocused synchrotron radiation offers the ability to analyze these particles in a polymer matrix in a non-destructive manner.

This discussion will focus on the development of a tender x-ray chamber for use at ALS Beamline 10.3.2 (see Fig. 1) and its use in nuclear forensics and nuclear safeguards. The tender x-ray data from the ALS will be compared with hard x-ray measurements taken at NSLS-II on similar samples. The tender x-ray chamber serves two goals. The first is the enabling of soft x-ray fluorescence for elemental analysis of particles. This is done in a helium environment which simplifies containment concerns and is possible to collect fluorescence on elements as light as oxygen (O K α at 525 eV). Particles contained in the existing polymer film method are available for light element fluorescence, including fluorine, a particularly important element for forensics and safeguards. The chamber also acts as an air-free containment for actinides, which are particularly important for interesting low valence compounds. This is demonstrated using $U\text{I}_3(\text{dioxane})_{1.5}$, a trivalent uranium complex which is highly air-sensitive.

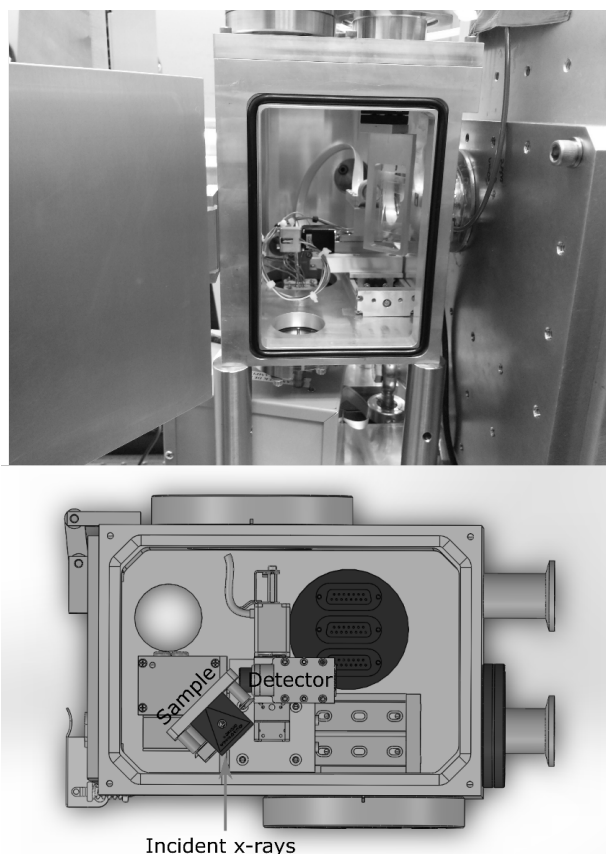


Fig. 1: Top: Image of the tender x-ray chamber installed at ALS beamline 10.3.2. Bottom CAD rendering of the beamline showing the sample orientation and detector positioning relative to the incident x-rays.

[1] Ditter, A. et al. A Chamber for Air-free Tender and Soft X-ray Fluorescence and Near-edge Spectroscopy for Actinides. To be submitted 2022

Spectroscopy for plutonium hydrolysed species in solution and application of model structures in data analysis.

T. Dumas,¹ M. Virost,² C. Micheau,² M. Cot-Auriol,² S. Dourdain,² Sergey I. Nikitenko,² C. Hennig,^{3,4} P. Solari,⁵ D. Menut,⁵ Philippe Moisy,¹ Geoffroy Chuppin,¹ Christelle Tamain,¹ Dominique Guillaumont.¹

¹ CEA, DES, ISEC, DMRC, Univ Montpellier, Marcoule, 30207 Bagnols sur Cèze, France

² ICSM, Univ Montpellier, CEA, CNRS, ENSCM, Marcoule, France

³ The Rossendorf Beamline at the ESRF, CS40220, 38043 Grenoble Cedex 9, France

⁴ Helmholtz Zentrum Dresden-Rossendorf, Institute of Resource Ecology, P.O. Box 510119, Dresden, Germany

⁵ Synchrotron SOLEIL, MARS Beamline, Gif Sur Yvette, France

Understanding the structure of plutonium ions in solution is crucial to develop effective separations technologies and predict the long term behavior of actinide containing materials in interaction with aqueous solutions. It is an euphemism to say that the plutonium chemistry in solution is complex. Diverse and multifaceted species has been identified and, most often, several of which coexist with each other. In this context, the structural information provided by EXAFS measurements can be a lighthouse for the chemist and the rich visible/near infrared plutonium absorption properties is an excellent asset too. Nevertheless none of which are easy to interpret because only few structural models are available for plutonium. This presentation aim to recall how multispectroscopic approaches can benefit from reference structures (crystallographic and/or theoretical) to identify plutonium compounds in solution focusing on plutonium hydrolysis compounds and polycondensation in aqueous solutions.

Single crystal X-ray diffraction and spectroscopies has been applied to describe small hexanuclear plutonium clusters in solution.[1-3] Apart from the structural description, this plutonium hexanuclear core resulted in a peculiar absorption spectrum in the visible range that can be a valuable footprint in other systems. Other actinide cluster geometries are known [4-7] and may be useful to support spectroscopic analysis in complex plutonium solution. **Figure 1.** is an example of EXAFS spectra derived from crystal structures and ab-initio calculations.[8] It shows how the cluster geometry and nuclearity translates into EXAFS scattering paths and may help to identify the plutonium clusters in solution. In addition, the larger plutonium clusters can be considered as model structures for PuO₂ nanoparticle (or colloids) and several structural properties of the nanosized plutonium oxides and colloids may be understood analyzing molecular bonds in plutonium clusters.[9-10] Ultimately, in the plutonium route from molecular ions to colloidal suspensions, polynuclear plutonium clusters may be an intermediate form, and the appropriate spectroscopic tools may help to capture it.

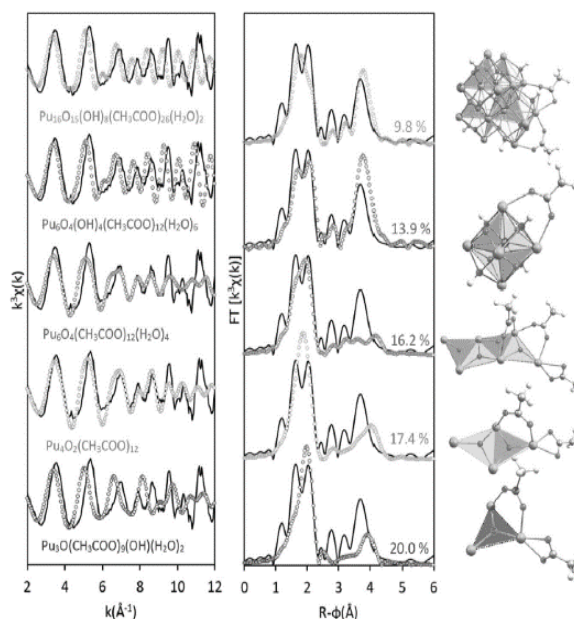


Fig. 1: Calculated EXAFS oscillations and corresponding FT for different polynuclear plutonium compounds.

[1] C. Tamain, T. Dumas, D. Guillaumont, C. Hennig and P. Guilbaud, *European Journal of Inorganic Chemistry*, 2016, 2016, 3536-3540.

[2] C. Tamain, T. Dumas, C. Hennig and P. Guilbaud, *Chemistry-a European Journal*, 2017, 23, 6864-6875.

[3] T. Dumas, M. Virost, D. Menut, C. Tamain, C. Micheau, S. Dourdain and O. Diat, *Journal of Synchrotron Radiation*, 2022, 29, 30-36.

[4] K. E. Knope, S. Skanthakumar and L. Soderholm, *Inorganic Chemistry*, 2015, 54, 10192-10196.

- [5] L. Soderholm, P. M. Almond, S. Skanthakumar, R. E. Wilson and P. C. Burns, *Angewandte Chemie-International Edition*, 2008, **47**, 298-302.
- [6] G. E. Sigmon and A. E. Hixon, *Chemistry-a European Journal*, 2019, **25**, 2463-2466.
- [7] R. E. Wilson, S. Skanthakumar and L. Soderholm, *Angewandte Chemie-International Edition*, 2011, **50**, 11234-11237.
- [8] G. Chupin, C. Tamain, T. Dumas, P. L. Solari, P. Moisy and D. Guillaumont, *Inorganic Chemistry*, 2022, **61**, 4806-4817.
- [9] C. Micheau, M. Viro, S. Dourdain, T. Dumas, D. Menut, P. L. Solari, L. Venault, O. Diat, P. Moisy and S. I. Nikitenko, *Environmental Science-Nano*, 2020, **7**, 2252-2266.
- [10] A. Romanchuk, A. Trigub, T. Plakhova, A. Kuzenkova, R. Svetogorov, K. Kvashnina and S. Kalmykov, *Journal of Synchrotron Radiation*, 2022, **29**.

Insights into the Enigmatic $\text{TcO}_2 \cdot x\text{H}_2\text{O}$ Structure via Atomistic Simulations and EXAFS

A. F. Oliveira,¹ A. Kuc,¹ T. Heine,^{1,2,3} U. Abram,⁴ A. C. Scheinost^{1,5}

¹ Helmholtz-Zentrum Dresden – Rossendorf (HZDR), Germany.

² Technische Universität Dresden, Germany.

³ Yonsei University, South Korea.

⁴ Freie Universität Berlin, Germany.

⁵ European Synchrotron Radiation Facility (ESRF), France.

Technetium is the lightest element without a stable isotope. The β -emitting ^{99}Tc is especially relevant for nuclear waste management due to its long half-life (ca. 2.1×10^5 years) and relatively high formation yield ($\geq 6\%$) in ^{235}U and ^{239}Pu nuclear reactors. In this context, redox reactions at mineral/water interfaces are crucial for the safety of nuclear waste repositories.

In the absence of complexing agents, Tc exists in water as Tc(VII) and Tc(IV). The former predominates in non-reducing conditions as TcO_4^- (aq), which is highly mobile in the environment due to its solubility and weak interaction with adsorbents. Studies show that Fe(II) minerals can reduce Tc(VII) to Tc(IV), which is then immobilized by adsorption onto or incorporation into the oxidized Fe mineral and by precipitation as $\text{TcO}_2 \cdot x\text{H}_2\text{O}$. However, even in the simpler case (precipitation) the structure of $\text{TcO}_2 \cdot x\text{H}_2\text{O}$ remains controversial.

Lukens et al. [1] demonstrated that, despite being amorphous, $\text{TcO}_2 \cdot x\text{H}_2\text{O}$ has a well-defined structure around the Tc atoms. Based on EXAFS measurements, they proposed that $\text{TcO}_2 \cdot x\text{H}_2\text{O}$ forms linear chains of equally spaced edge-sharing $\text{TcO}_4(\text{H}_2\text{O})_2$ octahedra, with terminal H_2O ligands at the apical positions. Vichot et al. [2] obtained similar results but, despite having extracted only one Tc-Tc distance from the EXAFS, proposed that Tc atoms would be separated by shorter and longer alternating distances as in the monoclinic TcO_2 crystal. More recently, Yalçintaş et al. [3] showed that both models can be fitted equally well to the EXAFS and, thus, the $\text{TcO}_2 \cdot x\text{H}_2\text{O}$ structure remained unsolved.

In this work, we use *density functional theory* (DFT) to investigate the polymeric $\text{TcO}_2 \cdot x\text{H}_2\text{O}$ structure. Our calculations reveal that, in contrast to previous models, a zigzag configuration with the terminal H_2O groups at neighboring positions of the octahedra is more likely. The zigzag configuration is energetically more favored and results in a better agreement with the EXAFS measurements.

[1] Lukens et al. (2002), *Environ. Sci. Technol.* 36, 1124-1129.

[2] Vichot et al. (2002), *Radiochim. Acta* 90, 575-579.

[3] Yalçintaş et al. (2016), *Dalton Trans.* 45, 17874-17885.

Complexation of Eu(III) and Cm(III) by EGTA related aminopolycarboxylic acids

S. Friedrich¹, J. Kretschmar¹, B. Drobot¹, T. Stumpf¹, A. Barkleit¹

¹ Helmholtz-Zentrum Dresden-Rossendorf, Institute of Resource Ecology, Bautzner Landstraße 400, 01328 Dresden, Germany

For radiation protection and chelation therapy, aminopolycarboxylic acids like ethylenediaminetetraacetic acid (EDTA) or diethylenetriaminepentaacetic acid (DTPA) are clinical approved decorporation agents. They show promising results in complexation of Ln(III)/An(III). For EDTA and DTPA related compound ethylene glycol-bis(β-aminoethyl ether)-N,N,N',N'-tetraacetic acid (EGTA), complexes with trivalent europium (Eu) have been characterized by NMR spectroscopy and x-ray diffraction. In these complexes, EGTA acts as an octadentate ligand.[1,2] In addition to this, the knowledge on the Eu-EGTA-system is extended by time-resolved laser-induced fluorescence spectroscopy (TRLFS), ²H-NMR spectroscopy and isothermal titration calorimetry (ITC). These speciation studies on Eu(III) show promising results for EGTA as a complexing agent (Fig. 1).

To expand this group of ligands, EGTA related compounds were synthesized (Fig. 2). With these compounds, the complexation behavior with Eu(III) and curium(III) were determined and comprehensively characterized with TRLFS from both sides: the ligands and metals perspective. The overall goal is a better understanding of the influence of the ligand design on the affinity to complex trivalent Ln and An. Hence, in the future these ligands may contribute to an advanced chelation therapy.

This work is funded by the German Federal Ministry of Education and Research (BMBF) under grant number 02NUK057A and part of the joint project RADEKOR.

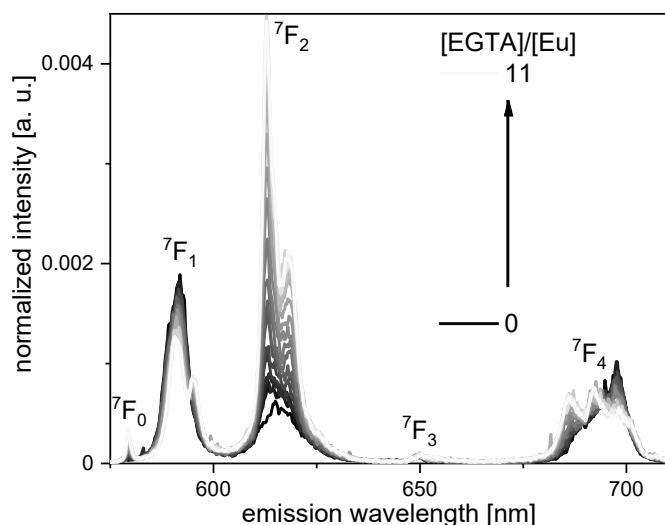


Fig. 2: Emission spectra of Eu(III) with EGTA obtained by TRLFS. pH = 3.0, [Eu(III)] = 10 μM, [EGTA] = 0 to 113 μM, I(NaClO₄) = 0,1 M.

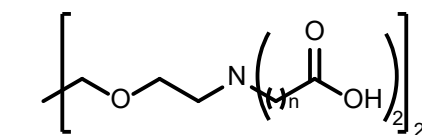


Fig. 1: Structure of EGTA and related ligands. n = 1 (EGTA), 2, 3.

- [1] S. Aime, A. Barge, A. Borel, M. Botta, S. Chemerisov, A. E. Merbach, U. Müller, D. Pubanz, *Inorg. Chem.* (1997), 36, 5104.
 [2] R. Xu, D. Li, J. Wang, Y. X. Kong, B. X. Wang, Y. M. Kong, T. T. Fan, B. Liu, *Russ. J. Coord. Chem.* (2010), 36, 810.

Structure and Stability of plutonium hexanuclear cluster in the gas phase and in solution

G. Chupin,¹ C. Tamain,¹ L. Berthon,¹ T. Dumas,¹ P. Moisy,¹ D. Guillaumont¹

¹ CEA, DES, ISEC,DMRC, Univ Montpellier, Marcoule, 30207 Bagnols-sur-Ceze, France

The chemistry of Plutonium(IV) is largely influenced by hydrolysis and condensation reactions leading to the formation of oxo/hydroxo oligomeric species. Such plutonium clusters are known as being an essential part of plutonium speciation in solution but their formation, stability and reactivity is yet largely unknown. For Pu(IV) and all tetravalent actinides, the hexamer is the most common unit that has been observed in solid state and in solution. Its core corresponds to $[An_6O_4(OH)_4]^{12+}$ and is stabilized with additional organic or inorganic ligands on its surface. With Pu(IV), two hexameric structures have been characterized by Single Crystal X-Ray Diffraction X with glycine [1] and with a polyaminocarboxylate acid (DOTA) [2]. For such polynuclear species, the main difficulty is to establish their presence and stability in solution. In the present work, we have combined DFT calculations with Vis-NIR, EXAFS spectroscopies and ESI-MS Mass Spectrometry in order to investigate plutonium cluster formation with acetate ligand. By coupling spectroscopic and theoretical methods it was possible to establish the presence of the hexameric core in the solution [3]. ESI-MS was applied to the acetate solution, a series of Pu(IV) hexameric clusters were detected indicating the strong stability of such clusters. The structure and thermodynamic stability of the clusters were further analyzed by using DFT calculations.

[1] Knope, K. E, Soderholm, L. (2013) *Inorg. Chem.* 52, 6770-6772.

[2] Tamain, C., Dumas, T., Guillaumont, D., Hennig, C., Guilbaud P. (2016) *Eur. J. Inorg. Chem.* 22, 3536-3540.

[3] Chupin, C., Tamain, C., Dumas, T., Solari, P., Moisy P., Guillaumont D. (2022) *Inorg. Chem.* 61, 4806-4817.

Multi-method investigation of the Eu/La complexation with HEDP

A. Heller¹, C. Senwitz¹, H. Foerstendorf², S. Tsushima², S. Paasch³, L. Holtmann⁴, L. Peters⁵, B. Drobot², J. Kretzschmar²

¹ Technische Universität Dresden, Radiochemistry/Radioecology and Central Radionuclide Laboratory

² Helmholtz-Zentrum Dresden-Rossendorf, Institute of Resource Ecology

³ Technische Universität Dresden, Bioanalytical Chemistry

⁴ Leibniz Universität Hannover, Institute of Radioecology and Radiation Protection

⁵ Rheinisch-Westfälische Technische Hochschule Aachen, Institute of Crystallography

In case actinides and lanthanides enter the food chain and are incorporated by humans, they pose a possible health risk due their radio- and/or chemotoxicity. In the event of U(VI) incorporation, HEDP (1-Hydroxyethylidene-1,1-diphosphonic acid; etidronic acid) is proposed to be a suitable decorporation agent *in vivo* [1,2]. However, HEDP is also capable of binding di- and trivalent metal ions. Therefore, we investigated the complexation of HEDP with lanthanides, which also serve as non-radioactive analogs of trivalent actinides.

Complexation studies were performed with Eu and La due to their excellent luminescence and NMR properties, respectively. A wide pH-range of 1 - 12 was investigated and ionic strength was kept constant at the physiological value of 0.1 M (NaCl). A variety of spectroscopic and analytical methods was applied and combined with theoretical calculations. First, the pH-dependent behavior of the HEDP ligand in aqueous solution was studied using infrared spectroscopy with attenuated total reflection (ATR-FT-IR) combined with density functional theory (DFT). Additionally, pK_a values were determined with nuclear magnetic resonance (NMR) spectroscopy. Then, the complexation of Eu with HEDP in aqueous solution was investigated using time-resolved laser-induced fluorescence spectroscopy (TRLFS), ATR-FT-IR, and mass spectrometry with electrospray ionization (ESI-MS) as well as with inductively coupled plasma (ICP-MS). Precipitates formed in Eu/La-HEDP-solutions were analyzed using solid-state-NMR, TRLFS, FT-IR with KBr pellets, DFT, and powder X-ray diffraction (P-XRD).

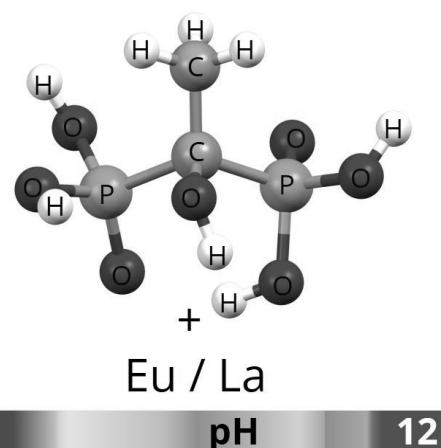


Fig. 1: Chemical structure of the HEDP ligand.

Depending on both the pH and the metal to ligand ratio, several Eu/La-HEDP complex species are formed. Within this study at least two soluble and two hardly soluble species were identified and characterized. At acidic and alkaline pH, soluble complexes with presumably 1:1 stoichiometry and monodentate binding of Eu/La via one of the phosphonate groups are formed. In contrast, within a broad pH-range (pH 3.5 - 10 at 10^{-5} M Ln and pH 1 - 11 at 10^{-3} M Ln), precipitation of hardly soluble species occurs. In these complexes with presumably 1:1 and 1:2 stoichiometry, Eu/La are most possibly complexed in bidentate or chelate binding mode via one or both phosphonate groups. Additionally, also Na from the background electrolyte has an influence on the Eu/La complexation with HEDP, especially the formation of the hardly soluble complex species. Hence, omitting the background electrolyte leads to differences in luminescence, XRD and NMR spectra both in aqueous solution and in precipitates.

This work is funded by the German Federal Ministry of Education and Research (BMBF) under grant number 02NUK057B and part of the joint project RADEKOR.

[1] E Fattal. et al. (2015) Adv. Drug Deliv. Rev. 90, 40-54.

[2] C. Jacopin et al. (2003) Inorg. Chem. 42(16), 5012-5022.

Study of actinide compounds using X-ray spectroscopy with high resolution X-ray spectrometer at Shanghai Synchrotron Radiation Facility

Yuying Huang^{1,2}, Hongliang Bao², Pequan Duan^{1,2}, Hanjie Cao^{1,2}, Jiong Li¹, Jing Zhou², Linjuan Zhang², Jian-Qiang Wang²

¹ Shanghai Synchrotron Radiation Facility, Shanghai Advanced Research Institute, Chinese Academy of Sciences

² Shanghai Institute of Applied Physics, Chinese Academy of Sciences

In this report, the development of instrumentation of X-ray spectroscopy with high resolution X-ray spectrometer at Shanghai Synchrotron Radiation Facility (SSRF) will be first introduced.

Then three applications on actinide compounds will be present. Uranium-induced changes in crystal-field and covalency effects of Th⁴⁺ in Th_{1-x}U_xO₂ Mixed Oxides were investigated by high-resolution X-ray absorption spectroscopy. The experiment results shown that the 6d orbit of Th was influenced when U is doped into ThO₂ crystal lattice. The broadening of 6d band and electron transfer to E_g band, the phenomenon is noticeable in Th_{0.25}U_{0.75}O₂ whose CEF splitting is decreased by approximately 10%, and covalent mixing between Th 6d t_{2g} and O 2p orbitals is substantially reduced compared to that of pure ThO₂.

Differential interplay between Ce and U on local structures of U_{1-x}Ce_xO₂ solid solutions was probed by X-ray absorption spectroscopy. The local structures of U and Ce in the U_{1-x}Ce_xO₂ were studied by EXAFS at the U L₃ edge and Ce K edge, respectively. The order degree in the local structure of U increases with the content of Ce when the Ce content is kept about 35% or more. In contrast, the disorder degree in the local structure of Ce increases with U content once U is added into CeO₂.

Local structure of uranium in polycrystalline α -U₂N_{3+x} film was probed by X-ray absorption spectroscopy, the polycrystalline α -U₂N_{3+ δ} sample was shown to be close to U₂N₃ with a narrow distribution of U-N bond lengths. The average valence of U was estimated to be 1.3 and the average bond distance of U-N was determined to be 2.30 Å.

In the last part of the report, the new progress of the instrumentation of X-ray spectroscopy with high resolution X-ray spectrometer of SSRF phase II beamline project will be present.

[1] Yuying Huang, et al. (2017) X-ray Spectrometry, 46, 12-18.

[2] Yuying Huang, et al. (2018) Inorganic Chemistry, 57, 11404–11413.

[3] Yuying Huang, et al. (2019) Journal of Nuclear Materials, 515, 238-244.

[4] Yuying Huang, et al. (2020) Journal of Nuclear Materials, 542, 152404.

Characterisation of actinide materials at the MARS beamline

M.O.J.Y. Hunault¹, D. Menut¹, P.L. Solari¹

¹ Synchrotron SOLEIL, L'Orme des Merisiers, Saint-Aubin, BP 48, 91192 Gif-sur-Yvette Cedex, France

The MARS (Multi-Analyses on Radioactive Samples) beamline at the SOLEIL synchrotron (France) is opened to the international community since 2010 and is dedicated to the study of radioactive samples [1] with a specific radioprotection safety design that fulfills the French ASN (Autorité de Sureté Nucléaire) requirements. The MARS beamline offers advanced structural and chemical characterizations of radioactive matter (solid or liquid, maximum 18.5 GBq per sample) using hard X-rays in the 3-35 keV energy range. Currently, different types of experiments are available: X-ray absorption spectroscopy (XAS) and X-ray emission spectroscopies (XES, HERFD and RIXS), Transmission X-ray diffraction (TXRD), High-Resolution X-ray diffraction (HRXRD), and associated X-ray microbeam techniques (μ XRF/ μ XRD/ μ XAS).[2] Small Angle and Wide Angle X-ray Scattering (SAXS/WAXS) are also available.[3]

This contribution presents the recent status of the MARS beamline with an emphasis on the most recent achievements using our x-ray emission spectrometer for the actinide material analysis. i) characterisation of bulk spent nuclear fuel thanks to specific shielding and ii) study of the role of the 5f states in the properties of uranium, plutonium and other actinide compounds using $M_{4,5}$ -edges RIXS [4,5].

[1] B. Sitaud, et al., *Journal of Nuclear Materials* (2012) 425 (1-3), 238–243.

[2] I. Llorens, et al. *Radiochimica Acta* (2014) 102 (11), 957–972

[3] Dumas, T. et al. *J Synchrotron Radiation* (2022) 29, 30–36

[4] M.O.J.Y. Hunault, et al. *Inorganic Chemistry* (2019) 58, 6858–6865.

[5] Hunault, M. O. J. Y., et al. *Crystals* (2021) 11, 56

Np(V) sorption onto zirconia: a combined spectroscopy, batch and modeling study

I. Jessat¹, A. Rossberg^{1,2}, A. Scheinost^{1,2}, J. Lützenkirchen³, H. Foerstendorf¹,

T. Stumpf¹, N. Jordan¹

¹ Helmholtz-Zentrum Dresden-Rossendorf, Institute of Resource Ecology, Bautzner Landstraße 400, 01328 Dresden, Germany

² Rossendorf Beamline at ESRF - European Synchrotron Radiation Facility, CS40220, 38043 Grenoble Cedex 9, France

³ Karlsruhe Institute of Technology, Institute for Nuclear Waste Disposal, 76021 Karlsruhe, Germany

When assessing the long-term safety of a nuclear waste repository, the interactions of dissolved long-lived radionuclides, such as the actinide neptunium, with corroded phases in the near-field of the repository have to be considered. Zirconia (ZrO_2) is the main corrosion product of the zircaloy cladding material of nuclear fuel rods and can constitute a first barrier against the release of mobilized radionuclides into the environment.

To gain a detailed understanding of the Np(V) sorption processes at the zirconia–water interface, a comprehensive multimethod approach was pursued. Molecular level information about the Np(V) surface species were derived by *in situ* Attenuated Total Reflection Fourier Transform Infrared Spectroscopy (ATR FT-IR) and Extended X-ray Absorption Fine Structure Spectroscopy (EXAFS). The Np L_3 -absorption edge (17,610 eV) is commonly used for EXAFS investigations of neptunium. However, the Zr K absorption edge (17,998 eV) is close in energy to the Np L_3 -edge, reducing the k-range that can be evaluated. Since attempts to use the Np L_2 -edge (21,600 eV) with an energy above the Zr K-edge were not successful, the Np L_3 -edge EXAFS spectra had to be used to gain information about the molecular environment of the sorbed Np(V) surface species. The short Np-Zr distance of approximately 3.6 Å derived from EXAFS spectra revealed the predominant formation of bidentate inner-sphere Np(V) surface complexes. ATR FT-IR experiments were conducted at different pH values and a shift of the asymmetric stretching vibration of Np(V) ($\nu_3(NpO_2^+)$) towards lower energies was observed at acidic pH, revealing the interactions between Np(V) and ZrO_2 . Furthermore, the sorption process was only slightly reversible, also indicating the formation of Np(V) inner-sphere complexes. However, with increasing pH, vibrational surface modes of the ZrO_2 matrix appeared, which were overlapping with Np(V) stretching frequency and impeding the investigation of the pH-dependent surface speciation of Np(V).

Batch sorption experiments (varying ionic strength, Np(V) concentration, and solid-to-liquid ratio (m/V)) as well as a sorption isotherm experiment at pH 6 were conducted to study the sorption processes of the Np(V)– ZrO_2 system on the macroscopic scale. The sorption of Np(V) was independent of ionic strength, also indicating the formation of Np(V) inner-sphere surface complexes. This was supported by zeta potential measurements in the presence of neptunium, where a shift to higher pH values of the isoelectric point of the neat ZrO_2 was observed. With increasing m/V the Np(V) sorption edge was shifted towards lower pH values, indicating the presence of different kinds of sorption sites, which was also deduced from the shape of the sorption isotherm.

Reliable information about the number and density of surface species obtained by spectroscopic and macroscopic investigations enable modeling approaches such as surface complexation modeling (SCM) to be robust. The results derived by SCM will in turn contribute to a more reliable prediction of the environmental fate of neptunium.

Ab initio modelling of magnetite surfaces for Pu retention

A. Katheras¹, K. Karalis¹, M. Krack², A.C. Scheinost³, S.V. Churakov^{1,2}

¹ University of Bern, Switzerland

² Paul Scherrer Institut, Switzerland

³ Helmholtz-Zentrum Dresden-Rossendorf, Germany

In many countries, thick-walled steel casks are used for the disposal of spent nuclear fuel in deep geological repositories. In contact with pore water, steel casks corrode over time and the corrosion products are expected to form mixed iron oxides, mainly magnetite (Fe_3O_4). After tens of thousands of years, casks may breach allowing the leaching of radiotoxic elements, such as plutonium (Pu) and technetium (Tc), by host rock pore-water. The dissolved radionuclides can then be retarded by interaction with the corrosion products. Possible retention mechanisms include surface adsorption and incorporation into the structure of solids. Our study aims to reveal the mechanisms of these interactions at an atomic scale using computer simulations alongside with X-ray absorption spectroscopy (XAS) [1].

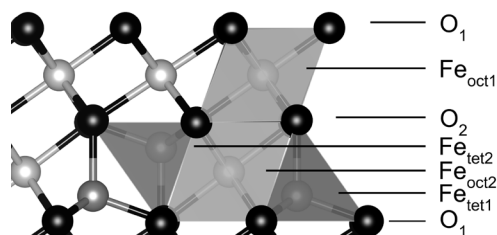


Fig. 1: Side view of magnetite (111) surface layers: two different oxygen layers and four different iron layers depending on octahedral (oct) or tetrahedral (tet) coordination.

In this computational study, we identified the structure and stoichiometry of dominant nano-magnetite surfaces at the repository relevant conditions based on Kohn-Sham density functional theory (DFT). This was done using the open-source code CP2K. The DFT+U method was employed for the strongly correlated 3d and 5f electrons of iron and plutonium, respectively. The Hubbard U parameter was determined by comparing experimental cell parameters and band gaps to the modelling prediction [2]. With this revised model, we examined the preferential magnetite crystal orientation plane (111) with different surface terminations (cf. Fig. 1) as a function of oxygen/water fugacity (cf. Fig. 2) and under different pH/redox conditions.

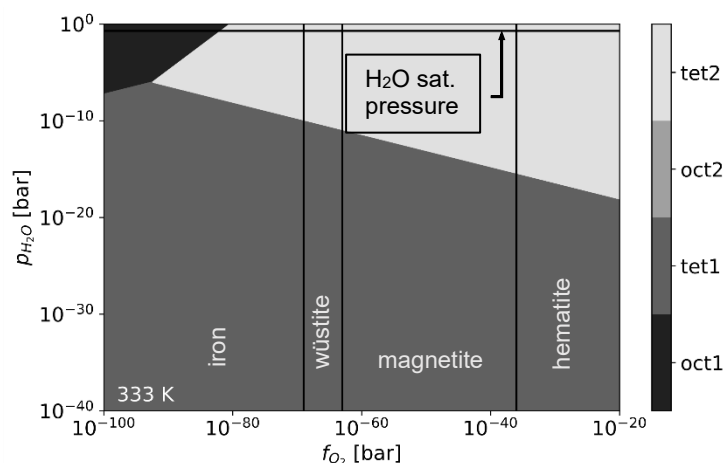


Fig. 2: Surface stability of different magnetite (111) surface terminations: One of the four occurring Fe coordinations (oct – octahedral, tet – tetrahedral) with coordinating oxygen and adsorbed hydrogen for charge neutrality. The vertical lines represent the oxygen fugacity ranges for iron and iron oxides based on mineralogical buffers, the horizontal line is the water saturation pressure at the expected long-time temperature of 333 K in a deep geological repository.

Based on our modelling, we found the most stable magnetite (111) surfaces under relevant repository conditions.

Moreover, we used classical and ab initio MD simulations to investigate the behavior of Pu at the water-magnetite interface based on experimentally proposed structures from XAS studies [3,4]. Further, we will use the obtained structures of incorporated and adsorbed Pu to simulate XAS spectra and contribute to the understanding of uptake mechanisms in deep geological repositories.

[1] Yalçintaş, E. et al. (2016), Dalton Trans. 45, 17874–17885.

[2] Kéri, A. et al. (2017), Environ. Sci. Technol. 51, 10585–10594.

[3] Kirsch, R. et al. (2011), Environ. Sci. Technol. 45, 7267–7274.

[4] Dumas, T. et al. (2019), ACS Earth Space Chem. 3, 2197–2206.

Multimodal multidimensional chemical imaging at the microXAS beamline of the Swiss Light Source

Makowska M.^{1,2}, Grolimund D.¹, Ferreira Sanchez D.¹, Meyer B.¹, Birri M.¹

¹ Swiss Light Source (SLS), Paul Scherrer Institute, Villigen PSI, Switzerland

² Laboratory for Nuclear Materials, Paul Scherrer Institute, Villigen PSI, Switzerland

The microXAS beamline of the Swiss Light Source (SLS), operated by the Chemical Imaging Group, provides unique capabilities for multimodal chemical and physical imaging in space and time in a wide range of spatial and temporal length scales.

The scanning imaging with submicron resolution is realized by achromatic KB mirror focusing down to a spot size of about 1 μm , however also smaller spot size down to 300 nm can be achieved by employing diffracting lenses. A special feature of this beamline is also the newly integrated x-ray beam position stabilization closed-loop system, which allows to maintain the focused beam position even during extended energy scans over a wider range of energies.

Mapping with submicron spatial resolution of chemical elements is performed by scanning X-ray fluorescence spectroscopy ($\mu\text{-XRF}$), which can be accompanied by simultaneous mapping of crystalline phases by means of X-ray diffraction ($\mu\text{-XRD}$) measurements. X-ray absorption spectroscopy – contrast microscopy can be performed both in scanning mode and via full field imaging, which can be combined with conventional attenuation contrast full field tomography. This variety of characterization techniques available at microXAS provides an invaluable capability to achieve complementary information corresponding to the full picture of the chemical characteristics combined with the microstructure of the studied systems during only one beamtime experiment.

These capabilities of microXAS are used by specialists from a very broad range of science, but what makes this beamline even more unique, is the possibility to investigate radioactive materials. Such studies are performed both in collaboration with external users as well as in close collaboration with the hot laboratory of the Nuclear Energy and Safety division of PSI. The newly installed FIB microscope in the hot laboratory is used to downsize samples to micro-scale from materials practically without upper limit of radioactivity, which opens up new possibilities for research on nuclear materials.

The potential of utilizing microXAS will be presented based on examples of recently performed research. As an outlook the perspectives of the new microXAS beamline after the major upgrade of the Swiss Light Source (SLS2.0) will be presented.

Extreme multi-valence states in mixed actinide oxides $U_{1-y}M_yO_{2\pm x}$

Ph. Martin¹, P. Fouquet-Métivier¹, L. Medyk¹, E. Epifano², F. Lebreton¹, M.O.J.Y. Hunault³, P.L. Solari³, D. Manara⁴, A.C. Scheinost⁶, C. Hennig⁶, D. Prieur⁶, T. Vitova⁷, K. Dardenne⁷, T. Pruessmann⁷, J. Rothe⁷

¹ CEA, DES, ISEC, DMRC, Univ. Montpellier, Marcoule, France

² CIRIMAT, UMR CNRS 5085, Univ. Toulouse III, France

³ Synchrotron SOLEIL, Gif-sur-Yvette, France

⁴ European Commission, JRC, Ispra, Italy

⁵ CEA, DES, ISAS, DPC, Université Paris Saclay, Gif-sur-Yvette, France

⁶ HZDR, Institute of Resource Ecology, Dresden, Germany

⁷ INE, KIT, Eggenstein-Leopoldshafen, Germany

In order to ensure the safety of nuclear reactors using oxide fuels, knowledge of the atomic-scale properties of $U_{1-y}M_yO_{2\pm x}$ (with $M=Pu, Am$) materials is essential. These compounds show complex chemical properties, as actinides may be present in different oxidation states. During irradiation in reactors, $UO_{2\pm x}$ and various ternary (or higher order) $U_{1-y}M_yO_{2\pm x}$ solid solutions can be encountered, such as fresh fuels ($M = Pu$), transmutation targets ($M = Np$ or Am) or irradiated fuels ($M =$ fission products, as d-transition metals and lanthanides). These materials are formed by substitution of uranium atoms (U^{4+}) with other cations, which are not necessarily in a tetravalent state. In these $U_{1-y}M_yO_{2\pm x}$ compounds, presenting mostly an ionic character, a direct connection exists between the cationic oxidation state and the oxygen stoichiometry, generally referred to as Oxygen/Metal (O/M) ratio. This is a crucial point for the safety assessment of nuclear fuels as changes in the O/M ratio can dramatically affect their thermal properties, for instance the melting point and the thermal conductivity, which determine their behaviour in reactors and safety margins.

By combining XRD, Raman microscopy, X-ray Absorption Spectroscopy (XANES, HERFD-XANES and EXAFS) in-depth study of atomic-scale properties of $U_{1-y}M_yO_{2\pm x}$ compounds can be performed. The first application of this methodology is dedicated to $U_{1-y}Am_yO_{2\pm x}$ on a wide compositional domain ($y \leq 0.70$) [1]. We provide evidences of the systematic co-existence of at least three different cations (U^{4+} , U^{5+} and Am^{3+}), even for stoichiometric compounds (O/M ratio = 2.00). For higher Am contents ($y \geq 0.50$), the presence of four cations (U^{4+} , U^{5+} , Am^{3+} and Am^{4+}) is demonstrated. Nevertheless, the fluorite structure is maintained throughout the whole composition range. Indeed, both XRD and EXAFS results show that the cationic sublattice is unaffected by the extreme multi-valence states, whereas complex defects are present in the oxygen sublattice.

The second application focuses on Pu-rich $U_{1-y}Pu_yO_{2-x}$ fuels dedicated to fast neutron reactors. In such materials, the accepted convention is a U^{4+} - Pu^{4+} configuration for stoichiometric (O/M=2.00) and the coexistence of Pu^{3+} , Pu^{4+} and U^{4+} for hypo-stoichiometric face centred cubic materials. However, our recent results clearly show a situation more similar to $U_{1-y}Am_yO_{2-x}$. Thanks to the gain in sensitivity provided by HERFD-XANES at actinide $M_{4,5}$ edges, the systematic presence of U^{5+}/Pu^{3+} , even for stoichiometric samples (O/M ratio = 2.00), is evidenced for Pu content up to 40 mol%. We observe that the relative concentration of U^{5+} and Pu^{3+} increases with the Pu content, reaching 10% for $Pu/(U+Pu) = 0.40$. One should note that the O/M ratios calculated from O/Pu, O/U and O/Am determined by HERFD-XANES are equal to the Raman [5] an XRD derived [6] values. Furthermore, the analysis of the microstructure (EPMA, μ -Raman) demonstrates that this multi-valence phenomenon cannot be attributed to the slight inhomogeneity of the samples, but to a real charge-compensation mechanism.

[1] E. Epifano et al., *Commun. Chem.* 2 (2019) 59.

[2] D. Prieur et al., *Inorg. Chem.* 50 (2011) 12437–12445.

[3] D. Prieur et al., *J. Nucl. Mater.* 434 (2013) 7–16.

[4] F. Lebreton et al., *Inorg. Chem.* 54 (2015) 9749–9760.

[5] C. Duriez et al., *J. Nucl. Mater.* 277 (2000) 143–158.

[6] L. Medyk et al., *J. Nucl. Mater.* 541 (2020) 152439.

Tc(VII) reductive immobilization by Sn(II) pre-sorbed on alumina nanoparticles

N. Mayordomo,¹ A. Rossberg,^{1,2} D. Prieur^{1,2} A. Scheinost,^{1,2} K. Kvashnina,^{1,2} K. Müller¹

¹ Helmholtz-Zentrum Dresden – Rossendorf e.V. (HZDR) Bautzner Landstraße 400 01348 Dresden (Germany).

² The Rossendorf Beamline (ROBL), 38043 Grenoble (France).

The interaction of highly mobile radioactive elements in the spent fuel with the different technical and geological barriers of a nuclear waste repository needs quantification and mechanistic understanding to allow a reliable safety assessment.

One of the most concerning mobile fission products is Tc-99. It is a long-lived radionuclide (half-life of 0.213 million years) that is expected to occur as Tc(VII) under oxidizing conditions and as Tc(IV) under reducing conditions. The anion pertechnetate (TcO_4^-) is the main species of Tc(VII) and it is known to be a highly mobile species since it barely interacts with mineral surfaces. On the contrary, TcO_2 is the main species of Tc(IV) and it is a hardly soluble solid. Therefore, the reduction of Tc(VII) to Tc(IV) limits the mobility of Tc in water and is triggered by reducing agents such as Fe(II) or Sn(II). [1] In a previous work, we have observed that pre-sorption of Fe(II) on alumina enabled the Tc(VII) reduction at the interface, even at low pH values when Tc(VII) reduction by Fe(II) was expected to be limited due to the low sorption of Fe(II) on alumina. [2] In this study we focus on the impact of Sn(II).

We have performed sorption experiments following a stepwise strategy to ensure that Tc(VII) reduction by Sn(II) occurred at the interface (heteroreduction). i) Sn(II) was sorbed on alumina, ii) the Sn(II) pre-sorbed on alumina solid was isolated and dried, iii) a solution of Tc(VII) was added to this modified alumina, and iv) the yield of Tc removal by Sn(II) pre-sorbed on alumina was analyzed. The resulting Tc-containing solid was analyzed by X-ray absorption spectroscopy (XAS) at the Rossendorf Beamline (ROBL) at the European Synchrotron Radiation Facility in Grenoble (France). Both Tc K-Edge and Sn K-Edge were recorded at 15 K.

Re-oxidation experiments were performed in samples where Tc(VII) reduction by Sn(II) was obtained by different pathways: i) Tc(VII) direct reduction by dissolved Sn(II) (homoreduction) and ii) Tc(VII) reduction by Sn(II) pre-sorbed on alumina (heteroreduction). The results show that Tc is removed from solution with a high yield (85-100% removal from solution), being maximum at pH values between 3.5 and 9.5, and minimum at pH 10. Re-oxidation studies show that Tc(IV) obtained by heteroreduction presents lower oxidation kinetics than Tc(IV) obtained by homoreduction. These results support that the presence of alumina plays an important role by preventing Tc(IV) re-oxidation.

Figure 1 shows that the spectrum of TcO_2 differs from those preliminary X-ray absorption fine structure (EXAFS) fits for the Tc-loaded samples. This indicates that Al or Sn might also interact with the resulting Tc(IV) species. Further analysis are needed to determine the exact molecular structure of Tc(IV) in the interaction.

Figure 1 shows that the spectrum of TcO_2 differs from those preliminary X-ray absorption fine structure (EXAFS) fits for the Tc-loaded samples. This indicates that Al or Sn might also interact with the resulting Tc(IV) species. Further analysis are needed to determine the exact molecular structure of Tc(IV) in the interaction.

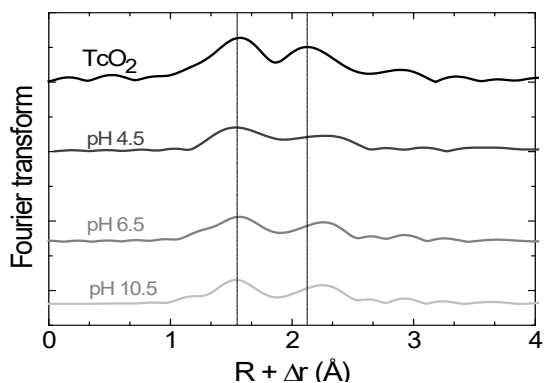


Fig. 1: Tc K-Edge EXAFS spectra (Fourier Transform) of TcO_2 and Tc-containing samples (1000 ppm) after interaction with Sn(II) pre-sorbed on alumina at different pH values.

ACKNOWLEDGEMENTS. The authors acknowledge the German Federal Ministry of Economic Affairs and Climate Action (BMWK) for the Vespa II project funding (02 E 11607B).

[1] Owunwanne, A. et al. (1977) Journal of Nuclear Medicine, 18, 822-826.

[2] Mayordomo, N. et al. (2020) Journal of Hazardous Materials, 388, 122066.

Report from the ALS: Pinpointing Actinide Bonding with Soft X-rays

S. G. Minasian¹, R. J. Abergel¹, J. Arnold¹, J. Autschbach², E. R. Batista³, J. A. Bradley³, J. Branson¹, A. S. Ditter¹, A. Gaiser¹, O. S. Gunther¹, J. Kasper³, A. A. Peterson¹, S. A. Kozimor³, W. W. Lukens¹, D.-C. Sergentu², D. K. Shuh¹, P. Yang³

¹ Lawrence Berkeley National Laboratory, Berkeley, CA 94720

² University at Buffalo, Buffalo, NY 14260

³ Los Alamos National Laboratory, Los Alamos, NM 87545

Controlling the outcome of chemical processes involving actinides requires accurate, predictive models of molecular structure and bonding. Towards this goal, recent chlorine K-edge X-ray absorption spectroscopy (XAS) studies on molecular actinide hexachlorides, $AnCl_6^{2-}$ ($An = Th$ to Am), provided direct and quantitative evidence of mixing between the 5f- and Cl 3p-orbitals [1,2]. However, because the 5f-orbitals are contracted for plutonium and overlap with ligand orbitals is small, these studies suggest that the relationship between 5f-orbital covalency and stability may be more complicated for heavier actinides such as plutonium. To understand the possible link between 5f-orbital mixing and the chemical behavior of plutonium and other actinides, we conducted F K-edge XAS and electron density mapping studies of the hexafluorides, AnF_6^{n-} ($An = Th$ to Bk , $n = 1$ or 2) Because values for the F and Cl valence orbital ionization potentials are known precisely, these comparisons provide an opportunity to control for changes in orbital energy and show if covalency is affected by overlap. However, the F K-edge (ca. 690 eV) is much lower in energy than that for Cl (ca. 2825 eV). Thus, acquiring quantitative F K-edge XAS results is complicated by weakly penetrating incident radiation that is potentially susceptible to surface contamination and saturation effects from the samples. The scanning transmission X-ray microscope (STXM) on the Advanced Light Source Molecular Environmental Science (ALS-MES) beamline 11.0.2 is ideally-suited for F K-edge XAS measurements on non-conducting molecular systems.

Although AnF_6^{n-} are structurally similar, the extent of $An-F$ bonding is anticipated to vary significantly as 5f-orbital energies and occupancies change with oxidation state and/or the identity of the actinide (Fig. 1). For example, comparisons between UF_6^{1-} ($5f^1$), NpF_6^{1-} ($5f^2$), and PuF_6^{1-} ($5f^3$), or between PuF_6^{2-} ($5f^4$), PuF_6^{1-} ($5f^3$) will show how decreasing 5f-orbital energies may result in increased An 5f and F 2p orbital mixing. To quantify the role of orbital overlap, we will compare these results with reported Cl K-edge XAS experiments on the analogous compounds, such as UCl_6^{1-} and $PuCl_6^{2-}$, among others. Interpretations of the F K-edge XAS will be facilitated by electronic structure calculations, and the percentage of F 2p character determined experimentally will be related to theoretical values determined from the Mulliken population analyses provided by electronic structure calculations with Autschbach (U. Buffalo) and Batista and Yang (LANL). Efforts to advance computational methodology for f-elements benefit greatly from these spectroscopic studies at the ALS, because the technique provides high energy resolution, feature-rich spectra while also probing interactions with both the f- and d-orbitals. This presentation will also discuss these results and technical aspects of performing actinide science at the ALS. In addition, we will describe as well as our more recent efforts to characterize a recently obtained supply of 249-Bk from Oak Ridge National Laboratory using complementary facilities at LBNL, including the Heavy Elements Research Laboratory.

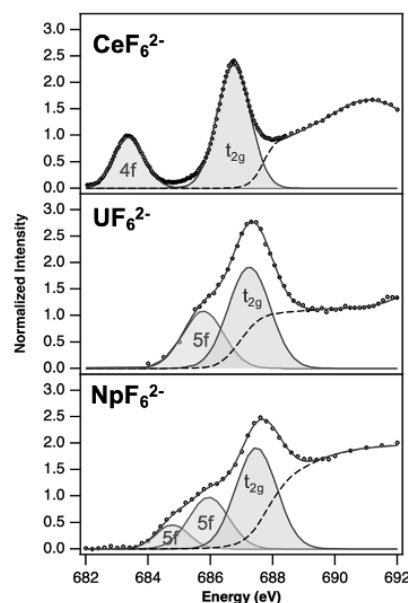


Fig 1. Fluorine K-edge STXM-XAS for MF_6^{2-} complexes where $M = Ce, U,$ and Np .

This work and the Advanced Light Source was supported by the Division of Chemical Sciences, Geosciences, and Biosciences, Office of Basic Energy Sciences, U.S. Department of Energy at LBNL (contract DE-AC02-05CH11231).

[1] Minasian, S. G. et al. (2012) *J. Am. Chem. Soc.* 134, 5586-5597

[2] Su, J. et al. (2018) *J. Am. Chem. Soc.* 140, 17977-17984

The Active Materials Laboratory and actinide research opportunities at Diamond Light Source

J.F.W. Mosselmans¹, R.E. Doull¹

¹ Diamond Light Source, Harwell campus, Didcot, Oxfordshire, U.K. OX11 0DE

The National Nuclear User Facility programme has funded the construction of an active materials laboratory (AML) for the handling of active materials at Diamond Light Source. The building, which is now operational, has been built containing dry and wet laboratories, a characterization room, and a storage room, which enables Diamond to accept samples that require secure handling.



Fig. 1: The AML Wet Laboratory showing the anaerobic Coy chamber

The AML has a range of equipment, e.g. glove-boxes, Coy chamber, 1200°C furnace, centrifuge, fume cupboards, to enable active samples to be handled and transformed chemically or physically before they are contained to be measured on one of Diamond's beamlines.

There are currently four beamlines at Diamond that are used routinely to perform X-ray spectroscopic studies on actinides. These cover a range of energies and beam sizes. Most actinide work has been done on the B18 Core XAS beamline. This has an energy range from 2.05-35 keV and is equipped with both

a 36 element Ge detector with Xspress4 electronics and a Si Drifts Vortex detector. The beamline has recently hosted a study on the sorption of strontium to uranium silicate particles [1]. The I20-scanning beamline can measure both L₃ EXAFS of dilute actinides samples using the 64 element Germanium detector with Xspress4 electronics (XANES has been collected on U samples with < 10 ppm concentration) and emission spectroscopies such as RIXS and HERFD at the L₃ edges. The current 3-crystal spectrometer will be replaced with a 14-crystal spectrometer towards the end of this year. Data from B18 and I20-scanning has been included in a study of Np and U interactions with iron minerals [2].

The I18 microfocus beamline covers the energy range 2.05 -20.5 keV. It can produce a focused beam of less than 2 x 2 micron and uses two 4-element Vortex detectors, one of which has 1 mm thick sensors. It is designed to measure heterogeneous samples using XRF, XAS and XRD. It has been used to look at Pu particles from a weapon testing site in Australia [3]. Next year a spectrometer designed for measuring the U M₄ and M₅ emission lines will become available on the beamline. The I14 beamline produces a focused X-ray beam of as small as 50 nm; it has an energy range of 5-23 keV and performs XRF, XANES mapping, XRD mapping, DPC imaging and Ptychography on suitable samples. Studies on the beamline include one on particles which originated in the Fukushima Daiichi power plant [4].

Diamond is planning for a machine upgrade in 2026/7, Diamond II; one of a suite of new beamlines will be a fast scanning XAS beamline SWIFT with an energy range of 4 -35 keV. Furthermore, Diamond now hosts a set of webpages developed by the CONEXS consortium which enables calculations in FDMNES, Orca, Quantum Espresso to be performed on Diamond clusters. The option to use the program Quanty will soon be added. The webpages help the user construct the input file while limiting the choice of options. The idea is to assist inexperienced users to use the programs and thus become more confident before starting to use more options.

[1] Neill, T.S. et. al. (2002) *Langmuir* 38, 3090-3097.

[2] Townsend, L.T. et. al. (2022) *Minerals* 12, 165.

[3] Cook, M. et. Al. (2021) *Sci. Rep.* 11, 10698.

[4] Morooka, K. et. al. (2021) *Sci. Total Environ.* 773, 145639.

Colloidal particulates in spent nuclear fuel storage: from fundamental properties to effluent treatment

Thomas S Neill^{4*}, Chris Foster^{1,2}, Samuel Shaw¹, Nick Bryan², Nicholas K Sherriff², Bruce Rigby³, Louise Natrajan⁴, Simon Kellett³, Katherine Morris¹

¹Research Centre for Radwaste Disposal and Williamson Research Centre, Department of Earth & Environmental Sciences, The University of Manchester, Oxford Road, Manchester, M13 9PL, UK

²National Nuclear Laboratory, Chadwick House, Warrington Road, Birchwood Park, Warrington, WA3 6AE, UK

³Sellafield Ltd., Hinton House, Birchwood Park Avenue, Risley, Warrington, Cheshire, WA3 6GR, UK

⁴Centre for Radiochemistry Research, Department of Chemistry, The University of Manchester, Oxford Road, Manchester, M13 9PL, UK

Colloids have the potential to mobilise radionuclides in radioactive waste decommissioning and disposal scenarios including the legacy ponds and silos complex at the Sellafield nuclear site, UK.¹ Here, we present results from investigations into U colloids under conditions relevant to Sellafield's legacy ponds and silos complex using a range of advanced analytical techniques including XAS, X-ray scattering and atomic-resolution TEM. Experimental results include both laboratory analysis of the fundamental colloidal and structural properties in U(IV) systems, exploration of U interactions with hydrotalcite colloids, and also analysis and characterisation of authentic samples taken from effluent treatment facilities on the Sellafield site. The findings underpin management of the legacy ponds and silos as well as develop the fundamental understanding of radionuclide-colloid properties and environmental mobility of actinides.

Firstly, the properties of intrinsic U(IV) colloids were investigated. Silicate was seen to have a significant role in stabilisation of colloidal U(IV), in both core-shell intrinsic U(IV)-silicate particles² and colloidal suspension of nano-UO₂ formed via corrosion of metallic uranium³. Particle size, using SAXS, TEM and ultrafiltration, and particle structure, using XAS, XRD and PDF, were investigated. In both cases, silicate enrichment on the particle surface increased colloidal stability. Intrinsic U(IV)-silicate particles had a UO₂-like core (~1 nm) surrounded by a silicate-rich U(IV)-silicate shell making up nanoparticles ~5 nm in size. HR-TEM imaging of nano-UO₂ particles exposed to silicate showed that these colloidal UO₂ particles had a silicate coating containing individual U atoms, while EXAFS indicated that the bulk particle structure did not change upon exposure to silicate. Experiments probing interactions of U(VI) aqueous species and U(IV) nanoparticles with hydrotalcite illustrated strong interactions between U and hydrotalcite. U(VI) interactions with hydrotalcite were dependent on U concentration and pH, with ternary U(VI)-carbonate sorption complexes dominating at high pH and low U(VI) loadings, confirmed by EXAFS and TRLFS.⁴ Interactions between hydrotalcite and nanoparticulate U(IV) phases were also investigated. Here, intrinsic U(IV)-silicate phases had a higher affinity for hydrotalcite than nano-UO₂ and silicate coated nano-UO₂. Ultrafiltration and TEM studies indicated that all 3 particle types investigated did interact with hydrotalcite, suggesting that hydrotalcite may be a vector for U as a 'pseudo-colloid' via sorption of solution complexes or nanoparticles.

Finally, authentic samples from a Sellafield effluent treatment facility treating effluents from the legacy ponds and silos were analysed. These samples contained stable colloidal U and Mg phases and radionuclides which were analysed by ultrafiltration, TEM and EXAFS for the first time. TEM and EXAFS measurements suggested U was present as both nano-UO₂ and U(VI)-carbonate sorption complexes. Pu L₃ edge XANES was representative of Pu(IV/V) mixed oxidation state speciation, consistent with Pu being associated with UO₂ nanoparticles at trace levels and highlighting the value in obtaining these challenging samples. Overall, these results illustrate the close relationship that U and Mg phases have in spent nuclear fuel storage. The laboratory studies closely mirror the authentic samples, and, in particular, illustrate the capability of hydrotalcite colloids to mobilise nanoparticulate U(IV) phases – a new type of 'pseudo-colloid'. This understanding is also of importance for long-term geological disposal of radioactive wastes where alkaline, reducing conditions are also expected.

[1] Z. Maher, *et al.*, *J. Nucl. Mater.* **2016**, 468, 84 [2] T. Neill, *et al.*, *Environ. Sci. Technol.* **2018**, 52, 16, 9118–9127 [3] T. Neill, *et al.*, *J. Nucl. Mater.* **2019**, 526, 151751 [4] C. Foster, *et al.*, *Langmuir* **2022**, 38, 2576-2589.

Actinide science of JAEA Beamline in SPring-8

T. Okane¹, T. Yaita¹, Y. Okamoto¹, K. Yoshii¹, S. Fujimori¹, H. Tanida¹, Y. Takeda¹, T. Kobayashi¹

¹ Japan Atomic Energy Agency, 1-1-1 Kouto Sayo-cyo, Sayo-gun, Hyogo 679-5148, Japan

Japan Atomic Energy Agency (JAEA) operates two beamlines with different energy ranges, i.e., hard X-ray and soft X-ray ranges, at the synchrotron radiation facility SPring-8. Both beamlines are installed in Radioisotope Laboratory (RI Lab.), which is specialized for measurements of radioactive materials, and JAEA is promoting actinide science combined with advanced experimental techniques using synchrotron radiation there.

In BL22XU ($E = 4 \sim 70$ keV), four experimental equipments, i.e., hard X-ray photoelectron spectroscopy (HAXPES) system, X-ray absorption fine structure (XAFS) measurement system, residual-stress measurement system, and diffractometer with a κ -type goniometer, are aligned tandem in the experimental hutch at RI Lab. For HAXPES and XAFS, microbeams with a spot size of submicron diameter, focused by using Kircpatrick-Baez (KB) mirrors, are available. The XAFS system (Fig. 1) is capable of obtaining extended XAFS (EXAFS) spectra in about 10 s by using a fast scanning monochromator, and has recently succeeded in measuring small amounts of Zr oxide molten salt at high temperatures up to 3500 K by using a pulse-heating furnace. We plan to advance this measurement to a mock-up experiment, which is useful for clarifying the progress scenarios of the Fukushima Dai-ichi Nuclear Power Plant accident.

BL23SU ($E = 0.37 \sim 1.8$ keV) is equipped with Angle-resolved photoelectron spectroscopy (ARPES) system, X-ray magnetic circular dichroism (XMCD) measurement system, scanning transmission X-ray microscopy (STXM) in RI Lab., while a photoelectron spectrometer for in-situ observation of surface reaction dynamics is installed at the conventional experimental hall where radioactive materials cannot be handled. ARPES and XMCD are used to study the superconductivity and magnetism of uranium compounds and related materials. Recently-installed STXM system has achieved a spatial resolution of ~ 60 nm, and is expected to be applied to a chemical analysis of various complicated materials, including materials related to nuclear power plants.

In order to contribute the decommissioning of Fukushima Dai-ichi Nuclear Power Plant (1F), JAEA plans to analyze the chemical properties of fuel debris from 1F at the JAEA beamlines in SPring-8. The application process to the Nuclear Regulation Authority of Japan for permission of using spent fuel at SPring-8 is now proceeding, and it is expected that we can pursue measurements for fuel debris from 1F at SPring-8 in the latter half of 2022. As a preparation for the analysis of fuel debris from 1F, we have performed micro X-ray fluorescence imaging, XAFS, and X-ray microtomography [1] for imitated fuel debris at BL22XU.

JAEA participates in “Advanced Research infrastructure for Materials and Nanotechnology in Japan” [2], which is the project of the Ministry of Education, Culture, Sports, Science and Technology (MEXT) of Japan. In this project, JAEA belongs to the research area of innovative energy conversion materials, and is planning especially to promote research for effective utilization of radiation from radioactive waste as energy. This project also aims to develop a system for data sharing to promote materials informatics.

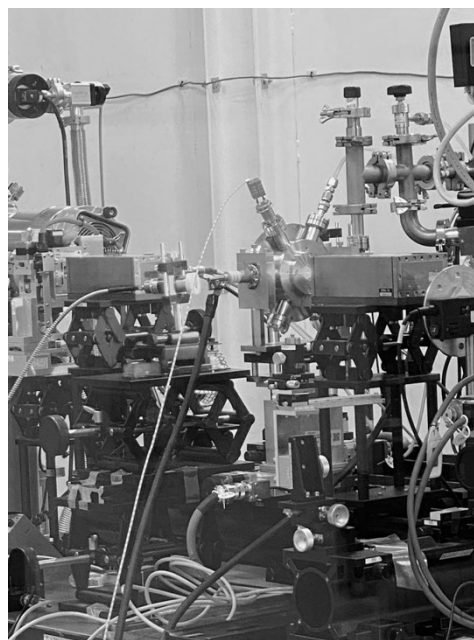


Fig. 1: XAFS measurement system at BL22XU, equipped with a pulse-heating furnace.

[1] Kitagaki, T., Yoshida, K., Liu, P. and Shobu, T. (2022) npj Materials Degradation 6, 13.

[2] <https://nanonet.mext.go.jp/page/dir000011.html>

Relativistic Multiconfigurational Ab Initio Calculation of XANES spectra and RIXS maps of radionuclide compounds

R. Polly,¹ K. Dardenne,¹ S. Duckworth,¹ X. Gaona,¹ J. Rothe,¹ D. Fellhauer,¹ M. Altmaier,¹ T. Neill,² B. Schacherl,¹ T. Vitova,¹ F. Weigend,³ H. Geckeis¹

¹ Institute of Nuclear Waste Disposal (INE), Karlsruhe Institute of Technology, Kaiserstraße 12, 76131 Karlsruhe, Germany

² Research Centre for Radwaste Disposal and Williamson Research Centre, School of Earth & Environmental Sciences, The University of Manchester, Manchester M13 9PL, U.K.

³ Department of Chemistry, Philipps University Marburg, Hans-Meerwein-Str. 4, 35043 Marburg, Germany.

X-Ray Absorption Near Edge Structure (XANES) spectroscopy and Resonant Inelastic X-ray Scattering (RIXS), combined with relativistic multiconfigurational ab initio Wave Function Theory (WFT) calculations including spin-orbit (SO) interactions, are a preferred combination of experimental and theoretical tools to explore the electronic structure of radionuclide compounds in different chemical environments (see e.g. [1-3]). We employed the RASSCF/RASPT2 methods with ANO-VTZ/VQZ basis sets and included Spin-orbit interaction via a mean-field SO operator using RASSI as available in OpenMolcas. We apply this powerful theoretical method to different systems to address open unresolved questions:

- (1) Tc L₃-Edge XANES of Tc(IV)-Gluconate complexes,
- (2) 3d4f RIXS map of Uranyl UO₂²⁺,
- (3) Cl K-edge XANES of [UO₂Cl₄]²⁻,
- (4) M_{4,5} XANES spectra of Np(VI)O₂²⁺ and Np(V)O₂⁺ and 3d4f RIXS map of Neptunyl Np(V)O₂⁺.

- (1) Tc L₃-Edge XANES of Tc(IV)-Gluconate complexes: recently we found a considerable change of the Tc L₃-Edge XANES from solid Tc(IV)O₂ to Tc(IV)-Gluconate complexes [1]. With the help of new accurate multiconfigurational calculations we could completely understand the reason for this change in the XANES spectra.
- (2) 3d4f RIXS map of Uranyl UO₂²⁺ [2]: The excellent agreement between our theoretical data and the measurements shows that the approach using the RASSCF/ RASPT2 methods followed by the inclusion of SO coupling is applicable to the accurate calculation of An M_{4,5} HR-XANES (in agreement with Sergentu et al. [3]) and 3d4f RIXS maps and reproduces the multiplet structure of the uranyl spectra faithfully. We show that the multiconfigurational protocol, which is nowadays applied as a standard tool to study the X-ray spectra of transition metal complexes, can be extended to the calculations of RIXS maps of An compounds. With this theoretical data we are able to provide a full assignment and understanding of the experimental data [4].
- (3) Cl K-edge XANES of [UO₂Cl₄]²⁻: the results of the calculations provide detailed information about the 5f and 6d contributions to metal-ligand bonds.
- (4) M_{4,5} XANES spectra of Np(VI)O₂²⁺ and Np(V)O₂⁺ and 3d4f RIXS map of Neptunyl Np(V)O₂⁺ we show the first results for these systems which are theoretical considerably more challenging due to the additional 5f¹ and 5f² occupation of the 5f shell.

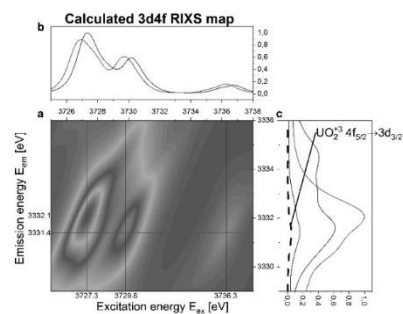


Figure 1: RASPT2 calculated 3d4f RIXS map of uranyl

This work is in part supported by the ERC Consolidator Grant 2020 under the European Union's Horizon 2020 research and innovation programme (grant agreement No. 101003292)

[1] K. Dardenne *et al.*, *Inorg. Chem.* 2021, 60, 16, 12285–12298.

[2] R. Polly *et al.*, *Inorg. Chem.* 2021, 60, 24, 18764–18776.

[3] D.-C. Sergentu *et al.*, *J. Phys. Chem. Lett.* 2018, 9, 18, 5583–5591.

[4] T. Vitova *et al.*, *Nat. Commun.* 2017, 8, 1–9.

Investigation on the Structural Incorporation of Dopants into the Uranium Oxide Structure

S. K. Potts¹, P. Kegler¹, G. Modolo¹, K. Dardenne², T. Prüßmann², J. Rothe², S. Hammerich³, I. Niemeyer¹, D. Bosbach¹, S. Neumeier¹

¹ Forschungszentrum Jülich GmbH, Institute of Energy and Climate Research – Nuclear Waste Management (IEK-6), 52428 Jülich, Germany

² Karlsruhe Institute of Technology, Institute for Nuclear Waste Disposal, 76021 Karlsruhe, Germany

³ Heidelberg University, Institute of Earth Sciences, 69120 Heidelberg, Germany

In the safeguards laboratories of Forschungszentrum Jülich an aerosol-based process for the production of microparticulate uranium oxide reference materials has been developed and implemented in order to support a sustainably robust quality control system of the International Atomic Energy Agency (IAEA) in particle analysis in nuclear safeguards [1]. This quality control system includes analytical instrument calibration, method validation as well as method development of analytical measurements of individual micrometer- and submicrometer particles. The well-designed microparticulate reference materials developed for this purpose must fulfill certain requirements, such as a precisely defined elemental and isotopic composition, size, morphology, and shelf-life, to ensure the reliability of the mass spectrometric analytical measurements. To enhance the mass spectrometric analytical measurements to even detect small amounts of fission products (e.g., lanthanides), the microparticulate reference materials must be refined. First attempts were made to synthesize Nd-mixed uranium oxide microparticles. But due to the yield limitations in the μg range, the characterization of these materials is challenging. Therefore, to unravel the incorporation mechanism of the dopants, such as lanthanides, Th, or Pu, into the uranium oxide structure, a co-precipitation method was adjusted to produce mixed bulk-scale materials [2]. Using TG-DSC measurements, the temperature range of the phase transition from UO_3 to U_3O_8 of the doped uranium-containing materials could be determined. According to the previously identified temperature ranges, the doped materials were calcined and characterized. For this purpose, methods for investigating long range order phenomena, e.g., XRD, as well as methods for investigating short range order phenomena such as Raman, IR, XAS were used. It could be observed that the phase transition from UO_3 to U_3O_8 of the undoped material forms orthorhombic U_3O_8 similar to the observations in the literature [3]. However, the lanthanide-doped materials show the formation of hexagonal U_3O_8 , which according to the literature only occurs for the pure U_3O_8 at temperatures above 350 °C. No segregated lanthanide-rich phases could be detected with XRD and Raman [4]. Various spectroscopic methods were used to investigate the incorporation of the lanthanides in the short-range order, *i.a.*, via XANES. Figure 1 shows a comparison of the vertically shifted U L3-XANES spectra of the doped materials. The XANES spectra of the doped materials are very similar to the U_3O_8 spectrum. The marginal shift of the white line of the doped U_3O_8 to higher energies

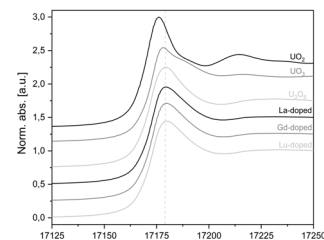


Fig. 1: XANES spectra of La-, Gd-, Lu-doped U_3O_8 samples and references (U_3O_8 , UO_3 , UO_2).

Tab. 1: Energy values of the white line position of U_3O_8 and doped U_3O_8 .

Sample	White line position
U_3O_8	17,179.0 eV
La-doped U_3O_8	17,179.4 eV
Gd-doped U_3O_8	17,179.7 eV
Lu-doped U_3O_8	17,179.8 eV

compared to the undoped U_3O_8 could indicate a shift in the uranium oxidation state to higher values than the average valence of 5.33 (for undoped U_3O_8). This presentation shows results related to the incorporation of lanthanides and Th into the uranium oxide structures and the phase transformation from orthorhombic U_3O_8 to hexagonal U_3O_8 crystal structure using state-of-the-art analytical methods (XRD, IR, Raman) and synchrotron methods.

[1] R. Middendorp, M. Durr, A. Knott, F. Pointurier, D. Ferreira Sanchez, V. Samson, D. Grolimund, *Anal. Chem.* 89, 4721-4728 (2017).

[2] P. Kegler, M. Klinkenberg, A. Bukaemskiy, G. L. Murphy, G. Deissmann, F. Brandt, D. Bosbach, *Materials* 14, 6160 (2021).

[3] R. Ackermann, A. Chang, C. A. Sorrell, *J. Inorg. Nucl. Chem.* 39, 75-85 (1977).

[4] S. K. Potts, P. Kegler, G. Modolo, S. Hammerich, I. Niemeyer, D. Bosbach, S. Neumeier, *MRS Adv.* 7, 128-133 (2022).

ROBL-II at ESRF: a synchrotron toolbox for actinide research

D. Prieur,^{1,2} J. Exner,^{1,2} C. Hennig,^{1,2} K. O. Kvashnina,^{1,2} D. Naudet,^{1,2}
 A. Rossberg,^{1,2} V. Svitlyk,^{1,2} T. Stumpf² A. C. Scheinost,^{1,2}

¹ The Rossendorf Beamline (BM20), European Synchrotron Radiation Facility, 71 Avenue des Martyrs, 38043 Grenoble, France

² Institute of Resource Ecology, Helmholtz Zentrum Dresden Rossendorf, Bautzner Landstrasse 400, 01328 Dresden, Germany

The Rossendorf Beamline has been operated at the ESRF since 1996 by Helmholtz-Zentrum Dresden-Rossendorf (HZDR) [1-3] and has been redesigned in 2016–2020 (ROBL-II) [4]. Embedded within the Helmholtz Association’s program on nuclear safety, ROBL-II is dedicated to research on actinides and other elements with no stable isotopes (Tc, Po, Ra) (Table 1).

ROBL-II provides four different experimental stations to investigate actinide and other alpha- and beta-emitting radionuclides at the new EBS storage ring of ESRF within an energy range of 3 to 35 keV.

The XAFS station consists of a highly automatized, high sample throughput installation in a glovebox, to measure EXAFS and conventional XANES of samples routinely at temperatures down to 10 K, and with a detection limit in the sub-p.p.m. range.

The XES station with its five bent-crystal analyzer, Johann-type setup with Rowland circles of 1.0 and 0.5 m radii provides high-energy resolution fluorescence detection (HERFD) for XANES, XES, and RIXS measurements, covering both actinide *L* and *M* edges together with other elements accessible in the 3 to 20 keV energy range.

The six-circle heavy duty goniometer of XRD-1 is equipped for both high-resolution powder diffraction as well as surface-sensitive diffraction techniques. Single crystal diffraction, powder diffraction with high temporal resolution, as well as high-pressure diffraction experiments can be performed at a Pilatus 2M detector stage (XRD-2). Elaborate radioprotection features enable a safe and easy exchange of samples between the four different stations to allow the combination of several methods for an unprecedented level of information on radioactive samples for both fundamental and applied actinide and environmental research.

Table 1 : Typical radionuclides and their radioprotection-relevant parameters, including their maximum amount not to exceed the 185 MBq limit for both solids and liquids under RAD-2 condition (sample in under-pressurized glovebox during measurements).

Nuclide (decay)	Half-life (years)	Specific activity (Bq mg ⁻¹)	Exemption limit (Bq)	Maximum amount (mg)
Tc-99 (β^-)	2.1×10^5	6.4×10^5	1.0×10^7	2.9×10^1
Po-209 (α)	1.0×10^2	6.2×10^8	1.0×10^4	3.0×10^{-1}
Ra-226 (α)	1.6×10^3	3.7×10^7	1.0×10^4	5.0×10^0
Th-nat (α)	1.4×10^{10}	8.2×10^0	1.0×10^4	2.3×10^7
Pa-231 (α)	3.3×10^4	1.7×10^6	1.0×10^3	1.1×10^2
U-nat (α)	4.5×10^9	2.6×10^1	1.0×10^4	7.1×10^6
Np-237 (α)	2.1×10^6	2.6×10^4	1.0×10^3	7.1×10^3
Pu-239 (α)	2.4×10^4	2.3×10^6	1.0×10^4	8.0×10^1
Pu-242 (α)	3.7×10^5	1.5×10^5	1.0×10^4	1.2×10^3
Am-243 (α)	7.4×10^3	7.4×10^6	1.0×10^3	2.5×10^1
Cm-246 (α)	4.8×10^3	1.1×10^7	1.0×10^3	1.7×10^1
Cm-248 (α)	3.4×10^5	1.6×10^5	1.0×10^3	1.2×10^3
Bk-247 (α)	1.4×10^3	3.8×10^7	1.0×10^4	4.9×10^0
Cf-251 (α)	9.0×10^2	5.8×10^7	1.0×10^3	3.2×10^0

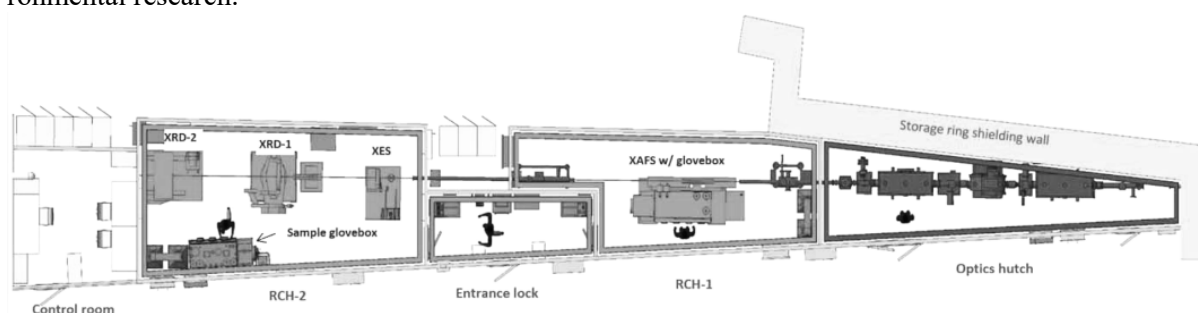


Fig. 1: Layout of ROBL-II, showing from right to left the X-ray Optics hut, the two experimental hutches (RCH-1 and RCH-2) connected by a common entrance lock room, and the control room. RCH-1 houses the XAFS experiment, RCH-2 a five-crystal spectrometer (XES), a six-circle goniometer for powder and surface diffraction (XRD-1), and a Pilatus 2M diffractometer (XRD-2).

- [1] Nitsche, H. (1995). *J. Alloys Compd.* 223, 274–279.
 [2] Matz et al. (1999). *J. Synchrotron Rad.* 6, 1076–1085.
 [3] Reich et al. (2000). *Radiochim. Acta*, 88, 633–637.
 [4] Scheinost et al. (2021). *J. Synchrotron Rad.* 28, 333–349.

Retention of Tc and Se on Fe-bearing clay minerals

Y.Qian^{1,2}, A.C. Scheinost^{3,4}, M. Marques¹

¹ Laboratory for Waste Management, Paul Scherrer Institut, Switzerland

² Institute for Geological Sciences, University of Bern, Switzerland

³ The Rossendorf Beamline at the European Synchrotron Radiation Facility (ESRF), France

⁴ Helmholtz Zentrum Dresden Rossendorf, Institute of Resource Ecology, Germany

The migration of (radio-)contaminants in deep geological repository is essentially controlled by geochemical factors such as mineralogical and chemical composition of the environment, pH, redox potential (Eh), solubility, biological (microbial) interactions and (redox) reaction kinetics. Clay minerals, as a major mineralogical component, play a key role in the retardation of contaminants in the multi barrier concept of a deep geological disposal for radioactive waste. In particular iron containing clay minerals might be able to affect the mobility and (bio)availability of redox sensitive elements by changing their oxidation state. Depending on the amount and location of redox active Fe, iron bearing clays might cover a large range of reducing potentials [1]. ⁹⁹Tc is one of the redox sensitive fission products with a long half-life (2.1×10^5 years) and high toxicity. Tc in its most oxidized heptavalent anionic form (TcO_4^-) is highly mobile, whereas it easily precipitates as rather insoluble $\text{TcO}_2 \cdot n\text{H}_2\text{O}$ -like species in its most reduced (in water), tetravalent oxidation state, thereby strongly retarding Tc groundwater migration. Se is of relevance since its stable isotope has only a very narrow concentration range between human deficiency and toxicity; furthermore, its radioisotope ⁷⁹Se is a potential risk driver for nuclear waste repositories. Se is considered as very immobile due to the low solubility of the predominant species Se^{II} and Se^0 under anoxic conditions, whereas Se^{VI} (as selenate (SeO_4^{2-})) and Se^{IV} (as selenite (SeO_3^{2-})) are much more mobile in oxic environments. Therefore, the interfacial reduction of Tc and Se have been proposed as a feasible remediation technology for radionuclides retention in repository.

Here, we will systematically address the retention of Tc^{VII} and Se^{IV} by $\text{Fe}^{\text{II}}/\text{Fe}^{\text{III}}$ containing clay minerals. We perform Tc and Se sorption experiments on native and reduced smectite clay samples with different $\text{Fe}^{\text{II}}/\text{Fe}^{\text{III}}$ ratios. The $\text{Fe}^{\text{II}}/\text{Fe}^{\text{III}}$ ratio and its local coordination in the clay mineral structure are determined by both Mössbauer and Fe K-edge XAFS spectroscopy. The reduced species after sorption experiments are identified by Tc and Se K-edge XANES and EXAFS. Reduction of Tc^{VII} to Tc^{IV} by Fe-bearing minerals has been observed, mainly forming $\text{TcO}_2 \cdot n\text{H}_2\text{O}$ surface precipitates [2,3]. Reductive precipitation of Se^{IV} to nanoparticulate Se^0 was observed when dissolved Fe^{II} is sorbed onto synthetic montmorillonite [4]. Most of these studies, however, were carried out at rather high Tc and Se loadings. The focus of our study is on low Tc and Se loadings, which are more environmentally relevant. By identifying the reduced surface products at low loading, we expect to have a better understanding of the geochemical redox reaction between Fe and Tc and Se, thus contribute to a more reliable prediction of Tc and Se retention in radioactive waste repositories.

-
- [1] Gorski, C.A., et al. (2013) Redox properties of structural Fe in clay minerals: 3. Relationships between smectite redox and structural properties. *Environ Sci Technol.*, **47**(23): p. 13477-85.
- [2] Jaisi, D.P., et al. (2009) Reduction and long-term immobilization of technetium by Fe(II) associated with clay mineral nontronite. *Chemical Geology*, **264**(1): p. 127-138.
- [3] Peretyazhko, T., et al. (2008) Heterogeneous reduction of Tc(VII) by Fe(II) at the solid–water interface. *Geochimica et Cosmochimica Acta.*, **72**(6): p. 1521-1539
- [4] Charlet, L., et al. (2007) Electron transfer at the mineral/water interface: Selenium reduction by ferrous iron sorbed on clay. *Geochimica et Cosmochimica Acta*, **71**(23): p. 5731–5749.

Electronic structure and bonding properties of U⁶⁺ by high-resolution X-ray spectroscopy and computations

H. Ramanantoanina,¹ T. Neil,² N. Müller,¹ B. Schacherl,¹ T. Prüssmann,¹ D. Hauschild,^{1,3} R. Steininger,¹ C. Heske,^{1,3} L. Weinhardt,^{1,3} M. Haverkort,⁴ T. Vitova¹

¹ Karlsruhe Institut für Technologie (KIT), DE-76344 Eggenstein-Leopoldshafen, Germany.

² University of Manchester, United Kingdom

³ University of Nevada Las Vegas (UNLV), 4505 Maryland Pkwy, Las Vegas, NV 89154, U.S.A.

⁴ University of Heidelberg, Philosophenweg 19, DE-69120 Heidelberg, Germany

Understanding the chemistry of actinide compounds is crucial in many fields including medical research, energy, and radioactive materials disposal, and accordingly a number of in-depth studies have been conducted. [1] However, the electronic structures and bonding properties of actinides have not been studied as deeply as those for lanthanides or transition metals. In this work, we describe the use of high-energy resolution X-ray absorption/emission spectroscopy (HR-XAS and HR-XES, respectively) and resonant inelastic X-ray scattering (RIXS) techniques to probe the local atomic and electronic structures of the molecular [(UO₂)F₅]³⁻, [(UO₂)Cl₄]²⁻, and [(UO₂)Br₄]²⁻ complexes. In addition, we also detail the methodological approach for predicting the ligand K-edge high-energy resolution XANES, and U M_{4,5}-edge core-to-core/valence band RIXS by means of first principles density-functional theory (DFT) calculations by using a time-dependent formalism and multiplet calculations, respectively, at the relativistic level (4-component Dirac Hamiltonian). [2] By comparing the theoretical and experimental spectra, our study also provides insight into the roles of the uranium 5*f* and 6*d* orbitals for the metal-ligand bonding as a function of the equatorial ligand (fluoride, chloride, and bromide). The X-ray spectroscopic experiments were performed at the Karlsruhe Research Accelerator (KARA) Light Source (Karlsruhe, Germany). The U M₄-edge and Br K-edge high energy resolution X-ray absorption emission and resonant inelastic X-ray scattering data were recorded at the ACT station of the CAT-ACT beamline, [3a] the Cl K-edge XANES at the INE-Beamline, [3b] and the F K-edge XANES at the X-SPEC beamline. [3c] This work is supported by the ERC Consolidator grant “the Actinide Bond” (N^o 101003292) under the European Union’s Horizon 2020 research and innovation program.

-
- [1] (a) Tobin, J.G.; Ramanantoanina, H.; Daul, C.; Poussel, P.; Yu, S.-W.; Nowak, S.; Alonso-Mori, R.; Kroll, T.; Nordlund, D.; Weng, T.-C.; Sokaras, D.; *Phys. Rev. B*, **2022**, *105*, 125129; (b) Ramanantoanina, H.; Kuri, G.; Martin, M.; Bertsch, J.; *Phys. Chem. Chem. Phys.*, **2019**, *21*, 7789; (c) Vitova, T.; Pidchenko, I.; Fellhauer, D.; Bagus, P.S.; Joly, Y.; Pruessmann, T.; Bahl, S.; Gonzalez-Robles, E.; Rothe, J.; Altmaier, M.; Denecke, M.A.; Geckeis, H.; *Nature Communications*, **2017**, *8*, 16053.
- [2] (a) Bagus, P.S.; Schacherl, B.; Vitova, T.; *Inorg. Chem.*, **2021**, *60*, 16090; (b) Polly, R.; Schacherl, B.; Rothe, J.; Vitova, T.; *Inorg. Chem.*, **2021**, *60*, 18764; (c) Vitova, T.; Pidchenko, I.; Biswas, S.; Beridze, G.; Dunne, P.Q.; Schild, D.; Wang, Z.; Kowalski, P.M.; Baker, R.J.; *Inorg. Chem.*, **2018**, *57*, 1735.
- [3] (a) Zimina, A.; Dardenne, K.; Denecke, M.A.; Grundwaldt, J.D.; Huttel, E.; Lichtenberg, H.; Mangold, S.; Pruessmann, T.; Rothe, J.; Steininger, R.; Vitova, T.; *J. Phys.: Conference Series*, **2016**, *712*, 012019; (b) Rothe, J.; Butorin, S.; Dardenne, K.; Denecke, M.A.; Kienzler, B.; Löble, M.; Metz, V.; Seibert, A.; Steppert, M.; Vitova, T.; Geckeis, H.; *Review of Scientific Instruments*, **2012**, *83*, 043105; (c) Weinhardt, L.; Steininger, R.; Kreikemeyer-Lorenzo, D.; Mangold, S.; Hauschild, D.; Batchelor, D.; Spangenberg, T.; Heske, C.; *J. Synchrotron Radiation*, **2021**, *28*, 609.

Investigation of complexation and redox reactions of actinides using CE-ICP-MS

T. Reich

Johannes Gutenberg University Mainz, Department of Chemistry, TRIGA Site, 55128 Mainz, Germany

The coupling of capillary electrophoresis (CE) with inductively coupled plasma mass spectrometry (ICP-MS) is a powerful experimental tool for studying the speciation of actinides at environmentally relevant concentrations. CE-ICP-MS benefits from the high separation capability of CE in combination with the possibility of multielement analysis at trace concentrations using ICP-MS. This presentation will highlight several applications of CE-ICP-MS for studying complexation and redox reactions of actinides.

The electrophoretic mobilities (μ_e) of the actinides Th, U, Np, Pu, and Am in different oxidation states have been determined by CE-ICP-MS at concentrations of 1×10^{-7} M in 1 M HClO₄ [1]. For the actinides U–Pu, the μ_e follow the order An(III) > An(VI) > An(V) > An(IV). The observed systematic trends in the μ_e values have been rationalized by speciation calculations and corresponding averaged effective charges of the actinides in the background electrolyte.

CE-ICP-MS was used to determine the stability constants of the acetate complexation of Am(III), Th(IV), Np(V), and U(VI) [2]. It was possible to investigate these actinides simultaneously at concentrations in the range of 5×10^{-8} M to 1×10^{-6} M. The stability constants that were extrapolated to zero ionic strength agree with the available literature data obtained at higher actinide concentrations. For U(VI) and Am(III) three successive acetate complexes were observed and for Th(IV) up to five. In contrast to literature data, only the formation of a 1:1 complex of Np(V) with acetate could be confirmed. The formation of a negatively charged Np(V) complex with more than one acetate ligand could be ruled out.

The investigation of the reaction of 5×10^{-5} Np(V) by hydroxylamine hydrochloride (HAHCl) in 1 M HCl in the temperature range from 30–70° C shows that CE-ICP-MS can be used to investigate redox processes of Np in aqueous solutions [3]. The reduction of Np(V) to Np(IV) was found to have a (pseudo)first order kinetics with respect to HAHCl. The activation energy equaled (72 ± 10) kJ/mol.

This presentation will conclude with a short outlook on future CE-ICP-MS studies of actinides in connection with the long-term safety analysis for future nuclear waste repositories.

[1] Willberger, C., Amayri, S., Häußler, V., Scholze, R., Reich, T. (2019) *Anal. Chem.* 91, 11537-11543.

[2] Willberger, C., Leichtfuß, D., Amayri, S., Reich, T. (2019) *Inorg. Chem.* 58, 4851-4858.

[3] Willberger, C., Amayri, S., Reich, T. (2018) *Electrophoresis* 39, 3013-3021.

Approaches to groundwater radionuclide remediation at Sellafield - in situ phosphate mineralisation

C. Robinson¹, S. Shaw¹, J.R. Lloyd¹, J. Graham² and K. Morris¹

¹ Research Centre for Radwaste Disposal, Department of Earth and Environmental Sciences, University of Manchester, Manchester, M13 9PL, UK

² National Nuclear Laboratory, Chadwick House, Birchwood Park, Warrington, Cheshire, WA3 6AE

Globally, nuclear fuel cycle activities over the last 70+ years have led to discharges of radionuclides to the sub-surface at key nuclear mega sites such as Hanford, USA and Sellafield UK leading to a significant legacy of radioactively contaminated land. Typically, contamination plumes contain co-contaminants including uranium and strontium-90 (⁹⁰Sr). Of these, Sr-90 is one of the more challenging radionuclides due to its relatively high mobility in the sub-surface. Developing remediation strategies for ⁹⁰Sr and U is therefore important in maintaining the stewardship of these complex sites in the medium to long term. Calcium phosphate minerals such as hydroxyapatite (HAp) have been suggested as promising radionuclide (including ⁹⁰Sr and U) sinks, as they can incorporate a range of radionuclides within their structure. The formation of HAp can be achieved in situ through both biotic and abiotic approaches. In previous studies conducted at the Hanford nuclear site, USA, aqueous injection of HAp-generating solutions have reduced the amount of mobile ⁹⁰Sr within contaminated groundwater on both laboratory and field scales [1].

In this study, focussed on the Sellafield facility in the North West of England, biotic (calcium citrate / sodium phosphate, glycerol phosphate) and abiotic (polyphosphate) phosphate amendments were tested using sediment microcosm experiments with the aim of developing a targeted remediation toolkit for ⁹⁰Sr and U remediation at Sellafield [2,3]. For both the U and Sr microcosms, aqueous geochemical results suggest the addition of phosphate generating amendments enhanced Sr and U removal from solution when compared to the sediment sorption controls. After treatment with calcium citrate / sodium phosphate and glycerol phosphate amendments U microcosm sediment endpoints were taken for U L_{III} x-ray absorption near edge structure (XANES) extended x-ray absorption fine structure (EXAFS) analysis. XANES identified the U was present as U(VI), with analysis of the EXAFS region showing evidence for a shell at ~3Å, suggesting that the U was present as a non-crystalline U(VI) phosphate, likely of the autunite group. For the Sr microcosm endpoints scanning electron microscopy in conjunction with energy dispersive x-ray spectroscopy was conducted on sediments after treatment with calcium citrate / sodium phosphate and glycerol phosphate amendments and showed the presence of Sr containing calcium phosphate phases deposited on the surface of larger sediment grains. Sequential leaching of these sediment endpoints suggested that some of this Sr may have become incorporated into these calcium phosphate phases. Finally, Sr K-edge EXAFS analysis was conducted on these treated sediments and a sorption control. For the sorption control sediment, fitting of the EXAFS data was achieved with a single shell of backscatterers containing nine oxygens, consistent with outer sphere sorption to sediment media [4]. However, shell-by-shell fitting of the treated sediments was best achieved using fitting parameters consistent with partial Sr incorporation into hydroxyapatite [5,6]. Here, statistically relevant P and Ca shells were used in the fit, confirming that some incorporation had occurred. The precipitation of these calcium phosphate phases and formation of U and Sr phosphates confirmed by XAS, demonstrates the potential for these techniques to provide a toolkit for remediation at nuclear sites.

-
- [1] Vermeul, V. R. et al. (2014) *Groundw. Monit. Remediat.* 34 (2), 28–41.
 - [2] Newsome, L et al (2015) *Environ. Sci. Technol.* 49 (18), 11070–11078.
 - [3] Szecsody, J. et al (2012) U.S. Department of Energy
 - [4] Wallace, S. H. et al (2012) *Appl. Geochemistry* 27 (8), 1482–1491
 - [5] Handley-Sidhu, S. et al (2011) *Biotechnol. Lett.* 33 (1), 79–87.
 - [6] Cleary, A. et al (2019) *Chem. Geol.* 509, 213–222.

Describing Radioactive Actinyl Cations in Water by Combining EXAFS + Molecular Dynamics

E. Sánchez Marcos,¹ G.Raposo-Hernández,¹ J.M.Martínez,¹ R.R.Pappalardo,¹ Ch. Den Auwer²

¹ Department of Physical Chemistry, University of Seville, 41012-Seville, Spain

² Université Côte d'Azur, CNRS, ICN, 06108 Nice, France

In this communication we present recent results on the physicochemical properties of the monovalent actinyl cations, PuO_2^+ and NpO_2^+ , species involved in the treatment of waste nuclear fuel and its recycling. Due to their chemical stability, their hazardous management and low concentrations, their physicochemical characterization is poor. Structural characterization of actinyl cations in water has been performed by both experimental and theoretical techniques. The experimental technique employed is the X-ray absorption spectroscopy (XAS), in particular the extended X-ray absorption fine structure (EXAFS).[1] This technique supplies short-range structural information around an specific atom, the absorbing atom, with a structural precision of one hundredth of angstrom for the first coordination shell distance and one unit in the coordination number.[2] From theoretical techniques, quantum-mechanical and computer simulations have also provided valuable information. The combination of XAS spectroscopy and MD simulations has been revealed as a useful strategy[3] to refine the structural properties of solutions where the standard fitting of the experimental spectra is clouded by different factors such as low concentrations, spectroscopical phenomena as multi-excitations or low signal/noise ratio. The good reproduction of an experimental spectrum by means of the use of the structural information derived from a statistical simulation has a double consequence.[4] On one hand, it allows the access to a direct EXAFS-structure assignment provided by the atomistic picture of the statistical trajectory. On the other hand, the agreement shows the ability of the interaction potentials employed in the statistical simulation when using classical force fields or the quantum-mechanical level in AIMD simulations to describe properly the system.

A specific set of cation-water intermolecular potentials based on ab initio potential energy surfaces has been built. Given the paramagnetic character of these actinyls, the cation-water interaction energies were computed from highly correlated wavefunctions using the NEVPT2 method. NVT and NPT MD simulations have been conducted. The TIP4P water model was adopted. Several structural, dynamical, and energetic properties of the aqueous solutions have been obtained and analysed. Experimental EXAFS spectra from dilute aqueous solutions of PuO_2^+ and NpO_2^+ , have been revisited and analysed, assuming tetra- and penta-hydration of the actinyl cations. Simulated EXAFS spectra have been computed from the snapshots of the MD simulations. (Figure 1 shows the PuO_2^+ case) A good agreement with the experimental information available is found. The global analysis leads us to conclude that monovalent actinyl cations in water are stable pentahydrated aqua ion. The comparison with other parent divalent cations shows the importance of dynamical and non-dynamical electron correlation in the interaction potential building. [6]

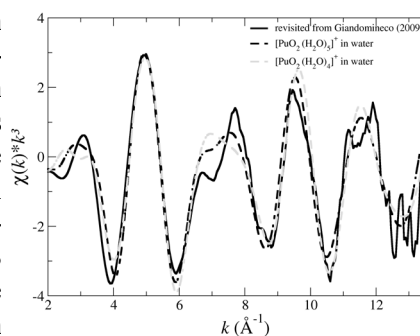


Figure 1: Comparison of Plutonyl(V) in water EXAFS spectra: simulated assuming CN=4

[1] M.A.Denecke, *Coord.Chem.Rev.*, 2006, 250, 730.

[2] K.E. Knope and L. Soderholm, *Chem. Rev.*, 2013, 113, 944.

[3] P.J.Merkling, A. Muñoz-Páez and E. Sánchez Marcos, *J. Am. Chem. Soc.*, 2002, 124, 10911.

[4] S.Pérez-Conesa, J.M.Martínez, R.R.Pappalardo and E. Sánchez Marcos, *Inorg.Chem.*, 2018, 57, 8089.

[5] S.Pérez-Conesa, J.M.Martínez, R.R.Pappalardo and E. Sánchez Marcos, *J.Chem.Phys.*, 2019, 150, 104504.

[6] S.Pérez-Conesa, J.M.Martínez, R.R.Pappalardo and E. Sánchez Marcos, *Inorg.Chem.*, 2022, 61, 8703.

Radionuclide research at the KIT synchrotron source – the INE and ACT experimental stations

B. Schacherl, T. Prüssmann, K. Dardenne, K. Hardock, V. Krepper, J. Rothe, T. Vitova, H. Geckeis.

Karlsruhe Institute of Technology (KIT), Institute for Nuclear Waste Disposal (INE), P.O. Box 3640, D-76021 Karlsruhe, Germany

X-ray absorption spectroscopy and related techniques became indispensable methods in actinide and radionuclide research. One important motivation are studies concerning the mobilization and retention of long-lived actinides, fission and activation products in geochemical processes relevant for safety studies of a potential deep geological nuclear waste repository. Therefore, reliable synchrotron based speciation techniques are needed and developed at, e.g., the INE-Beamline and the ACT experimental station of the CAT-ACT wiggler beamline at the Karlsruhe Institute of Technology (KIT) Light Source.[1] These beamlines are dedicated to the investigation of radionuclide containing materials with activities up to 1 million times the European exemption limit by various speciation techniques. The KIT facilities offer a highly versatile infrastructure - including on-site radiochemistry laboratories with inert-gas alpha boxes and a shielded box-line - for the investigation of radioactive materials in the context of the nuclear waste disposal safety case and fundamental actinide research.

One experimental technique especially powerful to differentiate oxidation states of actinides is the recently emerged actinide (An) $M_{4,5}$ -edge high-energy resolution X-ray absorption near-edge structure (HR-XANES). [2–4] This presentation highlights the latest technological developments at the ACT station, enabling, e.g., the HR-XANES spectroscopic technique for samples with low radionuclide loading down to 1 ppm in combination with a cryogenic sample environment reducing beam-induced sample alterations.[5,6] A critical part of this development is a versatile gas tight plexiglass encasement which ensures all beam paths in the five-analyzer-crystal Johann-type X-ray emission spectrometer run within He atmosphere. Also the exchange between different experiments (HR-XANES, conventional XAFS, high-energy or wide-angle X-ray scattering, tender to hard X-ray spectroscopy) is made quick and easy. The new setup paves the way for the *in-operando* examination of coupled redox/solid-liquid interface reactions. It opens up the possibility for the investigation of environmental samples, such as specimens containing transuranium elements from contaminated land sites or samples from sorption and diffusion experiments where molecular scale understanding of retention mechanisms can be achieved. Furthermore, a first glance on the currently ongoing further development of the XES spectrometer “NEXT generation probe of chemical bonding properties of actinides and lanthanides” will be presented in this contribution.

Complementing the method portfolio at the INE-Beamline is the setup for “tender” X-ray spectroscopy (spectral range, ~ 2 –5 keV) in transmission or total fluorescence yield detection mode on the basis of a He flow cell. With this setup also highly active samples can be investigated in fluorescence mode at low energies. For the first time, Tc L_{3} -edge measurements (~ 2.677 keV) of aqueous Tc specimens are reported. This method surpasses conventional K-edge spectroscopy as a tool to differentiate Tc oxidation states and coordination environments.[7,8]

We thank the Institute for Beam Physics and Technology (IBPT) for the operation of the storage ring, the Karlsruhe Research Accelerator (KARA). This project has received funding from the European Union's Horizon 2020 research and innovation program under grant agreement No. 847593. We also acknowledge funding from the ERC Consolidator Grant 2020 under the European Union's Horizon 2020 research and innovation programme (grant agreement No. 101003292). The Federal Ministry of Education and Research (BMBF) and the Helmholtz Association of German Research Centres (HGF) are acknowledged for funding within the HOVER project. We acknowledge the HGF as well for the VH-NG-734 grant. We also acknowledge the Strategic fund of KIT “NEXT generation probe of chemical bonding properties of actinides and lanthanides”.

-
- [1] J. Rothe, M. Altmaier, R. Dagan, K. Dardenne, D. Fellhauer, X. Gaona, E.G.-R. Corrales, M. Herm, K.O. Kvashnina, V. Metz, I. Pidchenko, D. Schild, T. Vitova, and H. Geckeis, *Geosciences* 9 (2019) 91.
 - [2] T. Vitova, I. Pidchenko, D. Fellhauer, P.S. Bagus, Y. Joly, T. Prüssmann, S. Bahl, E. Gonzalez-Robles, J. Rothe, M. Altmaier, M.A. Denecke, H. Geckeis, *Nat. Commun.* 8 (2017) 16053.
 - [3] P. Glatzel, T.-C.C. Weng, K. Kvashnina, J. Swarbrick, M. Sikora, E. Gallo, N. Smolentsev, R.A. Mori, *J. Electron Spectros. Relat. Phenom.* 188 (2013) 17–25.
 - [4] K.O. Kvashnina, S.M. Butorin, P. Martin, P. Glatzel, *Phys. Rev. Lett.* 111 (2013) 1–5.
 - [5] B. Schacherl, C. Joseph, P. Lavrova, A. Beck, C. Reitz, T. Pruessmann, D. Fellhauer, J.-Y. Lee, K. Dardenne, J. Rothe, H. Geckeis, T. Vitova, *Anal. Chim. Acta* 1202 (2022) 339636.
 - [6] B. Schacherl, T. Prüssmann, K. Dardenne, K. Hardock, V. Krepper, J. Rothe, T. Vitova, H. Geckeis, *J. Synchrotron Radiat.* 29 (2022) 80–88.
 - [7] K. Dardenne, S. Duckworth, X. Gaona, R. Polly, B. Schimmelpfennig, T. Pruessmann, J. Rothe, M. Altmaier, H. Geckeis, *Inorg. Chem.* 60 (2021) 12285–12298.
 - [8] S. Bauters, A.C. Scheinost, K. Schmeide, S. Weiss, K. Dardenne, J. Rothe, N. Mayordomo, R. Stuedtner, T. Stumpf, U. Abram, S.M. Butorin, K.O. Kvashnina, *Chem. Commun.* 56 (2020) 9608–9611.

Soft X-ray Chemical Speciation Mapping of Uranium Oxide Focused Ion Beam Sections

D. Shuh¹, A. Ditter¹, D. Smiles¹, J. Pacold¹, A. Altman¹, M. Mara¹, M. Bacchav², L. He², C. Deguldre³, D. Vine¹, S. Minasian¹, Z. Dai⁴, M. Davisson⁴, B. Chung⁴, S. Donald⁴

¹ Lawrence Berkeley National Laboratory

² Idaho National Laboratory

³ Lancaster University

⁴ Lawrence Livermore National Laboratory

The oxidation of uranium is a complex process, depending on temperature, humidity, dopants and morphology. It is also an important area of study with impacts in the fields of biology, nuclear forensics, nuclear fuels, and nuclear waste storage. For instance, the high temperature gradients and quantities of fission products make for a complex environment for UO_2 fuel to oxidize during burnup. The oxidation after burnup is also important as the volumetric expansion of the fuel can cause cracking, releasing gaseous fission products trapped in the fuel.

Soft x-ray spectromicroscopy is an unparalleled method for the study of these systems. The oxygen K-edge is particularly sensitive to the chemical state of the uranium oxide system, and the $\text{U N}_{4.5}$ -edges are also available for study. However, thin samples on the order of 100-200 nm are required for use in the scanning transmission x-ray microscope, and so a focused ion beam (FIB) was used to create thin lamella of uranium materials.

Two systems are discussed here, spent nuclear fuel and an agglomeration of UO_2 particles allowed to age under humid conditions. The spent fuel is measured at the oxygen K-edge and a modified form of non-negative matrix factorization is used to separate out the primary components, identifying a bulk species similar to UO_2 and an interfacial UO_{2+x} species (Fig. 1) [1]. This interfacial species forms near cracks and voids in the sample as well as the flat surface of the FIB section at a thickness of approximately 8 nm. This is confirmed through $\text{U-N}_{4.5}$ measurements which also show increased oxidation at the interface. Finally, the oxidation of Ce in spent fuel is measured and determined to be predominantly trivalent.

The agglomerated particles, aged for one year under 98% relative humidity atmosphere are also measured at the oxygen K-edge, showing three distinct species, a bulk UO_2 -like phase, an interfacial schoepite phase which forms at the interface of the sample with the air during aging, and a surface phase indicating sorption of water on the surface of the FIB stub [2]. The two uranium oxide phases are mapped across the entire section using carefully chosen energies to differentiate between the two phases. This is confirmed with $\text{U-N}_{4.5}$ measurements which can also distinguish oxidation state, a potentially useful result for other systems without oxygen or a suitable ligand to measure.

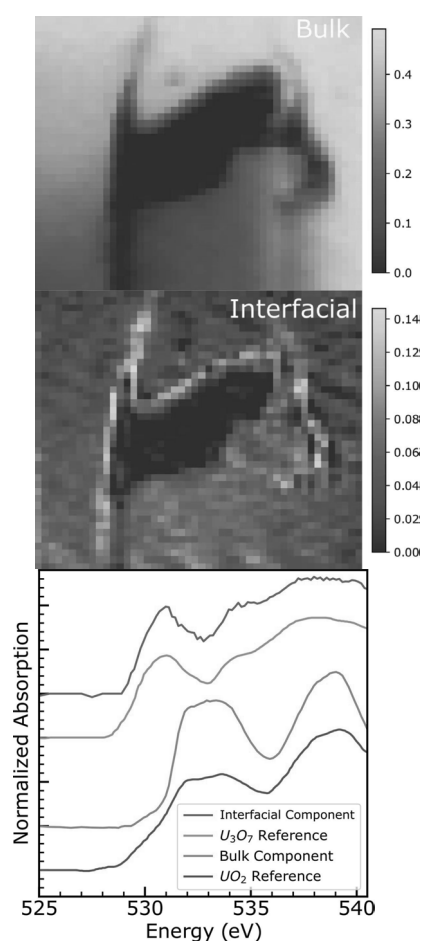


Fig. 1: Locations of the bulk UO_2 -like phase (top) and Interfacial UO_{2+x} phase (middle) in a FIB section of spent nuclear fuel. Comparison of the spectra of these phases with reference data identifying them.

[1] Ditter, A. S. et al., (2022) *J. Synchrotron Rad.* 29, 67-79. DOI: 10.1107/S1600577521012315

[2] Ditter, A. S. et al., (2022) *J. Vac. Sci. Technol. A* 40, 043202. DOI: 10.1116/6/001880

Seeing multiplets in UO₂ and UGa₂ with NIXS and tender RIXS

A. Marino¹, D. S. Christovam¹, M. Sundermann^{1,2}, A. Amorese^{1,3}, C.-F. Chang¹, P. Dolmantis¹, L. Havela⁴, P. Raison⁵, B. Keimer⁶, H. Gretarsson^{1,2,6}, L. H. Tjeng¹, A. Severing^{1,3}

¹Max Planck Institute for Chemical Physics of Solids, Dresden, Germany

²Deutsches Elektron-Synchrotron DESY, Hamburg, Germany

³Institute of Physics II, University of Cologne, Cologne, Germany

⁴Department of Condensed Matter Physics, Charles University, Prague, Czech Republic

⁵European Commission, Karlsruhe, Germany

⁶Max-Planck Institute for Solid State Research, Stuttgart, Germany

A central aspect in actinide research is the question of the $5f$ occupancy: in uranium intermetallics, the $5f$ states are usually believed to be itinerant with the expectation that DFT band structure approaches should provide a correct description. UGa₂ is a hexagonal intermetallic compound that orders ferromagnetically at 125K, with moments of about $3\mu_B$ along [100] [1-3]. For this binary, however, the magnitude of the magnetic moments indicates a more localized nature of the $5f$ electrons. DFT-based studies significantly underestimate the moments [4, 5] and correlation effects have to be taken into account [6]. Spectroscopic investigations also show remarkable evidence for a localized character of the $5f$ electrons [7-9], and here the crystal field aspect becomes important.

We will now show that the crystal-field aspect becomes important [10] and that the charge density of the $5f$ electrons in uranium compounds can be identified with x-ray Raman using non-resonant inelastic x-ray scattering (O -edge NIXS) [11-13].

Identifying the excited states, however, still remains an experimental challenge. It was a great success that soft x-ray resonant inelastic scattering (RIXS) experiments at the U N_4 -edge (780eV) by Lander *et al.* [14] show multiplets and crystal-field excitations in semiconducting UO₂. Trials on metallic uranium compounds, however, failed [15]. We therefore tried a new route, namely U M_5 edge RIXS in the tender x-ray regime (3.5keV), encouraged by XES results of Kvashnina *et al.* [15]. RIXS data at the U M_5 edge of UO₂ and also of metallic UGa₂ [10] were taken at the RIXS end-station at the P01 beamline at DESY/PETRA_III with its recently installed high resolution (150meV) quartz analyzer crystals. We see a plethora of multiplets in UO₂, and also in metallic UGa₂, and in both cases the multiplets arise from the f^2 configuration according to full multiplet calculations (Quanty code [16]).

We believe that O -edge NIXS and M -edge RIXS are the way forward for the investigation of the electronic structure of uranium and possibly also transuranium compounds because not only the cross-sections are favorable, in addition, cleaving in the tender x-ray regime is obsolete.

[1] A. Andreev *et al.*, Sov. Phys. JETP **48**, 1187 (1987).

[2] A. C. Lawson *et al.*, J.Magn. Magn. Mater. **50**, 83 (1985).

[3] R. Ballou *et al.*, J. Phys. Colloques **43**, CZ-279 (1982).

[4] M. Diviš *et al.*, Phys. Rev. B **53**, 9658 (1996).

[5] B. Chatterjee *et al.*, MRS Adv. **5**, 2639 (2020).

[6] B. Chatterjee *et al.*, Phys. Rev. B **103**, 205146 (2021).

[7] S. Fujimori *et al.*, J. Phys. Soc. Jpn. **85**, 062001 (2016).

[8] S. Fujimori *et al.*, Phys. Rev. B **99**, 035109 (2019).

[9] A. V. Kolomiets *et al.*, Phys. Rev. B **104**, 045119 (2021).

[10] A. Marino and D. S. Christovam *et al.*, unpublished

[11] M. Sundermann *et al.*, PNAS **113** (49) 13989 (2016)

[12] M. Sundermann *et al.*, Phys. Rev. B **98**, 205108 (2018)

[13] A. Amorese *et al.*, PNAS **117** (48) 30220 (2020)

[14] G. Lander *et al.*, J. Phys.: Condens. Matter **33**, 06LT01 (2020)

[15] A. Amorese, unpublished

[16] K. Kvashnina *et al.*, Phys. Rev. B **95**, 245103 (2017)

[17] M.W. Haverkort *et al.*, Phys. Rev. B **85**, 165113 (2012)

Relativistic correlated electronic structure and the calculation of accurate ground-state, core and valence properties of heavy element species

Loïc Halbert¹, Xiang Yuan^{1,2}, Florent Réal¹, Valérie Vallet¹, André Severo Pereira Gomes¹ (andre.gomes@univ-lille.fr)

1. Univ. Lille, CNRS, UMR 8523 - PhLAM - Physique des Lasers Atomes et Molécules, F-59000 Lille, France

2. Department of Chemistry and Pharmaceutical Sciences, Faculty of Science, Vrije Universiteit Amsterdam, de Boelelaan 1083, 1081 HV Amsterdam, The Netherlands.

Accurate electronic structure calculations have become an indispensable tool to understand the molecular properties of heavy and superheavy elements. Such approaches help make sense of the underlying complex physical processes probed by experiments, or in the case such experiments are unfeasible due to the heavy elements' radioactivity.

In this contribution I will outline our efforts pertaining to the development of coupled cluster approaches based on four-component Hamiltonians for ground-state properties as well as for valence and core excitation and ionization spectra [1-4], and their application to investigating actinides and super heavy elements [2, 3, 5].

Furthermore, I will outline how these can be combined with more approximate approaches through embedding theories [6], to enable the investigation of heavy element species in complex environments such as in solution.

Funding: ANR-11-LABX-0005-01, ANR-19-CE29-0019, ANR-16-IDEX-0004, DE-AC05-00OR22725.

[1] J. Pototschnig *et al.*, J. Chem. Theory Comput. (2021) **17**, 5509 [10.1021/acs.jctc.1c00260](https://doi.org/10.1021/acs.jctc.1c00260)

[2] X. Yuan, L. Visscher, A. S. P. Gomes, J. Chem. Phys. (in press) (2022). [10.1063/5.0087243](https://doi.org/10.1063/5.0087243)

[3] A. Shee, T. Saue, L. Visscher, A. S. P. Gomes, J. Chem. Phys. (2018) **149**, 174113 [10.1063/1.5053846](https://doi.org/10.1063/1.5053846)

[4] L. Halbert, M. L. Vidal, A. Shee, S. Coriani, A. S. P. Gomes, J. Chem. Theory Comput. (2021) **17**, 3583 [10.1021/acs.jctc.0c01203](https://doi.org/10.1021/acs.jctc.0c01203)

[5] S. Kervazo, F. Réal, F. Viot, A. S. P. Gomes, V. Vallet, Inorg. Chem. (2019) **58**, 14507 [10.1021/acs.inorgchem.9b02096](https://doi.org/10.1021/acs.inorgchem.9b02096)

[6] Y. Bouchafra, A. Shee, F. Réal, V. Vallet, A. S. P. Gomes, Phys. Rev. Lett. (2018) **121**, 266001 [10.1103/PhysRevLett.121.266001](https://doi.org/10.1103/PhysRevLett.121.266001)

Fe(II) Induced Reduction and Sulfidation of U(VI)-incorporated Goethite

Samuel Shaw^{1*}, Olwen Stagg¹, Katherine Morris¹; Liam Abrahamsen-Mills²; Luke Townsend¹, Thomas S. Niell¹, J. Frederick W. Mosselmans³

¹ Research Centre for Radwaste Disposal and Williamson Research Centre, Department of Earth & Environmental Sciences, The University of Manchester, Oxford Road, Manchester, M13 9PL, UK

² National Nuclear Laboratory, Chadwick House, Warrington Road, Birchwood Park, Warrington, WA3 6AE, UK

³ Diamond Light Source Ltd., Diamond House, Harwell Science and Innovation Campus, Didcot, OX11 0DE, UK

Uranium is a significant contaminant in the global legacy of radioactive waste and contaminated land, with higher activity wastes destined for deep underground geological disposal, and radioactively contaminated land now being decommissioned. Iron (oxyhydr)oxide phases are ubiquitous in and around these engineered and natural environments formed via a variety of processes including metal corrosion and microbially induced reactions. These can lead to the formation of nanoparticulate iron (oxyhydr)oxide phases (e.g. goethite, α -FeOOH). There are numerous reports of uranium-incorporation into iron (oxyhydr)oxides, therefore it has been suggested that these phases may be an additional barrier to the migration of uranium (and other radionuclides) in the environment (e.g. subsurface contaminated land system). However, the long-term stability of these phases and the uranium within them during environmental perturbations are largely unexplored. Specifically, U-incorporated iron (oxyhydr)oxide phases may interact with aqueous Fe(II) and sulphide species in the subsurface. Firstly, significant electron transfer may occur between adsorbed Fe(II) and stable iron oxyhydroxides (e.g. goethite), with potential for changes in the speciation of incorporated uranium e.g. oxidation state changes and/or release into solution. Secondly, on exposure to aqueous sulfide, iron (oxyhydr)oxides may undergo extensive reductive dissolution and recrystallisation to iron sulphide phases e.g. mackinawite (FeS) or erdite ($\text{NaFeS}_2 \cdot 2\text{H}_2\text{O}$). Understanding the fate of incorporated uranium during these process in key to understanding its environmental behaviour in a variety of systems.

A series of experimental studies were undertaken where U(VI)-goethite was synthesized then reacted with either aqueous Fe(II) or S(-II) at different pH's, and the system monitored over time using geochemical analysis and X-ray absorption spectroscopy (XAS) techniques e.g. U L_{III}-edge and M_{IV}-edge HERFD-XANES. Reaction with aqueous Fe(II) resulted in significant electron transfer between Fe(II) and U(VI)-goethite, with >50% U(VI) reduced to U(V). XAS analysis revealed that all the U remained within the goethite structure, and electron transfer only occurred within the outermost atomic layers of goethite. which led to the reduction of U(VI) to U(V). Minimal recrystallisation of goethite (2%) occurred following electron transfer, with both U(VI) and U(V) retained within the structure. Rapid reductive dissolution of U(VI)-goethite occurred on reaction with aqueous sulfide at pH 7. Over the first day of sulfidation, a transient release of aqueous U was observed, likely due to intermediate uranyl(VI)-persulfide species. Despite this, overall U was retained in the solid phase, with the formation of nanocrystalline U(IV)O₂, along with a persistent U(V) component. On reoxidation, U was associated with an iron (oxyhydr)oxide phase, either as an adsorbed uranyl or an incorporated U species. In contrast, the sulfidation of U adsorbed to ferrihydrite at pH 12.2 led to the immediate release of U (<10% U_{total}). A U(VI)-associated colloidal erdite phase also formed immediately and was stable throughout the experiment, with U(VI) likely encapsulated within the structure. Moreover, in the bulk phase the surface of ferrihydrite was passivated by sulfide, and U was found to have been trapped within surface associated erdite-like fibres.

Overall, these studies further understanding of the long-term behaviour of U-incorporated iron (oxyhydr)oxides under environmental perturbations and support the overarching concept of iron (oxyhydr)oxides acting as a barrier to U migration in the environment.

High-energy-resolution X-ray spectroscopy and actinides research at SLAC

Dimosthenis Sokaras, SLAC National Accelerator Laboratory

Nowadays, high-energy-resolution x-ray spectroscopy is a well-established and powerful tool available in state-of-the art synchrotron facilities. The suppression of the core-hole lifetime contribution within the conventionally broad spectroscopic features of actinide series has revitalized the role of x-ray spectroscopy in the study of actinide complexes and intermetallics. Numerous studies have leveraged the fine structure of M or L absorption edges resonances to sensitively probe and quantify the oxidation state, 5f delocalization, and ligation of the actinides species. The increasing availability of large solid angle instruments coupled with high flux beamlines is quickly enabling such advanced studies for dilute samples or samples under special sample environments. In this presentation we will summarize the high-resolution tender and hard x-ray spectroscopy advances at SLAC and the actinides research program that these capabilities have enabled during the last decade.

Simulating Uranyl Oxygen K-edge XANES using Multiconfigurational RASSCF Methods

K. Stanistreet-Welsh,¹ A. Kerridge¹

¹ Lancaster University Chemistry Department, Lancaster University, United Kingdom LA1 4YB, k.stanistreet-welsh@lancaster.ac.uk

X-ray absorption near-edge spectroscopy (XANES) is useful for probing metal-ligand interactions in f-element complexes to quantify orbital mixing and hence covalency.[1] Time-dependent density functional theory (TDDFT) is commonly used to aid in the interpretation of XANES spectra. However, TDDFT methods typically require large energy shifts to align predicted spectra with experiment, due to a number of limitations when obtaining core-excited states,[1,2,3] one limitation being the exclusion of occupied-orbital relaxations in the presence of the core-hole.[3] Recently, restricted active space self-consistent field (RASSCF) methods have been used to address TDDFT limitations, leading to greater agreement with experiment.[1] In this contribution, the results of oxygen K-edge XANES simulations, using a RASSCF methodology including spin-orbit coupling, for free uranyl and $\text{UO}_2\text{Cl}_4^{2-}$ are presented. RASSCF approaches can be computationally expensive, but we take a truncated-CI approach to simulations which allows a degree of control over the amount of correlation included, hence managing simulation cost. The simulated spectrum of free uranyl shows strong agreement with experimental XANES undertaken by Denning et al. but without the need for large energy shifts to align with experiment (Fig. 1).[4] Analysis of theoretical peaks using spin-orbit natural orbitals show predictions compare well to the original characterization made by Denning et al. Initial QTAIM analysis and orbital decomposition has allowed an examination of uranyl bonding and provides a method for verifying covalency information derived from XANES. Simulations on $\text{UO}_2\text{Cl}_4^{2-}$ show the approach can be expanded to explore the influence of the local crystal environment and QTAIM analysis is used to rationalize a red-shift with respect to experiment. The results presented here offer proof of concept for this truncated RASSCF methodology, which is now being actively adapted to obtain metal $M_{4,5}$ edge data in uranyl(V), uranyl(VI) and neptunyl(VI). Preliminary metal-edge results will be presented to further demonstrate the applicability of RASSCF methods for XANES simulations.

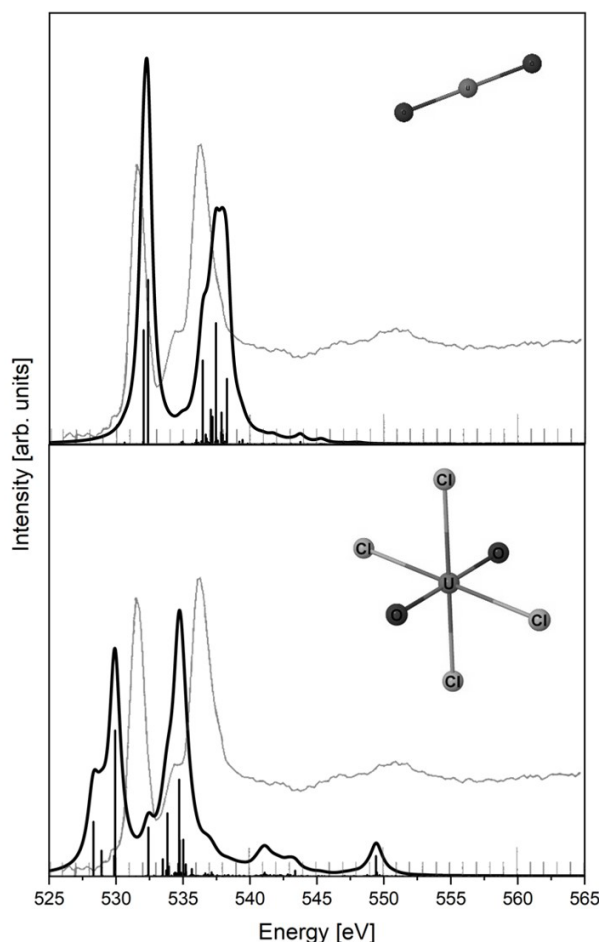


Fig. 1. Uranyl (Top) and uranyl chloride RAS-CISDT (bottom) simulated (thick-line) oxygen K-edge XANES compared to experiment [4] (thin-line).

- [1] D.-C. Sergentu, T. J. Duignan and J. Autschbach, *The Journal of Physical Chemistry Letters* 9, 5583-5591 (2018).
 [2] S. G. Minasian, J. M. Keith, E. R. Batista, K. S. Boland, D. L. Clark, S. A. Kozimor, R. L. Martin, D. K. Shuh and T. Tyliszczak, *Chem. Sci.* 5, 351-359 (2014).
 [3] L. P. Spencer, P. Yang, S. G. Minasian, R. E. Jilek, E. R. Batista, K. S. Boland, J. M. Boncella, S. D. Conradson, D. L. Clark, T. W. Hayton, S. A. Kozimor, R. L. Martin, M. M. MacInnes, A. C. Olson, B. L. Scott, D. K. Shuh and M. P. Wilkerson, *Journal of the American Chemical Society* 135, 2279-2290 (2013).
 [4] R. G. Denning, J. C. Green, T. E. Hutchings, C. Dallera, A. Tagliaferri, K. Giarda, N. B. Brookes and L. Braicovich, *The Journal of Chemical Physics* 117, 8008-8020 (2002).

Speciation and accumulation of uranium in mussels *Mytilus Galloprovincialis*

Romain Stefanelli^[1-2], Jean Aupiais^[2], Marguerite Monfort^[2], Maria-Rosa Beccia^[1], Christophe Moulin^[1,3], Pier-Lorenzo Solari^[4], Sophie Pagnotta^[5], Christophe Den Auwer^[1]

[1] Institut de chimie de Nice, UMR 7272, Université Côte d'Azur, 06108 Nice, France

[2] CEA, DAM, DIF, F-92297 Arpajon, France

[3] SGDSN, 51 boulevard de la Tour-Maubourg, 75007 Paris 07 SP, Seconded from CEA

[4] Synchrotron Soleil, Saint-Aubin, F-91192 Gif-sur-Yvette, France

[5] CCMA - Centre Commun de Microscopie Appliquée, Université Côte d'Azur, 06108 Nice, France

The marine environment constitutes the major part of the earth's surface and can be monitored as a pollution bellwether. Uranium is a radioelement belonging to the actinide series of the Periodic Table. It is naturally present in seawater and marine ecosystems, but its presence may increase due to human activities^[1]. In the context of the study of the impact of nuclear activities on ecosystems, and in particular on the marine compartment, it is essential to be able to understand how it interacts with marine organisms, how it is (bio)accumulated or transferred to the trophic chain^[2]. In seawater, uranium speciation is mainly in the form of a dicalcium complex of uranyl tricarbonate, $\text{Ca}_2\text{UO}_2(\text{CO}_3)_3$ ^[3].

This project aims to describe the speciation of uranium in a lamellibranch bivalve mollusc (*Mytilus Galloprovincialis*). This sedentary marine organism is present in abundance throughout the world and used in numerous biomonitoring programs as a bioindicator of metals contaminations (NOAA-Mussel Watch program)^[4]. But in many cases speciation data are lacking. We have used complementary spectroscopic and imaging techniques to map the speciation of uranium in marine organisms, although this is challenging given the low concentrations present in tissues (1-10 ppm).

Specimens of *M. galloprovincialis* were contaminated in the laboratory with uranium-doped seawater. Different compartments of *M. galloprovincialis* were separated and analyzed by ICP-MS (Inductively Coupled Plasma Mass spectroscopy). The distribution of uranium concentration is : byssus > hepatopancreas > gill > mantle > visceral body > foot. Moreover, imaging techniques SEM (Scanning Electron Microscopy), μ -XRF (X-ray fluorescence), SIMS (Secondary-ion mass spectrometry) have been used to observe the repartition of uranium and to understand its accumulation at the cellular/subcellular level. Spatial and speciation correlations using the different imaging techniques have been attempted. Speciation in the organs of interest, especially byssus and hepatopancreas, was more specifically studied with EXAFS (Extended X-ray Absorption Fine Structure) at the U edge and TRLIF (Time Resolved Laser Induced Fluorescence) spectroscopy.



Figure Mussel section contaminated with uranium-doped seawater. Uranium L_{II} mapping (top part in the byssus) (bottom part in the hepatopancreas).

[1] CCREM Canadian Water Quality Guidelines. Canadian Council of Resource and Environment Ministers, Inland Waters Directorate, Environment Canada, 1991.

[2] Kim J-I. The chemical behavior of transuranium elements and barrier functions in Natural Aquifer Systems - Mrs SpringerLink 1992.

[3] Maloubier M, Solari PL, Moisy P, Monfort M, Auwer CD, Moulin C. Xas and TRLIF spectroscopy of uranium and neptunium in seawater. Dalton Transactions 2015.

[4] Kimbrough, K.L., W.E. Johnson, G.G. Lauenstein, J.D. Christensen, and D.A. Apeti. 2008. An assessment of two decades of contaminant monitoring in the nation's coastal zone. NOAA Technical Memorandum NOS NCCOS 74. Silver Spring, MD. 105 pp.2008

Revealing long-range and long-term properties of actinides with diffraction at the Rossendorf Beamline

V. Svitlyk,^{1,2} C. Hennig^{1,2}

¹Helmholtz-Zentrum Dresden-Rossendorf, Institute of Resource Ecology, 01314 Dresden, Germany

²Rossendorf Beamline (BM20), European Synchrotron Radiation Facility, 38000 Grenoble, France

The Rossendorf Beamline (ROBL BM20, European Synchrotron Radiation Facility (ESRF), Grenoble, France) is dedicated to actinide and nuclear waste research and is managed by the Institute of Resource Ecology, Helmholtz-Zentrum Dresden-Rossendorf, Dresden, Germany. Diffraction station of ROBL features a unique combination of two diffractometers: XRD-1 High Resolution Powder (Fig. 1, left) and XRD-2 Multipurpose (Fig. 1, right) machines [1].

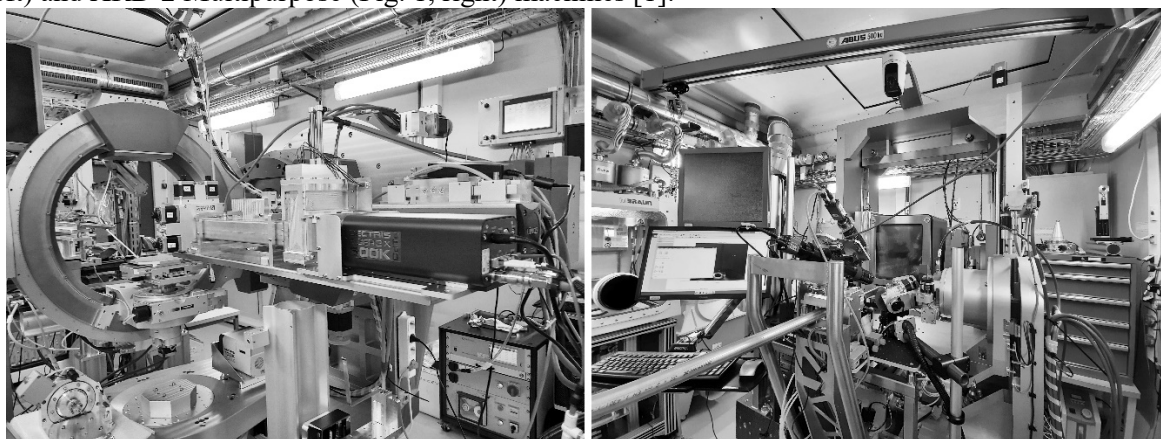


Fig. 1. XRD-1 High Resolution Diffractometer (left) and XRD-2 Multipurpose Diffractometer (right) at the Rossendorf Beamline (BM20, ESRF).

The XRD-1 machine relies on Dectris Eiger2X 500k CdTe photon counting detector mounted on a heavy-duty 2θ arm coupled with an angular encoder. High precision movements combined with small pixel size of the detector ($75 \times 75 \mu\text{m}^2$) and symmetrically focalized beam (down to $100 \times 100 \mu\text{m}^2$) yields resolution in terms of $\delta d/d$ down to 1.8×10^{-4} and diffraction peaks with FWHM of 0.009° . Resulting high resolution powder diffraction data with a symmetrical line profile enables identification of low-symmetry structures in multi-phase samples with a subsequent full structural refinement. In particular, precise unit-cell parameters, atomic coordinates together with anisotropic thermal parameters, strain and grain size can be reliably obtained from data collected with the XRD-1 diffractometer. Performance of this machine will be illustrated, in part, on the example of Th-doped Y-stabilized zirconia system where an interplay between fine structure, symmetry and solubility limit of Th was found [2].

The XRD-2 Multipurpose Diffractometer is equipped with a large area Pilatus3 X 2M detector. This enables fast data collection both on polycrystalline and monocrystalline samples at ambient conditions or *in situ* under extreme temperatures (5 - 1473 K) or high pressure (HP, up to 20 GPa). Application of HP is used to simulate possible phase instabilities of systems containing radiotoxic elements which are placed in underground storage. Moreover, extreme pressures allow to accelerate corresponding processes potentially occurring in buried nuclear waste from million years down to a week of experiment at the beamline. Relevant examples of *in situ* diffraction studies under extreme condition of temperature and pressure performed at ROBL will be presented on example of doped zirconia phases.

-
- [1] Scheinost A C, Claussner J, Exner J, Feig M, Findeisen S, Hennig C, Kvashnina K O, Naudet D, Prieur D, Rossberg A, Schmidt M, Qiu C, Colomp P, Cohen C, Dettona E, Dyadkin V and Stumpf T 2021 ROBL-II at ESRF: a synchrotron toolbox for actinide research *J. Synchr. Rad.* **28** 333–49
- [2] Svitlyk V, Weiss S and Hennig C 2022 Immobilization of radiotoxic elements with Y-stabilized zirconia: the Thorium case *J. Am. Ceram. Soc.* <https://doi.org/10.1111/jace.18543>

Molecular Design of Pentadentate Planar Ligand and Its Coordination with UO_2^{2+} towards Uranium Recovery from Seawater

K. Takao,¹ T. Mizumachi,¹ M. Sato,¹ M. Kaneko,² T. Takeyama,¹ S. Tsushima^{1,3}

¹ Laboratory for Zero-Carbon Energy, Institute of Innovative Research, Tokyo Institute of Technology

² Japan Atomic Energy Agency

³ Institute of Resource Ecology, Helmholtz-Zentrum Dresden-Rossendorf

Seawater is dissolving most of naturally occurring elements including U. While its concentration is very small (3.3 ppb), its net amount is approx. 10^3 times greater than the terrestrial U resources available. Therefore, U in seawater is a promising resource option for securing nuclear fuel materials in the future. In the past, various adsorbents have been tested for efficient and selective recovery of U under seawater condition. While several organic and inorganic adsorbents for the U uptake from seawater have been found, we believe that there is still much space to design and optimize a molecular structure of the adsorbing site on the basis of deep understanding of coordination chemistry of U present there. Herein, we propose a new pentadentate planar ligand structure designed for the U recovery from seawater, and report its actual coordination behavior with UO_2^{2+} under seawater condition.

It is well known that UO_2^{2+} most typically accepts five-fold coordination in its equatorial plane. On this implication, we have developed $\text{H}_2\text{saldian}$ (Figure 1a) as a water-compatible pentadentate planar ligand. Under the simulated seawater condition (0.5 M NaCl + 2.30 mM $\text{HCO}_3^-/\text{CO}_3^{2-}$ at pH 8.00(3)), $\text{H}_2\text{saldian}$ exhibits 5-step acid dissociation/association equilibria pronounced by $\text{p}K_{\text{a}1} = 4.15$, $\text{p}K_{\text{a}2} = 8.06$, $\text{p}K_{\text{a}3} = 9.51$, $\text{p}K_{\text{a}4} = 11.29$, and $\text{p}K_{\text{a}5} = 14.97$. A reaction of $\text{H}_2\text{saldian}$ with $\text{UO}_2(\text{NO}_3)_2 \cdot 6\text{H}_2\text{O}$ in ethanol immediately afforded orange powder of $\text{UO}_2(\text{saldian})$ (Figure 1b), where all 5 donating atoms of saldian^{2-} are located in the equatorial plane of UO_2^{2+} to make a stable chelate as expected. A stability constant of $\text{UO}_2(\text{saldian})$ ($\log \beta_{11}$) under the simulated seawater condition was determined to be 28.05 ± 0.07 by UV-vis titration experiments (Figure 1c). The characteristic absorption bands of $\text{UO}_2(\text{saldian})$ were well corroborated by the TDDFT calculations. Due to much greater stability compared with that of $\text{UO}_2(\text{CO}_3)_3^{4-}$ ($\log \beta_{13} = 21.84$), $\text{UO}_2(\text{saldian})$ is predominantly formed in the range from pH 4.3 to pH 12.7 including the seawater condition, pH ~ 8 . This indicates that saldian^{2-} is a promising ligand towards U recovery from seawater. Thanks to the unique pentadentate planar coordination, good selectivity for UO_2^{2+} from other metal ions (alkaline metals, alkaline earths, Al^{3+} , divalent d-block metals, Zr^{4+} , VO_2^+ , and MoO_4^{2-}) coexisting in seawater was also achieved as demonstrated by their separation factors at 10^3 - 10^9 .

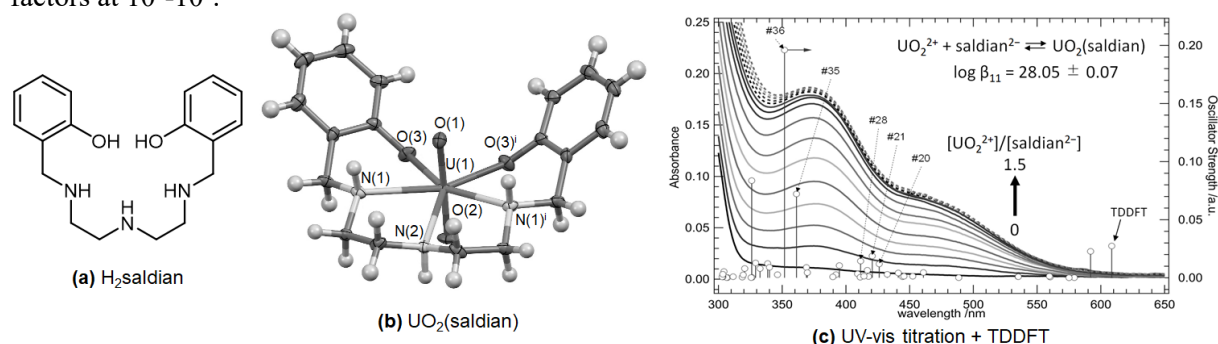


Figure 1. Molecular structures of (a) $\text{H}_2\text{saldian}$ and (b) $\text{UO}_2(\text{saldian})$ together with (c) UV-vis absorption spectra of aqueous solution of $\text{H}_2\text{saldian}$ (0.1 mM) at different total $[\text{UO}_2^{2+}]$ under the simulated seawater condition.

This work was supported in part by JAEA Nuclear Energy S&T and Human Resource Development Project through concentrating wisdom Grant Number JPJA19P19209861, Grants-in-Aid for Scientific Research (20H02663, 21J11942), and World Research Hub (WRH) Program of International Research Frontiers Initiative (IRFI), Tokyo Institute of Technology.

[1] Mizumachi, T. et al. (2022) *Inorg. Chem.* 61, 6175-6181.

Sorption of radionuclides by oxidized carbons: from graphene oxide to super-oxidized high surface area carbons.

A.V, Talyzin¹.

¹Department of Physics, Umeå University, Umeå, SE-901 87, Sweden

Functionalization of carbon surfaces with various oxygen-containing groups is favorable for sorption of radionuclides. For example, graphene oxide (GO) shows high sorption capacity for radionuclides and various heavy metals.^[1] GO is non-stoichiometric material functionalized mostly with epoxy and hydroxyl groups on the planar surface, while the edges of flakes are terminated mostly by carbonyls and carboxylic groups. Moreover, the defects (holes and vacancies) are an essential part of the GO structure.

Our recent studies demonstrated that an increased number of defects and carboxylic groups in GO is correlated with the improvement of sorption capacity for several radionuclides.^[2] This trend led us to the synthesis of extremely defect-rich modification of GO (dGO). The dGO has been prepared using Hummers oxidation of the defect-rich reduced graphene oxide (rGO) and demonstrated excellent sorption properties towards U(VI) with up to a 15-fold increase compared to standard GO.^[3] The material was also demonstrated promising benefits for the sorption of organic pollutants.^[4] The enhanced sorption of radionuclides has been correlated in these studies to interactions with carboxylic groups on the edges of flakes or holes and vacancy defects.^[2-3] However, synthesis of dGO is relatively complex and might be challenging to scale up for real applications. Moreover, both GO and dGO need to be dispersed in water in order to make their high surface area accessible.

Therefore, we designed an alternative approach to preparing carbon sorbents with similar to GO oxidation state using common high surface area carbon materials as precursors. High surface area activated reduced graphene oxide (arGO) was oxidized using two types of treatments and transformed into a 3D analogue of dGO. Surface oxidation of arGO results in carbon to oxygen ratio C/O=3.3, similar to the oxidation state of graphene oxide while preserving relatively high BET surface area. Analysis of surface oxidized arGO showed high abundance of oxygen functional groups which converted hydrophobic precursor into hydrophilic material. The “3D graphene oxide” showed high sorption capacity for U(VI) removal in an extraordinary broad interval of pH. Notably, the surface oxidized carbon material has a rigid 3D structure with micropores accessible for penetration of radionuclide ions. Therefore, the bulk “3D GO” can be used as a sorbent directly without dispersing, the step required for GO to make its surface area accessible for pollutants.^[5] The mechanism of sorption was studied using EXAFS data and HERFD-XANES spectra. The HERFD-XANES spectra recorded from oxidized samples after sorption of U(VI) are different compared to spectra of arGO after U(VI). The change in relative height of the main features of HERFD-XANES spectra correlates with the degree of oxidation. Our results indicate that experimental data are compatible with U(VI) adsorbed in hole defects for the more oxidized materials.

Tab. 1: Capacity for U(VI) sorption onto precursor arGO and two types of surface oxidized materials calculated by applying the Langmuir model at pH 5.1 vs BET surface area and oxidation degree (C/O)

Sample	BET Surface area (m ² /g)	C/O	Maximum sorption capacity Q _{max} , μmol/g
arGO	2730	55	644 ± 78
HNO ₃ Oxidized arGO	1810	8.2	1590 ± 38
(NH ₄) ₂ S ₂ O ₈ oxidized arGO	880	3.3	1950 ± 64
dGO	< 5	2.7	2250 ± 53

- [1] A. Y. Romanchuk, et al, *Phys Chem Chem Phys* **2013**, *15*, 2321-2327.
 [2] A. S. Kuzenkova, et al, *Carbon* **2020**, *158*, 291-302.
 [3] N. Boulanger, et al, *Acs Appl Mater Inter* **2020**, *12*, 45122-45135.
 [4] S. Khaliha, et al, *Flatchem* **2021**, *29*.
 [5] N. Boulanger, et al *Adv Mater Interfaces* **2022**, *9*.

The Underlying Simplicity of 5f Unoccupied Electronic Structure

J. G. Tobin^{1,*}, S. Nowak², S.-W. Yu³, P. Roussel⁴, R. Alonso-Mori², T. Kroll²,
D. Nordlund², T.-C. Weng², and D. Sokaras²

¹University of Wisconsin-Oshkosh, Oshkosh, WI, USA 54901, USA

²SLAC National Accelerator Laboratory, Menlo Park, CA 94025, USA

³Lawrence Livermore National Laboratory, Livermore, CA, 94550, USA

⁴AWE plc, Aldermaston, Reading, Berkshire, RG7 4PR, UK

*Contact Author Email: tobinj@uwosh.edu

Using a simple empirical model based upon the Bremsstrahlung Isochromat Spectroscopy (BIS) of elemental Th [1], it is possible to explain the recent High Energy Resolution Fluorescence Detection (HERFD) measurements of UF₄ (n = 2) and UCd₁₁ (n = 3) as well as the new Inverse Photoelectron Spectroscopy (IPES) of Pu₂O₃ (n = 5), where n is the 5f occupation number. [2] A critical issue in this analysis is the assumption that the Th 5f states are essentially empty, which was confirmed both experimentally and computationally. Additionally, this model can be extended to understand the observations for an n = 2/3 system, U₃O₈ [3,4], and qualitatively rationalize the earlier Bremsstrahlung Isochromat Spectroscopy (BIS) results for US and UTe. [5,6] Thus, for 5f systems, this simple model provides a unified and consistent picture of 5f Unoccupied Density of States (UDOS) in simple, localized systems, as the 5f occupation varies in the early part of the series, for n = 2/3, 2, 3, and 5, and for the impact of weak 5f delocalization in uranium monochalcogenides.

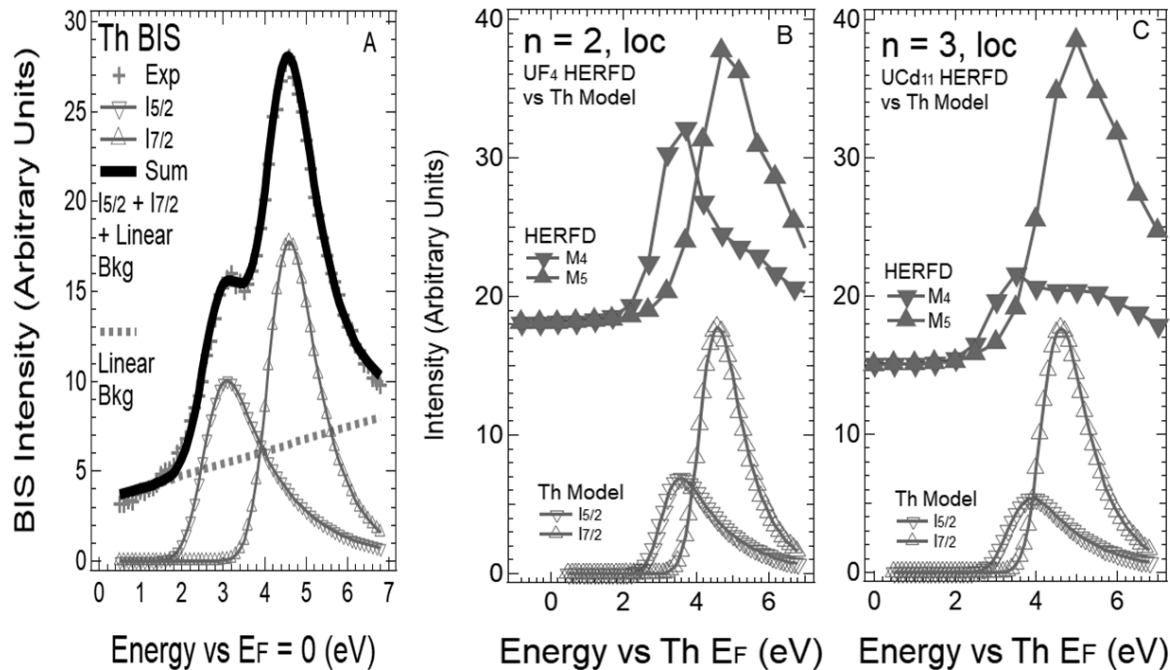


FIG. 1. Th model and n = 2 and 3 localized cases. (a) Shown here are the results of the fitting of the Th BIS experimental curve (+) [1]. The background was linear. (b) Presented here is a comparison between the HERFD XAS results for uranium tetrafluoride and the prediction of the Th model for localized n = 2. (c) Illustrated here is a comparison between the HERFD XAS results for uranium cadmium and the prediction of the Th model for localized n = 3. See Ref 2, 3 and 5 for further detail and full citations.

[1] Y. Baer and J. K. Lang, Phys. Rev. B **21**, 2060 (1980).

[2] J. G. Tobin, S. Nowak, S.-W. Yu, P. Roussel, R. Alonso-Mori, T. Kroll, D. Nordlund, T.-C. Weng, D. Sokaras, J. Vac. Sci. Tech. A **39**, 043205 (2021), <https://doi.org/10.1116/6.0001007>.

[3] J. G. Tobin, S. Nowak, S.-W. Yu, P. Roussel, R. Alonso-Mori, T. Kroll, D. Nordlund, T.-C. Weng, D. Sokaras, J. Vac. Sci. Tech. A **39**, 066001 (2021), <https://doi.org/10.1116/6.0001315>.

[4] P. Le Pape, L. Stetten, M. O. J. Y. Hunault, A. Mangeret, J. Brest, J.-C. Boulliard, and G. Morin, Appl. Geochem. **122**, 104714 (2020).

[5] J. G. Tobin, S. Nowak, S.-W. Yu, P. Roussel, R. Alonso-Mori, T. Kroll, D. Nordlund, T.-C. Weng, D. Sokaras, J. Vac. Sci. Tech. A **40**, 033205 (2022), <https://doi.org/10.1116/6.0001754>.

[6] Y. Baer, Handbook on the Physics and Chemistry of the Actinides, edited by A. J. Freeman and G. H. Lander (North Holland, Amsterdam, 1984), Vol. 1, p. 271.

Structural characterisation of advanced Cr & Mn doped UO₂ fuels using X-ray Absorption Spectroscopy

H. Smith¹, L. T. Townsend¹, R. Mohun¹, T. Cordara¹, M. C. Stennett¹, J. F. W. Mosselmans², K. Kvashnina^{3,4}, C. L. Corkhill¹

¹ NucleUS Immobilisation Science Laboratory, Department of Materials Science and Engineering, The University of Sheffield, UK

² Diamond Light Source, Harwell Science and Innovation Campus, Didcot, UK

³ Helmholtz-Zentrum Dresden-Rossendorf (HZDR), Institute of Resource Ecology, PO Box 510119, 01314, Dresden

⁴ The Rossendorf Beamline at ESRF – The European Synchrotron, CS40220, 38043 Grenoble Cedex 9, France

Advancements in UO₂ fuel technology are key in the generation of safe and efficient nuclear energy. The doping of UO₂ with transition metals, such as Cr and Mn, provides a method for improving properties, such as increased grain size, improved plasticity, and reduced pellet-cladding interactions. All these enhanced properties result in more accident tolerant and efficient fuels. Despite the implementation of Cr and Mn-doped UO₂ technology within the nuclear industry, there is a lack of fundamental understanding surrounding the local Cr/Mn coordination environment upon incorporation into the UO₂ matrix. Furthermore, the mechanisms by which Cr/Mn are accommodated within the UO₂ lattice are not well established. Here, a variety of spectroscopic techniques, including X-ray absorption spectroscopy (XANES, EXAFS, and HERFD-XANES) and Raman spectroscopy, provide significant insight into mechanisms behind the incorporation of Cr/Mn upon incorporation into the UO₂ structure. In the Mn-doped UO₂ system, Mn²⁺ is substituted onto the U⁴⁺ site, with vacancies and U⁵⁺ forming to maintain charge balance. A similar incorporation mechanism is observed in the Cr-doped UO₂ however, the UO₂ matrix accommodates Cr as a Cr²⁺ on the U⁴⁺ site. Following further heat treatment (to simulate nuclear fuel synthesis), Cr is present as several different species (including, Cr²⁺ and Cr³⁺) in a variety of locations within the UO₂ fuel. The findings of these studies provide significant new insight into the fundamental chemistry behind doped UO₂ fuels and offer new opportunities for advanced nuclear fuels to be further developed and implemented within the nuclear industry.

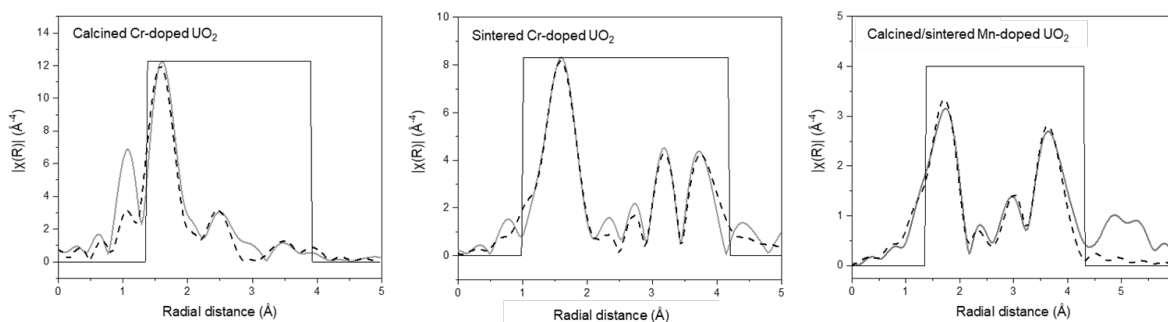


Fig. 1: Fourier transforms of the Cr & Mn K-edge EXAFS spectra for calcined and sintered Cr/Mn-doped UO₂.

Selective binding of uranyl(VI) by protein through polar and hydrophobic interactions.

S.Tsushima^{1,2}

¹ Helmholtz-Zentrum Dresden-Rossendorf (HZDR), Dresden, Germany

² Tokyo Institute of Technology, Tokyo, Japan

Interaction of protein with actinides have great importance in connection with health impact of contamination of organisms by actinides. Although interactions between uranyl(VI) and protein (or peptide) generally occur through carboxylic groups of negatively charged residues of proteins, it was also previously demonstrated that additional interaction to “yl”-oxygen of uranyl(VI) could also take place and could greatly enhance the affinity and selectivity for capturing uranyl(VI).^[1]

In this presentation, it will be demonstrated that such interactions take place also in various other examples and can enhance the affinity of uranyl(VI) to protein. In one instance, it was confirmed through molecular dynamics (MD) simulations that uranyl(VI) interacts with bovine serum albumin (BSA) protein in a specific manner so that the equatorial shell of uranyl(VI) is coordinated by three carboxylic groups from Asp307, Asp311, and Asp313 whereas additional coordination from hydrogen of isopropyl group of Val314 is also taking place. Eventually, one “yl”-oxygen of UO_2^{2+} is “soaked” into the hydrophobic core of the protein whereas the other “yl”-oxygen is surrounded by bulk waters. This coordination pattern corroborate with experimental finding that photo-illumination of uranyl(VI)-bound BSA results in the cleavage of the protein at the Va314-Cys315 site.^[2] Presumably photo-excited state of uranyl(VI) abstract hydrogen from the sidechain of Val314 resulting in the cleavage of the protein at Va314-Cys315.

In another instances, two peptides having high affinity to uranyl(VI) have been identified. A modified EF Hand of calmodulin consisting of 33 amino acids has been identified to fully “capture” uranyl(VI) ion through equatorial shell as well as through the interaction with “yl”-oxygen of UO_2^{2+} .^[3] Much shorter cyclic peptide with only 10 amino acids was also found to capture uranyl(VI) ion in the equatorial plane, and additionally hold “yl”-oxygen through hydrophobic interaction. Apparently, peptides need to be well-designed to enhance their interactions with UO_2^{2+} through electrically charged residues as well as hydrophobic ones.

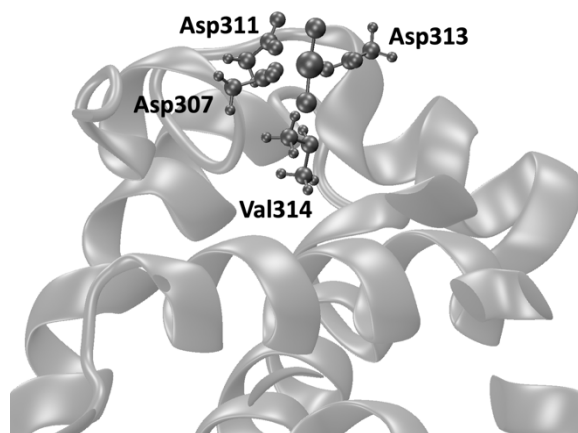


Fig. 1: Uranyl(VI) ion interaction with bovine serum albumin (BSA) as obtained by classical molecular dynamics (MD) simulations showing coordination of three carboxylic groups of Asp to the equatorial plane of the BSA as well as additional interaction between isopropyl group of Val to the “yl”-oxygen of UO_2^{2+} .

[1] Zhou, L. et al. (2014) Nat. Chem. 6, 236-241.

[2] Duff, M.R. and Kumar, C. (2006) Angew. Chem. Int. Ed. 45, 137-139.

[3] Tsushima, S. and Takao, K. (2022) Phys. Chem. Chem. Phys. 24, 4455-4461.

Exploring luminescence properties of uranyl-based complexes by TRLFS and *ab initio* method

V. Vallet^{1*}, H. Oher^{1,2}, F. Réal¹, T. Vercoouter², A. S. P. Gomes¹, Richard E. Wilson³

¹ Université Lille, CNRS, UMR8523-PhLAM- Physique des Lasers Atomes et Molécules, F-59000 Lille, valerie.vallet@univ-lille.fr

² DEN-Service d'Etudes Analytiques et de Réactivité des Surfaces (SEARS), CEA, Université Paris-Saclay, F-91191 Gif-sur-Yvette, France

³ Chemical Sciences and Engineering Division, Argonne National Laboratory, Argonne Illinois USA

Uranyl complexes have been the subject of many research works for fundamental chemistry of actinides, environmental issues, or nuclear fuel cycle processes. The formation of various uranyl complexes, with organic and inorganic ligands in solution must be characterized for a better understanding of U(VI) speciation. As uranyl-ligand interactions and the symmetry of the complexes affect the electronic structure of U(VI) and thus its luminescence properties, time-resolved laser induced fluorescence spectroscopy (TRLFS) is one of the major techniques to characterize U(VI) complexes, with high sensitivity and selectivity. However, most of the relevant systems have complex chemical composition in solution and the identification of each species from spectroscopic data is challenging.

In our study, the synergy between TRLFS and *ab initio*-based interpretation appears as a promising route for complexation data. Luminescence spectra of uranyl complexes in solution show in general a narrow energetical range about 6000 cm⁻¹ and we can identify a single electronic transition between the initial and target states with the vibrationally resolved band [1].

The main challenge consists in exploiting a computationally cheap and effective theoretical approach, in a relativistic context, to characterize the main spectral parameters of the ground and luminescent states of symmetrical uranyl compounds (*i.e.* UO₂Cl₄²⁻, UO₂F₅³⁻, UO₂(CO₃)₃⁴⁻, UO₂(NO₃)L₂) with different organic or inorganic counter ions after the photo-excitation. We will illustrate that TD-DFT with the CAM-B3LYP functional is able to provide accurate excitation/emission energies for these systems, together with accurate vibronic progressions allowing the assignment of experimental data.

As a benchmark system serving the purpose of assessing the accuracy of our theoretical protocol, the uranyl tetrachloride UO₂Cl₄²⁻ was selected because of the extensive amount of structural and spectroscopic data available [2]. A good agreement was found between ours and previously obtained theoretical data (structural parameters, orbitals nature, excitation energies) [3]; the final luminescence spectrum is in remarkable agreement with our TRLFS measurements [4]. We will also quantify the effects of organic or inorganic counterions [5, 6], along with that of first-sphere ligands that might perturb the uranyl(VI) moiety.

This work showcases how one can predict vibrationally resolved spectra to assign the recorded TRLFS data, and shed light on the relationship between the uranyl coordination and its luminescence properties.

[1] J. Visnak et al. (2006) EPJ Web Conf. 128:02002.

[2] R.G. Denning et al. (1991) Chem. Phys. Lett. 180, 101.

[3] K. Pierloot et al. (2005) J. Chem. Phys. 123, 204309.

[4] H. Oher et al. (2020) Inorg. Chem. 59, 5896.

[5] H. Oher et al. (2020) Inorg. Chem. 59, 15036.

[6] H. Oher et al. (2022) Inorg. Chem. 61, 890.

Actinide bonding properties – stability relations probed by high resolution X-ray spectroscopy

¹T. Vitova, ¹B. Schacherl, ²M. Tagliavini, ³K. Popa, ³O. Walter, ⁴L. Maron, ¹C. Vollmer, ¹N. Palina, ¹T. Prüßmann, ¹A. Beck, ¹T. Neill, ¹H. Kaufmann, ¹H. Ramanantoanina, ⁵P. Bagus, ⁵M. Mazzanti, L. ²M. Haverkort

¹Karlsruher Institut für Technologie (KIT), Hermann-von-Helmholtz-Platz 1, DE-76344 Eggenstein-Leopoldshafen, Germany

²University of Heidelberg, Philosophenweg 19, DE-69120 Heidelberg, Germany

³European Commission, Joint Research Centre, Karlsruhe, Germany

⁴LPCNO, University of Toulouse, INSA Toulouse 135, avenue de Rangueil, Toulouse cedex 31077, France

⁵Department of Chemistry, University of North Texas, Denton, Texas 76203-5017, USA

⁶Institut des Sciences et Ingénierie Chimiques, Ecole Polytechnique Fédérale de Lausanne (EPFL), 1015 Lausanne, Switzerland

Understanding the electronic structure and chemical bonding properties of the actinide (An) elements poses a great challenge [1]. The An_{4,5} absorption edges core-to-core and valence band resonant inelastic X-ray scattering (CC/VB-RIXS) and high energy resolution X-ray absorption near edge structure (HR-XANES) techniques probe the occupied and unoccupied parts of the valence band of the actinide elements with extraordinary energy resolution and thus unique information on the chemical bonding can be obtained [1]. A deep insight into the An electronic structure is for example essential to understand actinide environmental behavior. All An M_{4,5} edge RIXS and HR-XANES studies are performed at the ACT station of the CAT-ACT beamline at the KIT Light Source [2].

Spectroscopic and computational tools for probing in detail the An-ligand (U, Np, Pu or Am) bond covalency will be discussed [2-5]. Examples of applications describing the link between covalency and stability/reactivity of different actinide materials will be presented. We will address questions like for example: 1) how Fe(II) influences the electronic structure U(V)O₂¹⁺ and thus increases the U(V) stability in the environment [5]; 2) how the binding properties of equatorial ligands influence the electronic structure and stability of U, Np or Pu in solutions or solids [4, 6].

We acknowledge the funding from the European Union's Horizon 2020 research and innovation program, ERC Consolidator Grant 2020 "The ACTINIDE BOND" under grant agreement No. 847593. PSB acknowledges support by the U.S. DOE, Office of Science, Office of Basic Energy Sciences, CSGB through its Geosciences program at PNNL.

[1] Vitova, T. et al. Nature Communications 2017, 8, 16053.

[2] Schacherl, B. et al. Journal of Synchrotron Radiation 2022, 29 (1), 80-88.

[3] Bagus, P. S. et al. Inorganic Chemistry 2021, 60 (21), 16090-16102.

[4] Vitova, T. et al. Inorganic Chemistry 2020, 59 (1), 8-22.

[5] Vitova, T. et al., M. Mazzanti, L. Maron et al., submitted

[6] Neill, T. et al, in preparation

Actinide oxalates as key intermediates in actinide chemistry

O. Walter, K. Popa

¹ European Commission, DG Joint Research Centre, Directorate G - Nuclear Safety and Security, PO Box 2340, D-76125 Karlsruhe, GER

Among the existing applications engaging actinides those based on actinide materials represent the major part; so up to present the actinide oxides for nuclear based energy production are dominating the applications, but new applications are under development or applied on a smaller scale such as the application of radionuclides for medical tumour treatment

For all these possible applications at the very beginning stands the synthesis and of the actinide material. This is industrially applied in the case for the reactor fuel in the nuclear fuel cycle. But for example the synthesis of target materials for the production of radionuclides for medical applications can still be improved and developed.

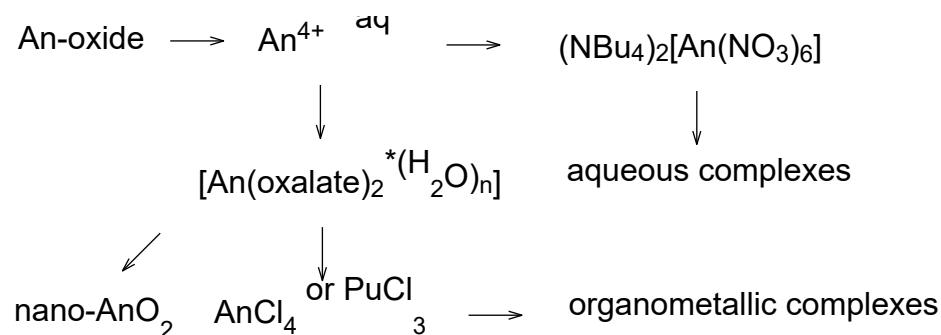


Fig. 1: Overview on the actinide chemistry based on oxides as the starting material

The starting point for all actinide chemistry and their materials is the mining from natural sources or recycling from the spent fuel. The separated actinides are normally gained in form of the oxides which are then to be re-dissolved for further transformations (Figure 1).

The presentation will briefly summarise and give an overview on what we have done to develop this kind of chemistry and showing the bridge to the materials. In more detail the main reaction pathways as depicted in Figure 1 will be explained; based on the actinide oxides as the starting point and the oxalates as one key intermediate the formation of actinide dioxide nano-materials, complexes in aqueous environment but as well organometallic complexes will be presented.

-
- [1] Dutkiewicz, M.S., Goodwin, C.A.P., Perfetti, M., Gaunt, A.J., Griveau, J.-C., Colineau, E., Kovács, A., Wooles, A.J., Caciuffo, R., Walter, O., Liddle, S.T., (2022) *Nature Chemistry*, 14 (3), pp. 342-349.
- [2] Apostolidis, C., Kovács, A., Morgenstern, A., Rebizant, J., Walter, O., (2021) *Inorganics*, 9 (6), art. no. 44, .
- [3] De Bona, E., Balice, L., Cognini, L., Holzhäuser, M., Popa, K., Walter, O., Cologna, M., Prieur, D., Wiss, T., Baldinozzi, G., (2021) *Journal of the European Ceramic Society*, 41 (6), pp. 3655-3663.
- [4] Corradetti, S., Carturan, S.M., Ballan, M., Eloirdi, R., Amador Celdran, P., Walter, O., Staicu, D., Dieste Blanco, O., Andrighetto, A., Biasetto, L., (2021) *Scientific reports*, 11 (1), p. 9058.
- [5] Radoske, T., März, J., Patzschke, M., Kaden, P., Walter, O., Schmidt, M., Stumpf, T., (2020) *Chemistry - A European Journal*, 26 (70), pp. 16853-16859.
- [6] Walter, O., (2019) *Chemistry - A European Journal*, 25 (12), pp. 2927-2934.

Selective Am(III)-(V) oxidation by multiphoton excitation

T. Yaita¹, Y. Matsuda¹, K. Yokoyama¹, T. Okane¹

¹ Japan Atomic Energy Agency, 1-1-1 Kouto Sayo-cyo, Sayo-gun, Hyogo 679-5148, Japan

Neighboring lanthanides and actinides with the same valence are recognized as a chemically similar group of elements because there is almost no difference in their ionic radii (Tb^{3+} - Dy^{3+} : 0.01Å, Am^{3+} - Cm^{3+} : 0.02Å) and the electron configuration in the outermost shell is identical. A group of series elements filling electrons in the f orbitals of the inner shell, the absorption bands originating from dipole forbidden f-f transitions have an extremely sharp band structure like atomic orbitals. Therefore, it seems possible in principle to induce oxidation reactions based on selective electronic excitation reactions by utilizing this band, which does not overlap with other elements. Thus, our research group has been conducting experiments to induce selective oxidation reactions of targeted elements through multiphoton excitation, in which dipole forbidden f-f transitions followed by allowed f-d transitions are continuously induced, as shown in Fig. 1. In this study, we focused on the oxidation reaction of Am(III), which is under investigation as a separation method from high-level liquid waste, and tried to detect the oxidation reaction of Am(III) by irradiating Am(III) with a precisely tuned short-pulse laser.

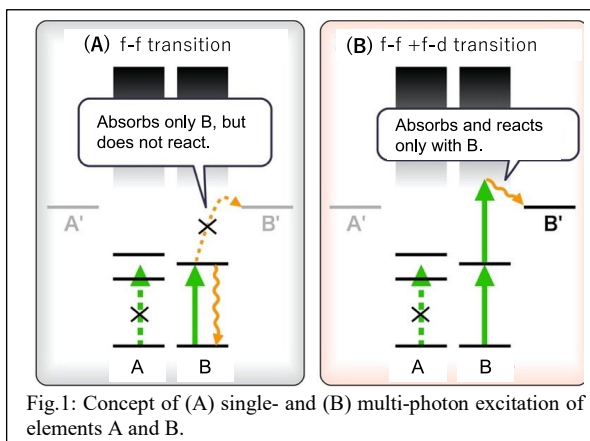


Fig.1: Concept of (A) single- and (B) multi-photon excitation of elements A and B.

For the experiments, 0.4 mM $^{234}\text{Am}(\text{III})$ was prepared with various concentrations of nitric acid, injected with a micropipette into a screw-capped quartz cuvette, and sealed. The sample volume in the cuvette was $2 \times 5.2 \times 10 \text{ mm}^3$ and the optical path length was 10 mm. A nanosecond OPT laser (EKSPLA NT342B, $\sim 5 \text{ ns}$, $< 34 \text{ mJ}$, 10 Hz) was used to excite Am(III). The energy of the laser pulse was measured using a power detector (Gentec electro-optics, UP19K-30H-VH) coupled to a power monitor (Gentec electro-optics, TPM-300-CE). Valence identification was performed using a UV-visible spectrophotometer (JASCO V-670); the typical absorbance at 503 nm was measured to be 0.15. Nd-L3 EXAFS experiments at similar solution concentrations were performed to perform speciation of Am in nitric acid solutions at the BL22XU of SPring-8.

A part of the result is shown in Fig. 2A, where the decrease of Am(III) at 503 nm and the increase of Am(V) peak at 715 nm were observed by laser irradiation at 503 nm, and the oxidation reaction of $\text{Am}(\text{III}) \rightarrow \text{Am}(\text{V})$ was observed for the first time. Fig. 2B shows the slope analysis for the dependence of the reaction rate on laser power. The slope exceeds 1, indicating that the oxidation reaction is due to more than one photon absorption, i.e., multiphoton absorption such as f-f+f-d transitions. At the same time, the formation of nitrite was also observed. Nd-L3 EXAFS analysis further showed that the oxidation is most efficient when an almost 1:1 complex is formed. Thus, the oxidation reaction by multiphoton excitation was successfully detected. This oxidation reaction by multiphoton excitation caused oxidation of only Am. No oxidation other than that of Am has been observed for Am in solutions containing various lanthanides and actinides. Advancement of this technique may have a great impact on the next generation of separation chemistry, including the reduction of secondary wastes and separation processes.

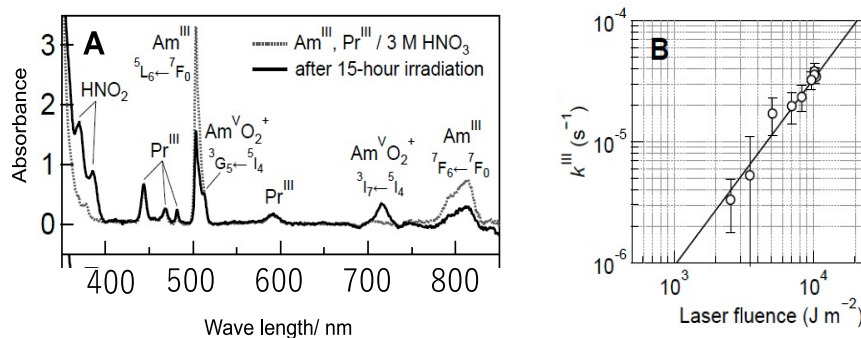


Fig. 2A: Absorption spectrum of Am and Pr in nitrate solution before and after Laser irradiation at 503nm; B Slope analysis of rate constant of oxidation reaction of Am(III)-Am(V) against Laser fluence.

[1] Mstuda. et al. (2022) *Science Advances*, 8, 1-11.

Chemical Bonding and Electronic Structure Enabled by 5f-Electrons

Ping Yang, Enrique Batista, Rebecca Carlson, Andrew Gaunt, Stosh A Kozimor, Ivan A. Popov, Jing Su, Aaron Tondreau

Los Alamos National Laboratory, Los Alamos, NM 87545, USA
 pyang@lanl.gov

The complicated electronic structure of actinide complexes leads to their versatility of chemical bonding, reactivity, and spectral properties. Advances in high-performance computing and quantum chemistry have greatly accelerated the understanding of complex systems at the molecular level. In this talk, I will present our recent work on the novel chemical bonding and spectroscopy of heavy elements across the actinide series using advanced quantum chemical techniques. Our close collaboration with experimental teams has demonstrated that the synergy between theory and experiments can greatly accelerate the understanding of f-orbital participation in chemical bonding.

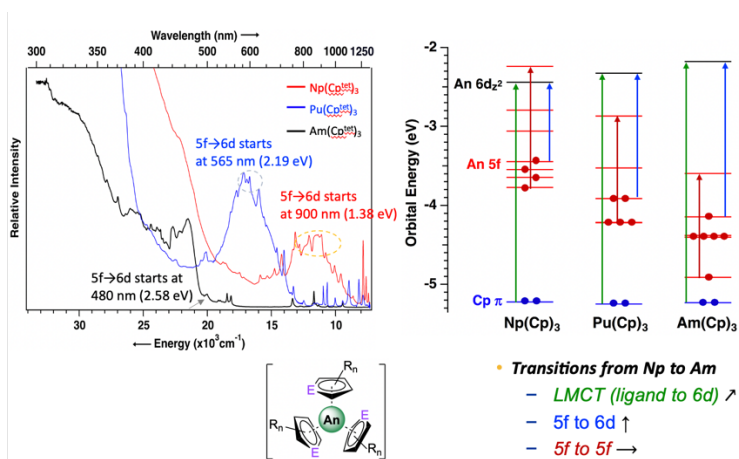


Figure 1. Frontier molecular orbital energy level diagram for An-complexes and their UV-Vis spectra. [3]

1. MP Kelley, IA Popov, J Jung, ER Batista, P Yang, Nature Communication, 2020, 11, 1558
2. CAP Conrad, J Su, *et al.* Nature, 2021, 599, 7885, 421-424
3. J Su, ER Batista, P Yang, Rare Earth Elements and Actinides: Progress in Computational Applications, 2021, Chapter 14, pg 283-327
4. J Su, T Cheisson, A McSkimming, CAP Goodwin, I DiMucci, T Albrecht-Schoenzeit, B Scott, ER Batista, A Gaunt, SA Kozimor, P Yang, EJ Schelter, Chemical Science. 2021, 12, 13343-13359
5. J Su, ER Batista, P Yang, *et al.* Journal of the American Chemical Society, 2018, 140, 17977-17984
6. CAP Conrad, J Su, *et al.* Angew Chem Int Ed, 2019, 58, 11695-11699
7. IA Popov, BS Billow, SH Carpenter, ER Batista, JM Boncella, PM Tondreau, P Yang, Chem Eur J, 2022, e202200114

5th International
Workshop on Advanced
Techniques in Actinide
Spectroscopy



9th Workshop on
Speciation, Techniques
and Facilities for
Synchrotron Radiation

Poster Abstracts

Poster number	Name	First Name	Laboratory	Poster Title
P-1	BAZARKINA	Elena	Helmholtz-Zentrum Dresden-Rossendorf (HZDR)	Exploring actinide state and properties with HERFD
P-2	BES	Rene	University of Helsinki	The Center for X-ray Spectroscopy: a new XAS/XES facility at the University of Helsinki
P-3	CHIORESCU	Ion	Technische Universitaet Muenchen	On the Sorption mode of Actinide ions at Calcium Silicate Hydrate: An Exemplary Density Function Study for U(IV)
P-4	DARDENNE	Kathy	Karlsruhe Institute of Technology	Combining Tc K /L3 edge X ray absorption spectroscopy and ab initio calculations of Tc redox speciation in complex aqueous systems: A success story.
P-5	JESSAT	Isabelle	Helmholtz-Zentrum Dresden-Rossendorf	Spectroscopic investigations of the U(VI) sorption onto the zircaloy corrosion product ZrO2
P-6	LESSING	Jessica	Helmholtz-Zentrum Dresden-Rossendorf (HZDR)	Influence of the competition of Al on the retention of trivalent actinides and their homologues in orthoclase.
P-7	MENUT	Denis	Synchrotron Soleil	Enhanced X-Ray Diffraction and Total Scattering opportunities at the MARS beamline
P-8	MISAEAL	Wilken	CNRS UMR 8523 - USTL	X-ray Absorption Spectra and Photoionization of Actinide Compounds with Relativistic Electronic Structure Approaches
P-9	MUELLER	Katharina	Helmholtz-Zentrum Dresden-Rossendorf (HZDR)	A mechanistic view on curium(III) sorption on natural K-feldspar surfaces
P-10	OHER	Hanna	CNRS UMR 6226 - Université Rennes 1	Chemistry and speciation of protactinium – a first principles study
P-11	ORLAT	Simon	University of Helsinki	Combining U L3 HERFD-XAS and FDMNES computations to study the uranium electronic structure in MUO3 (M = K, Na and Rb)
P-12	ROTHE	Joerg	Karlsruhe Institute of Technology	XAFS investigation of fission and activation products in irradiated light water reactor fuels
P-13	RUIZ FRESNEDA	Miguel Angel	Universidad de Granada	Biological reduction of selenate in the deep geological repository case (DGR): a spectroscopic and microscopic study.
P-14	SMITH	Patrick	Lawrence Berkeley National Laboratory	Covalency in UX6n- (X = F, Cl, Br; n = 1, 2) Complexes Probed Using Ligand- and Metal-Based XAS
P-15	SOLARI	Pier Lorenzo	Synchrotron Soleil	How to get to MARS?
P-16	VEJAR	Manuel	University of Notre Dame	Uptake and reduction behavior of plutonium on Al-substituted hematite (α -Fe2O3) and goethite (α -FeOOH)
P-17	VOLLMER	Christian	Karlsruhe Institute of Technology (KIT)	Bonding properties of uranium carbonate species in liquid and solid state in multiple oxidation states studies by U M4-edge high resolution X-ray spectroscopy
P-18	ZIMMERMANN	Thomas	Helmholtz-Zentrum Dresden-Rossendorf (HZDR)	Investigating the complex interaction of technetium with magnetite nanoparticles

Exploring actinide state and properties with HERFD

E.F. Bazarkina^{1,2}, K.O. Kvashnina^{1,2}

¹ Rossendorf Beamline at ESRF – The European Synchrotron, CS40220, 71 Avenue des Martyrs, 38043 Grenoble Cedex 9, France

² Institute of Resource Ecology, Helmholtz Zentrum Dresden-Rossendorf (HZDR), PO Box 510119, 01314 Dresden, Germany

High-Energy Resolution Fluorescence Detection (HERFD) is a powerful technique for the exploration of the properties and state of actinides, lanthanides, and other elements. The principles of HERFD are based on the selection of emitted fluorescence with an X-ray emission spectrometer with the help of crystal analyzers. The X-ray emission spectrometer recently developed at ROBL [1] is equipped with 5 crystal analyzers and has 2 possible configurations (0.5m and 1m). The main advantages of HERFD were discussed in many contexts in literature [1, 2]. For actinides, the most important aspects are:

1) Near-zero background counts of HERFD allow to decrease in the detection limit on the one hand, and, on the other hand, to study complex systems with the main constituents of the matrix with overlapping fluorescence and/or the scattering signal. Both XANES and EXAFS spectra can be measured in samples for which total fluorescence measurements are not efficient.

3) The use of HERFD at $M_{4,5}$ edges in actinides (i.e. tender X-rays) allows probing f electrons, i.e. fingerprinting of the oxidation state of the actinides. The maximum of $M_{4,5}$ HERFD-XANES spectra is shifted by energy with oxidation state [3, 4, 5].

4) Better energy resolution of HERFD-XANES spectra improves the accuracy of XANES quantitative analyses. For example, the Ce(III)/Ce(IV) mixture with low Ce(IV) can be accurately quantified by HERFD-XANES [6, 7].

5) Energy position of the fluorescence lines (and especially the $K\beta$ ones) provides better energy resolution of the recorded XANES transitions. For example, HERFD-XANES at the $L\beta_5$ emission line of U allows to resolve the crystal field splitting in UO_2 [5, 8].

6) With the help of an emission spectrometer, other spectroscopic techniques such as valence-to-core XES or RIXS can be applied to better discriminate between the different ligands in the first coordination sphere of actinides [9, 10].

This work was supported by ERC grant 759696.

[1] Kvashnina, K. O. and Scheinost, A. C. (2016) *J. Synchrotron Radiat.* 3, 836–841.

[2] Proux O. et al. (2017) *J. Environ. Qual.* 46, 1146–1157.

[3] Kvashnina, K.O. et al. (2013) *Phys. Rev. Lett.* 111, 253002.

[4] Kvashnina, K.O. and Butorin, S. M. (2022) *Chem. Commun.* 58, 327–342.

[5] Kvashnina, K.O. et al. (2014) *J. of Elect. Spectros. and Relat. Phenom.* 194, 27-36.

[6] Cafun J.-D. et al. (2017) *ACS Nano*, 2013, 7, 10726–10732.

[7] Plakhova, T.V. et al. (2019) *Nanoscale*, 2019, 11, 18142-18149.

[8] Kvashnina, K.O. et al (2015) *Anal. Chem.* 87, 8772-8780.

[9] Kvashnina, K.O. and De Groot, F.M.F. (2014) *J. of Elect. Spectros. and Relat. Phenom.* 194, 88-93.

[10] Butorin, S.M. (2021) *J. Chem. Phys.* 155, 164103.

The Center for X-ray Spectroscopy: a new XAS/XES facility at the University of Helsinki

R. Bes^(1,2)

¹ Department of Physics, University of Helsinki, P.O. Box 64, FI-00014 Helsinki, Finland

² Helsinki Institute of Physics, Department of Physics, University of Helsinki, P.O. Box 43, FI-00014 University of Helsinki, Finland

X-ray absorption spectroscopy (XAS) and emission spectroscopy (XES) have demonstrated themselves as an essential approach for the study of actinide materials in various research fields from chemistry, physics, biology, geosciences and environmental research. However, conventionally implemented at beam lines in synchrotron radiation sources, those techniques are bearing the constraints of synchrotron highly competitive and limited access. Therefore, numerous studies, especially routine experiments, are suffering from the lack of a credible alternative in the laboratory.

During the last decade, and especially in the last few years, several important efforts were made in developing laboratory-based spectrometers to implement XAS techniques at laboratory level [1, 2]. Today, these nascent laboratory instruments are opening new research opportunities, and they are attracting continuously increasing interest from laboratories worldwide, notably thanks to their commercial availability [3].

Fully aware of those opportunities and limitations, the Center for X-ray Spectroscopy was created at the University of Helsinki [4]. This new facility aims to increase XAS and XES usage at laboratory by enhancing its teaching and learning from experiment preparation to data analysis/modeling, by allowing routine experiments to be performed and by ultimately acting as a unique facility opened to external users, as a complement to synchrotron radiation facilities.

In this contribution, the facility mission and values will be described, as well as our available spectrometers, the on-going instrumental developments, all illustrated by few example of applications.

[1] Seidler et al. Review of Scientific Instruments 85 (2014).

[2] Honkanen et al. Review of Scientific Instruments 90 (2019).

[3] <http://easyxafs.com>

[4] <https://www2.helsinki.fi/en/infrastructures/center-for-x-ray-spectroscopy>

On the Sorption mode of Actinide Ions at Calcium Silicate Hydrate: An Exemplary Density Function Study for U(IV).

I. Chiorescu,¹ A. Kremleva,¹ S. Krüger¹

¹ Theoretische Chemie, Technische Universität München, 85748 Garching, Germany

U(IV) has been chosen as an exemplary actinide ion to study actinide sorption at cement. Uranium is the main actinide element in highly active radioactive waste and under long-term reducing conditions of a geological repository for highly radioactive waste U(IV) will be the dominant oxidation state. In such a repository, cement will be introduced as construction and barrier material as well as as a matrix of solidified waste. Thus, the interaction of actinides with cement in its typical high pH environment will be of interest to understand their chemical reactions and potential of dissipation and migration. Calcium silicate hydrate (CSH) is the main product of cement hydration and has been shown to be the essential sorbing phase for actinide ions interacting with cement [1,2]. We

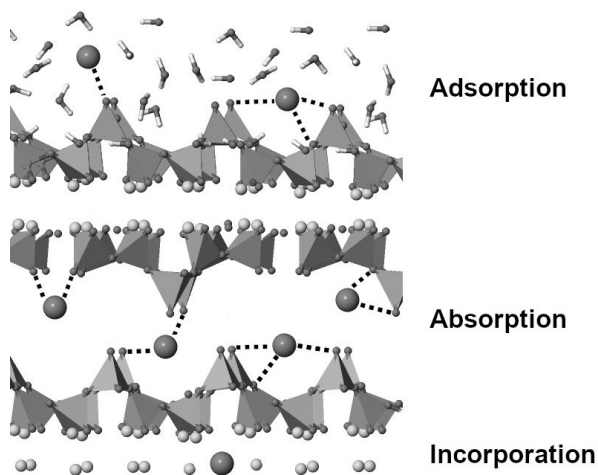


Fig. 1: Structure of calcium silicate hydrate with exemplary sorption sites of U(IV) indicated as large balls.

modeled CSH with a tobermorite like structure (Fig. 1), which is accepted for lower Ca/Si ratios of aged cement. Tobermorite shows a layered structure consisting of CaO sheets decorated on both sides with silica chains (Fig. 1). For this mineral structure we considered U(IV) sorption at a (001) surface, absorption of U(IV) in the interlayer, and incorporation into the CaO layer of CSH. Various sorption sites for each sorption mode have been modeled quantum mechanically, applying a density functional approach. A combined dynamic equilibration and optimization approach has been used to generate a set of representative stable sorption complexes, including defect sites.

U(IV) sorbs as hydroxo complex with 2-5 ligands. Comparison of energies shows a tendency to monodentate coordination to the substrate for adsorption and absorption. Surface adsorption tends to be preferred over absorption in the interlayer, probably because this sorption mode provides more steric flexibility. Incorporation of U(IV) in the CaO layer yields the most favorable sorption site and a second one, which is degenerate with the favorable surface adsorption site. This result is supported by qualitative agreement of structures with EXAFS results for other actinides in the oxidation state IV. Calculated average U-O distances are in good agreement with measured ones for Np(IV) [2] and Pu(IV) [3] for a coordination number (CN) of 6, while a CN of 8 has been measured. U-O distances for U(IV) incorporation show a CN of 7 and overestimate the measured values by about 5 pm. Four measured U-Si distances of about 360 pm are in good agreement with the longer ones of 5-6 calculated U-Si distances for U incorporation, while for other sorption modes only 1-2 of these distances have been obtained. The experiment for Pu(IV) provides in addition two short U-Si distances of about 320 pm, fitting the shortest of the calculated ones for U(IV) incorporation. For adsorption and absorption only 1-4 U-Ca distances are obtained. U(IV) incorporation yields 6 of them, which is more compatible with the experimental result of 8. 3-4 of these distances are close to the measured result of about 415 pm.

Sorption of Np(IV) at CSH has previously been interpreted in favor of interlayer adsorption [1]. Our structure results show instead the best agreement with experiment for U(IV) incorporation in the CaO layer of CSH. This interpretation is supported by sorption energies, suggesting incorporation of U(IV) as the main sorption mode in CSH.

[1] Macé, N.; Wieland, E.; Dähn, R.; Tits, J.; Scheinost, A. C. (2013) *Radiochimica Acta* 101, 379-389.

[2] Gaona, X.; Dähn, R.; Tits, J.; Scheinost, A. C.; Wieland, E. (2011) *Environmental Science & Technology* 45, 8765-8771.

[3] Reich, T. private communication.

Combining Tc K-/L₃-edge X-ray absorption spectroscopy and ab initio calculations of Tc redox speciation in complex aqueous systems: A success story

K. Dardenne, N. DiBlasi, S. Duckworth, R. Polly, X. Gaona, T. Pruessmann, J. Rothe, M. Altmaier, H. Geckeis

¹ Institute for Nuclear Waste Disposal (INE), Karlsruhe Institute of Technology, P.O. Box 3640, D-76021 Karlsruhe, Germany

⁹⁹Tc is a low energy beta emitter with a high fission yield from both ²³⁵U (~6.1%) and ²³⁹Pu (~5.9%). Its long half-life ($t_{1/2} = 2.121 \times 10^5$ a) and large inventory in spent nuclear fuel, makes it a radionuclide of particular interest in the context of safety assessment of repositories for radioactive waste. Many small organic molecules capable of strong aqueous complexation interactions, such as gluconate (GLU), citrate, and ethylenediaminetetraacetic acid (EDTA), may be present in nuclear waste disposal scenarios which can potentially increase the solubility and mobility of Tc. For these reasons, it is essential to understand the impact of complexing organic ligands on the speciation and oxidation state of Tc under relevant boundary conditions.

A new setup for “tender” X-ray spectroscopy (spectral range ~2–5 keV) in transmission or total fluorescence yield detection mode based on a He flow cell has been developed at the INE-Beamline for radionuclide science (KIT Light Source, KIT, Germany). This setup allows handling of radioactive specimens with total activities up to one million times the exemption limit. For the first time, Tc L₃-edge X-ray absorption near edge structure (XANES) measurements (~2.677 keV) of Tc species in liquid (aqueous) media are reported [1], clearly outperforming conventional K-edge spectroscopy as a tool to differentiate Tc oxidation states and coordination environments.

In the gluconate system, the combination of wet-chemistry experiments (measurements of pH, E_h, and [Tc]) and advanced spectroscopic techniques (K- and L₃-edge X-ray absorption fine structure spectroscopy) confirms the formation of a very stable Tc(V)–gluconate complex under anoxic conditions, whereas Tc(IV)-GLU complexes dominate the aqueous speciation of Tc under reducing conditions [1].

In this contribution, we report on a series of Tc oversaturation solubility studies under reducing, anoxic conditions coupled with spectroscopic measurements and theoretical calculations. The same methodology as applied for the Tc-GLU system is used to investigate two additional organic ligands (L) with relevance for repository conditions: L = EDTA and citrate. Tc is added to the aqueous solutions as NaTc(VII)O₄ and reacted at constant pH = 9, ionic strength (0.7 M NaCl-NaOH-Na_xL), and ligand concentration (100 mM), employing SnCl₂ as a redox buffer. Long-term equilibrated solutions are analyzed by pH and E_h measurements, liquid scintillation counting to determine aqueous Tc concentration, UV-Vis-NIR spectroscopy as well as Tc K- and L₃-edge XANES for selected samples.

The coupling of L₃-edge XANES spectroscopy measurements and relativistic multiconfigurational ab initio methods opens new perspectives in the definition of chemical and thermodynamic models for Tc species of relevance in the context of nuclear waste disposal, environmental remediation or pharmaceutical applications.

Acknowledgements: This work is partly funded by the German Federal Ministry for Economic Affairs and Climate Action (BMWK) within the framework of the VESPAII project (02E11607C). We thank the Institute for Beam Physics and Technology (IBPT) for the operation of the storage ring, the Karlsruhe Research Accelerator (KARA).

[1] Dardenne, K. et al. (2021) Inorg. Chem. 60, 12285-12298.

Spectroscopic investigations of the U(VI) sorption onto the zircaloy corrosion product ZrO₂

I. Jessat¹, H. Foerstendorf¹, K. Heim¹, A. Rossberg^{1,2}, A. Scheinost^{1,2}, T. Stumpf¹, N. Jordan¹

¹ Helmholtz-Zentrum Dresden-Rossendorf, Institute of Resource Ecology, Bautzner Landstraße 400, 01328 Dresden, Germany

² Rossendorf Beamline at ESRF - European Synchrotron Radiation Facility, CS40220, 38043 Grenoble Cedex 9, France

For a safety assessment of a repository for nuclear waste, the interactions of actinides with corroded phases in the near-field must be taken into account. Most commercial fission reactors use uranium-based fuels and the spent nuclear fuel still contains approximately 95 % of uranium, making it the largest fraction of the spent nuclear fuel by mass. Zirconia (ZrO₂) is the main corrosion product of the zircaloy cladding material of nuclear fuel rods and can act as a first barrier against the release of mobilized radionuclides from the spent nuclear fuel into the environment. Furthermore, the complexation of dissolved radionuclides with common inorganic ligands, such as carbonate, in the groundwater can have a significant influence on the formation and structure of actinide surface species and thus their mobility in the environment.

In situ Attenuated Total Reflection Fourier Transform Infrared Spectroscopy (ATR FT-IR) and Extended X-ray Absorption Fine Structure Spectroscopy (EXAFS) were applied to investigate the U(VI) speciation at the ZrO₂-water interface. A pH-dependent speciation of U(VI) at the zirconia surface could be observed under inert gas conditions with EXAFS and the preliminary results indicated the presence of two inner-sphere U(VI) surface species with different structural environments. The EXAFS results can be compared to the literature results of Lomenech et al., where also two U(VI) surface species on the ZrO₂ surface were observed (a tridentate U(VI) surface species at pH 3 and a bidentate surface species at higher pH) [1,2].

The sorption of U(VI) onto ZrO₂ under inert gas conditions was also studied with ATR FT-IR at pH 3.5 and 5.5 and a pH-dependent U(VI) speciation was observed, supporting the findings from the EXAFS investigations. The observed red shift of the asymmetric stretching vibration of the free uranyl aqua ion ($\nu_3(\text{UO}_2^{2+})$) in the presence of ZrO₂ at pH 5.5 was due to the U(VI)-ZrO₂ interactions. At a lower pH of 3.5 a second U(VI) surface species with a less pronounced red shift of the ν_3 vibration was identified. A pH-dependence of the sorption of atmospheric carbonate on the zirconia surface was observed and a spectral splitting ($\Delta\nu$) of approximately 200 cm⁻¹ of the symmetric and asymmetric stretching vibration modes indicated the presence of bidentate bound carbonate species on the surface. The U(VI) sorption onto zirconia pre-equilibrated with atmospheric carbonate was also studied at pH 5.5 and 3.5. Compared to the experiments conducted under inert gas conditions, the red shift of the ν_3 mode of U(VI) at pH 5.5 was more pronounced in the presence of carbonate, indicating an influence of carbonate on the formed U(VI) surface species. In addition, changes in the frequency of the asymmetric and symmetric stretching vibrations of carbonate sorbed to the zirconia surface were observed in the presence of U(VI), also hinting towards structural changes in the surface species.

EXAFS and ATR FT-IR investigations provided valuable structural information about the formed U(VI) sorption species on the ZrO₂ surface in the presence and absence of carbonate. The improved molecular level understanding of such sorption processes will enable more reliable predictions of the environmental fate of U(VI). Such results will be complemented with batch sorption experiments as well as thermodynamic surface complexation modeling.

[1] Lomenech, C. et al. (2003) *Radiochim. Acta* 91(8), 453-461.

[2] Lomenech, C. et al. (2003) *J. Colloid Interface Sci.* 261(2), 221-232.

Influence of the competition of Al on the retention of trivalent actinides and their homologues in orthoclase

J. Lessing,¹ M. Schmidt,¹ T. Stumpf¹

¹ Helmholtz-Zentrum Dresden-Rossendorf e.V., Institute of Resource Ecology, Bautzner Landstraße 400, 01328 Dresden, Germany, email: j.lessing@hzdr.de

Most countries worldwide consider disposal in a deep geological formation as the safest concept for nuclear waste disposal. For a realistic safety assessment of such a repository, understanding the mechanisms of the prevalent retention processes is of utmost importance. Sorption of radioactive elements on many minerals is well described in literature, but there is a lack of data regarding the influence of other natural cations especially Al^{3+} [1]. These cations will be present in all scenarios as Al^{3+} is the third most common element (following O and Si) in the earth crust, and will occur locally e.g. due to the dissolution of minerals (especially alumino-silicates). Its concentration can be expected to exceed that of the actinides manifold. In addition to competition for sorption site, Al^{3+} can then also re-precipitate on a primary mineral's surface and form a secondary phase, which will impact the interaction of the radionuclides with these minerals.

Alumino-silicates, such as feldspars (orthoclase) and mica, together with quartz are the main components of crystalline rock, which is considered as possible host rock for radioactive waste repositories. The other common option are clay formations, which also consist of alumino-silicate minerals. The retention of trivalent actinides by feldspars was already investigated thoroughly [2,3]. The minor actinides (Np, Am, and Cm) as well as plutonium dominate the radiotoxicity of spent nuclear fuel over geological time scales. Am and Cm are predominantly trivalent in aqueous solution and Pu is also expected to occur at least partly in its trivalent state, due to the expected reducing conditions in deep geological formations. The less radiotoxic lanthanide Eu^{3+} is often used as homologue for the trivalent actinides with excellent luminescence properties.

Here, we study the effect of dissolved Al^{3+} on the retention of trivalent actinides (Cm^{3+}) and lanthanides (Eu^{3+}) on orthoclase. The quantitative effect of different $[\text{Al}^{3+}]$ on actinide retention was first evaluated in batch sorption experiments using Eu^{3+} as an analogue. For further analysis on a molecular level, time resolved laser spectroscopy (TRLFS) was applied, from which information about the formed surfaces complexes can be gained. We will discuss the results with respect to the impact of Al^{3+} on quantity and speciation of An^{3+} sorption on feldspars.

The derived speciation and quantitative retention data is foreseen to be implemented into a surface complexation model, with parameters available in thermodynamic databases. Ultimately this will provide a better understanding of the fundamental mechanisms of sorption process of the minor actinides Am and Cm on naturally occurring mineral phases under close to natural conditions.

[1] Fendorf, S. et al. (1994) World Congr. Soil Sci., No. VI.

[2] Neumann, J. et al. (2021) J. Colloid Interface Sci. 591, 490-499.

[3] Lessing, J. et al. (2022) in preparation.

Enhanced X-Ray Diffraction and Total Scattering opportunities at the MARS beamline

D. Menut¹, M. O. J. Y. Hunault¹, P.L.Solari¹

¹ Synchrotron SOLEIL, L'Orme des Merisiers, Saint-Aubin, BP 48, 91192 Gif-sur-Yvette Cedex, France

The MARS beamline provides two different experimental stations to investigate actinides and/or fission-products that are formed in materials after neutron-irradiation for experiment and/or during their industrial use within an energy range of 3 – 35 keV.

The four-circle high-resolution diffractometer is equipped for both high-resolution powder diffraction as well as surface-sensitive techniques. Thus, powder diffraction in the direct space to investigate structural modification, high resolution surface analyses with combined texture and residual-stress analysis, reflectometry and reciprocal space maps (in 2D and 3D measurements) can be operated. In routine operation, two banks of twelve Tl(NaI) scintillator detectors are scanned to measure the diffracted intensity as a function of 2θ . Each detectors is preceded by an Ge(111) analyser crystal and each channel are nominally $2,6^\circ$ apart to cover a full angular range of $67,5^\circ$. Even though well established, this high-resolution detector presents a few drawbacks. In particular, the axial acceptance of the detectors behind the analyser crystals plays a significant role limiting the quality of the data. In order to mitigate these problems if irradiation spectrum of the sample does not require the use of analyzer crystals as bandpass filter, a 2-dimensionnal Hybrid Photon Counting detector can be operated simultaneously between banks of analyzer.

This arrangement offers new possibilities in terms of data handling and processing as for instance complex microstructure disentangled (i.e. coexistence of larger single-crystal grains and powder diffraction signals). Fast shutters set up on the incident X-ray beam are controlled by a feedback loop to protect detectors from too intense reflections during goniometer and detector movements in the reciprocal space.

The XAFS end station hosting a new motorised detector support opens capabilities for multimodal *in situ* analyses by combining X-ray Fluorescence detection with X-ray Diffraction and total scattering SAXS/WAXS measurements with the use of a Pilatus 2M and a He-flushed flying tube.

The enhanced X-ray diffraction and total scattering opportunities to characterize phases in radioactive materials at the MARS beamline will be illustrated with results from neutron irradiated austenitic and zirconium-based claddings [1], UO₂ fuels (powder-like and single-crystal analysis), Pu(IV) intrinsic colloids [2, 3] and simulated corium [4] analysis.

[1] Menut, D. et al. (2015) J. Mater. Res. 30(9), 1392-1402.

[2] Micheau, C. et al. (2020) Environ. Sci. Nano. 7, 2252.

[3] Dumas, T. et al. (2022) J. Synchrotron Rad. 29, 30-36.

[4] Jizzini, M et al. (2022) Nuclear Materials and Energy 31, 101183.

X-ray Absorption Spectra and Photoionization of Actinide Compounds with Relativistic Electronic Structure Approaches

W. A. Misael¹, A. S. P. Gomes¹

¹ Université de Lille, CNRS, UMR 8523 – PhLAM – Physique des Lasers, Atomes et Molécules, F-59000 Lille-France.

Actinides are used in several fields of science and technology, e.g., as catalysts in chemical processes, fuel in nuclear plants, among other applications [1]. In order to characterize their electronic structure and morphology one often employs spectroscopic techniques, and given their great sensitivity and selectivity, X-ray spectroscopies have been playing a major role in the investigation of actinide-containing materials.

Within this context, due its physical chemistry proprieties, uranium complexes have been used as a probe to explore phenomena at the bottom of the period table. And with the development and introduction of advanced instrumentation and X-ray spectroscopic techniques in light sources in recent years it has become possible to go even further in the acquisition of data to explore these materials, with techniques such as High Energy Resolution Fluorescence Detected X-ray Absorption Near Edge Structure (HERFD-XANES) and Resonant Inelastic X-ray Scattering (RIXS) being useful in the investigation of phenomena ranging from soft to hard X-rays [2]. However, analyzing such spectra requires robust theoretical models capable of describing the electronic structure of these species in both ground and excited states, always including a proper description of the electronic correlation and relativistic effects embedded in these heavy species [3,4].

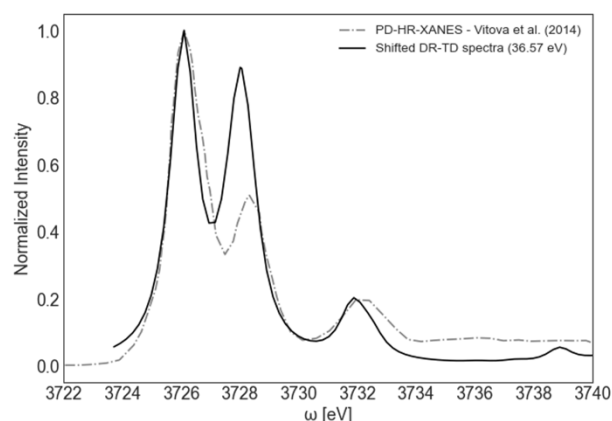


Fig. 1: U M_4 -edge XANES spectra. Experimental data digitalized from [8].

In this work we employ the Core–Valence-Separated Equation-of-Motion Coupled-Cluster Singles and Doubles (CVS-EOM-CCSD) framework [5] recently implemented in the DIRAC code [6] and Time-Dependent Density Functional Theory (TD-DFT) calculations to investigate the core excited and ionized states of the uranyl ion (UO_2^{2+}) in the gas phase and in the $Cs_2UO_2Cl_4$ crystal, the latter being treated with the frozen density embedding (FDE) method, as previously done for valence processes [7].

Our calculations are in accordance with previous experimental and theoretical reports, showing first the importance of the Hamiltonian in order to obtain qualitative results at O K -, U M_4 - and U L_3 -edges, and second that embedded models can adequately reproduce the interaction of the uranyl ion and its equatorial ligands in the crystal environment for core states.

-
- [1] Jennifer Leduc et al. In: ACS Catalysis 9.6 (2019), pp. 4719–4741.
 [2] JG Tobin et al. In: Surface Science 698 (2020), p. 121607.
 [3] RG Denning. In: The Journal of Physical Chemistry A 111.20 (2007), pp. 4125–4143.
 [4] Lan Cheng. In: The Journal of chemical physics 151.10 (2019), p. 104103.
 [5] Loic Halbert et al. In: Journal of Chemical Theory and Computation 17.6 (2021), pp. 3583–3598.
 [6] Trond Saue et al. In: The Journal of Chemical Physics 152.20 (2020), p. 204104.
 [7] ASP Gomes et al. In: Physical Chemistry Chemical Physics 15.36 (2013), pp. 15153–15162.
 [8] T Vitova et al. In: Inorganic chemistry 54.1 (2015): 174–182.

A mechanistic view on curium(III) sorption on natural K-feldspar surfaces

M. Demnitz,¹ S. Schymura,² J. Neumann,^{1,3} M. Schmidt,¹ T. Schäfer,⁴ T. Stumpf,¹ K. Müller^{1*}

¹ Helmholtz-Zentrum Dresden-Rossendorf e.V., Institute of Resource Ecology, Bautzner Landstraße 400, 01328 Dresden, Germany

² Helmholtz-Zentrum Dresden-Rossendorf e.V., Institute of Resource Ecology, Research Site Leipzig, 04318 Leipzig, Germany

³ Current address: Argonne National Laboratory, Chemical Science and Engineering Division, 9700 S Cass Ave, Lemont, IL 60439, United States

⁴ Friedrich-Schiller-Universität Jena, Institute for Geosciences, Burgweg 11, 07749 Jena, Germany

For a reliable safety assessment for future deep underground repositories for highly active nuclear waste a comprehensive understanding of the radionuclide retention by the surrounding host rock is required. Several parameters such as mineral heterogeneity and surface roughness, as well as pore water chemistry, influence radionuclide retention. Although many studies have been performed to investigate individual parameters, their interplay with each other is not yet well understood.

In our study, we focus on the sorption of trivalent curium on K-feldspar, a representative for the large alkali feldspar fractions contained in most crystalline rocks. We use cleaved macroscopic K-feldspar crystals and perform experiments at different pH values (5.5 and 6.9) to determine its impact on surface sorption with varying surface roughness. Furthermore, we investigate a K-feldspar mineral grain, which is part of a complex heterogeneous crystalline rock, obtained from the Grimsel Test Site.

To assess the sorption dependencies, we apply a correlative spectromicroscopy approach. In detail, the topography and surface roughness of the K-feldspar crystals as well as the mineral thin section is determined by vertical scanning interferometry. In addition, Raman microscopy delivers information about the thin section's surface mineralogy. The quantitative amount of sorbed Cm(III) is obtained by calibrated autoradiography and partially μ TRLFS (micro-focus time-resolved laser-induced fluorescence spectroscopy), which is also the only method capable of measuring Cm(III) surface speciation on the molecular level via analysis of luminescence spectra and lifetimes.

Our results indicate that rougher K-feldspar surfaces exhibit increased Cm(III) uptake and stronger surface complexation. Similarly, the increase in pH leads to higher surface loading and stronger Cm(III) binding to the surface. Results obtained on the thin section reveal, that within a heterogeneous mineralogical system, sorption is affected by dissolution of neighboring minerals and competitive sorption between different mineral phases, such as mica and feldspar. The obtained findings express a need for investigating relevant processes on multiple scales of dimension and complexity to better understand radionuclide retention by potential repository host rocks.

The authors acknowledge funding provided by the German Federal Ministry of Education and Research (iCross project 02NUK053B), the Helmholtz Association (iCross project SO-093 and CROSSING project PIE-0007), as well as by the German Federal Ministry of Economics and Technology (SMILE project 02E11668B). We thank F. Bok R. Moeckel, S. Beutner and S. Schöne.

Chemistry and speciation of protactinium – a first principles study

H. Oher^{1,2} V. Vallet,³ R. Maurice^{1,2}

¹ Univ Rennes, CNRS, ISCR (Institut des Sciences Chimiques de Rennes) – UMR 6226, France

² SUBATECH, UMR CNRS 6457, IN2P3/IMT Atlantique/Université de Nantes, France

³ Université de Lille, CNRS, UMR 8523 –PhLAM– Physique des Lasers Atomes et Molécules, France

It is of fundamental interest to understand and predict the chemistry of rare radioelements. In this work, we focus on protactinium ($Z = 91$), an element that is sandwiched in between thorium and uranium in the periodic table. Protactinium may naturally occur in environment (protactinium-231 results from the decay of naturally occurring uranium-235) and also appear in thorium-based nuclear fuel cycles. From a chemical point of view, protactinium is a crossing point in the actinide series [1] and its chemistry is hard to predict [2,3]. We hypothesize that relativistic quantum chemistry should allow us to understand the enigmatic chemistry of protactinium and even predict it.

For our first study, we have chosen to focus on the coordination sphere of protactinium and on the computation of equilibrium constants for experimentally known systems [3–5]. The occurrence of 1:1, 1:2 and 1:3 complexes of protactinium(V) with sulfate and oxalate ligands is thus studied by means of quantum mechanical calculations, in particular based on density functional theory. The solvent effects, inherent to solution chemistry, are introduced by means

of a polarizable continuum model [6] and the explicit treatment of water molecules (micro solvation). The coordination sphere of protactinium has been obtained by geometry optimizations performed both in the gas phase and in solution. It involves an oxygen atom from the Pa=O mono-oxo bond and also oxygen atoms from the bidentate ligands, and in some cases from additional water molecules. The computation of equilibrium constants and comparison with experimental data is more subtle. First, only apparent constants were experimentally determined. Since the occurrence of a mono-oxo bond was confirmed by EXAFS [5] even in the case of the 1:3 complex with oxalate ligands (corresponding to the stronger complexation), we hypothesize that this bond is also present in all the studied complexes. Second, number of explicitly treated water molecules should not be randomly chosen, it should ideally (i) lead to saturation of the coordination sphere of protactinium and (ii) be sufficient to stabilize the anionic ligands. We find that adding CN+1 water molecules is enough to satisfy both conditions in all the six studied complexes. By doing so and computing ligand-exchange equilibrium constants, we reproduce well the experimental trends for the exchange of 2 and 3 ligands, while the exchange of only one ligand (1:1 complexes) is still hard to reproduce from computations.

We report recent progress concerning the basic chemistry of protactinium. We have shown that its coordination sphere may include up to 8 oxygen atoms (from the original mono-oxo bond and from ligand and solvent molecule complexation) and find an approximate way of determining trends in equilibrium constants, opening the way for future predictions.

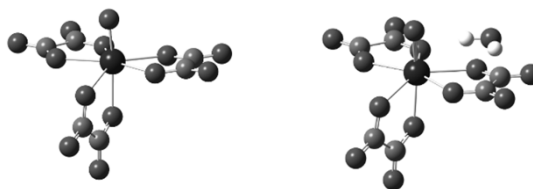


Fig. 1: Fully coordinated (left) and solvated (right) protactinium (V) oxalate complex obtained by R-ECP DFT/PBE0 calculations.

Tab. 1: First coordination sphere of selected protactinium complexes.

CN	1:1	1:2	1:3
SO ₄ ²⁻	8	8	7
C ₂ O ₄ ²⁻	8	8	7

[1] Wilson R. *et al.* (2018) Nat. Commun. 9, 622.

[2] Wilson R. (2012) Nat. Chem. 4, 586.

[3] Le Naour C. *et al.* (2019) Radiochim. Acta, 107, 979-991.

[4] Le Naour C. *et al.* (2005) Inorg. Chem. 44, 9542.

[5] Mendes M. *et al.* (2010) Inorg. Chem. 49, 9962-9971.

[6] Barone *et al.* (1997) J. Chem. Phys. 107, 3210-3221.

Combining U L_3 HERFD-XAS and FDMNES computations to study the uranium electronic structure in MUO_3 ($M = K, Na$ and Rb)

S. Orlat¹, R. Bes^{2,3}, F. Tuomisto², P. Martin¹, P. Moisy¹, G. Leinders⁴, K. Kvashnina^{5,6}

¹ CEA, DES, ISEC, DMRC, University of Montpellier, Marcoule, France

² Department of Physics, University of Helsinki, P.O. Box 64, FI-00014 Helsinki, Finland

³ Helsinki Institute of Physics, Department of Physics, University of Helsinki, P.O. Box 43, FI-00014 University of Helsinki, Finland

⁴ Belgian Nuclear Research Centre (SCK CEN), Institute for Nuclear Materials Science, Boeretang 200, B-2400 Mol, Belgium.

⁵ The Rossendorf Beamline at ESRF, The European Synchrotron, CS40220, 38043 Grenoble Cedex 9, France

⁶ Institute of Resource Ecology, Helmholtz Zentrum Dresden-Rossendorf (HZDR), PO Box 510119, 01314 Dresden, Germany

As a key chemical element of the nuclear industry, uranium has been the focus of substantial research. This element has a complex chemistry due to the large number of oxidation states allowed by its $[Rn]7s^26d^15f^3$ ground state electronic configuration. From a fundamental perspective, uranium has a complex electronic structure with 5f electrons showing a duality in localisation. Indeed, 5f electrons are often found in radially dispersed and hybridized bands, but they remain sometimes localized [1,2].

The study of this duality is difficult theoretically due to the same magnitude of the crystal field splitting, spin orbit coupling and electron-electron interaction. The latter can be overcome by studying pure pentavalent compounds meaning uranium $[Rn]5f^1$ configuration. One example of a pure pentavalent uranium compound is the potassium uranate KUO_3 which crystallizes in a cubic perovskite structure where U and K atoms are octahedrally ($U-O = 2.147 \text{ \AA}$ [3]) and cub-octahedrally coordinated by oxygen atoms, respectively. Considering the absence of distortion in both uranium and potassium coordination shells, KUO_3 can be considered as a perfect U(V) reference material. Other metal uranates such as $RbUO_3$ and $NaUO_3$, similarly are pure pentavalent uranium compounds and thus worth studying. $RbUO_3$ crystallizes in the same cubic perovskite structure ($U-O = 2.161 \text{ \AA}$ [3]) whereas $NaUO_3$ exhibits a distorted perovskite structure ($U-O$: two oxygen atoms at 2.142 \AA and four at 2.151 \AA [3]).

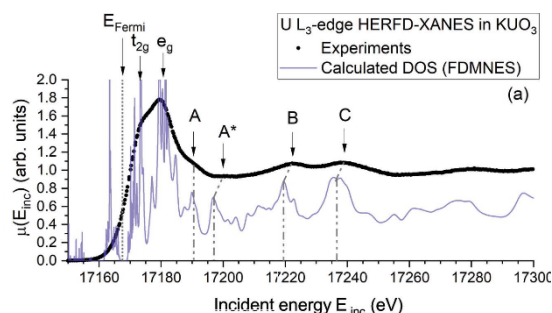


Fig. 1: Uranium L_3 -edge HERFD-XANES in KUO_3 and corresponding simulated spectrum using $FDMNES$ [4]

In this contribution, we will discuss the analysis of high energy resolution fluorescence detected data obtained at the U L_3 edge in $MU^{(V)}O_3$ compounds with $M = K, Na$ and Rb . The experimental spectra are compared to theoretical computations performed using the Finite Difference Method for Near-Edge Structure ($FDMNES$) code [4]. As illustrated by recent results obtained on KUO_3 [5] and on $NaUO_3$ [6], this combined experimental and theoretical approach allows to study the impact of the U-O interatomic distance and the structural distortion on the uranium valence electronic structure.

[1] Guziewicz et al., Phys. Rev. B 69 (2004) 045102.

[2] Y. A. Teterin et al., Russ. Chem. Rev. 73 (2004) 541.

[3] S. Van den Bergh et al, J. Solid State Chem. 177 (2004) 2231.

[4] Bunău et al., J. Phys. Condens. Matter. 21 (2009) 4260.

[5] Bes et al., J. Synch. Rad. 29 (2022) 21.

[6] S. M. Butorin et al., Chem. Eur. J. 22 (2016) 9693.

XAFS investigation of fission and activation products in irradiated light water reactor fuels

T. König, K. Dardenne, M. Herm, V. Metz, T. Pruessmann, J. Rothe, H. Geckeis

Karlsruhe Institute of Technology, Institute for Nuclear Waste Disposal (KIT-INE), P.O. Box 3640, D-76021 Karlsruhe, Germany

For several countries (e.g., Sweden, Finland or Germany) utilizing nuclear fission as energy source, the direct disposal of spent nuclear fuel (SNF) in a deep geological repository (DGR) for high active waste is the favored option for the back end of the nuclear fuel cycle. Regarding the long-term isolation of radiotoxic actinides or fission and activation products generated during in-reactor service of the fuel, various multi-barrier concepts are currently discussed. In general, the concepts envisage (i) a technical barrier, consisting of the irradiated fuel pellets inside their cladding tubes and a metallic container holding the fuel rod assemblies, (ii) a geotechnical barrier formed by construction materials of emplacement rooms and backfill materials retarding the ingress of solutions or - in case of the failure of the first barrier - retarding the release of radionuclides (RN) before reaching (iii) the geological barrier, i.e., the host rock surrounding the DGR and a possible overburden. As the initial barrier relevant for the potential release of RN from the DGR is the waste matrix (SNF and cladding) itself, precise information on SNF isotopic composition and RN speciation is of utmost importance in any safety analysis of the repository concept. While all actinide isotopes (^{238}U , unburned $^{235}\text{U}/^{239}\text{Pu}$ and all transuranic isotopes formed from ^{238}U by neutron capture and consecutive β -decay) tend to remain immobilized in a fluorite-type lattice as in pristine UOx (UO_2) or mixed oxide (MOX: $(\text{U,Pu})\text{O}_2$) fuel, certain highly mobile fission and activation product isotopes are of major concern for safety assessments due to their initial prompt release from the SNF matrices upon ground water contact (e.g., the cesium isotopes, ^{129}I as well as the activation product ^{36}Cl).

Reports on XAFS investigations of RN speciation in irradiated SNF samples are generally scarce, mainly focusing on the actinides [1,2], noble gases [3] or a few selected fission product elements, e.g. [4]. Research at the INE-Beamline and ACT stations of the KIT Light Source benefits from the unique proximity of hot cell lab facilities, where fragments of genuine nuclear waste forms (vitrified high active waste concentrates from reprocessing, SNF or cladding segments) can be conditioned, extracted and transported to the nearby beamlines for X-ray based speciation measurements (XAFS, HR-XANES, XRF, XRD). In this contribution we will focus on recent XANES measurements of the β -emitter ^{36}Cl , generated via neutron activation of impurities of the natural isotope ^{35}Cl in the cladding, the pristine fuel and adjacent construction materials, and the γ -emitting, long-lived fission product ^{129}I , both for the first time directly analyzed by XAFS as anionic species in SNF bulk fragments. Besides forming solid solutions with the original $\text{UO}_2/(\text{U,Pu})\text{O}_2$ lattice, some fission product cations with incommensurable ionic radii are expected to accumulate in separate oxide or perovskite-type phases in the SNF matrix, sometimes denoted as ‘grey phases’ (e.g., $(\text{Ba,Sr})(\text{U,Pu,Zr})\text{O}_3$). Those have been recently addressed by comprehensive Sr K-edge EXAFS measurements on a SNF bulk fragment and reference compounds.

[1] C. Degueldre et al., *J. Phys. Chem. Sol.* 75, 358–365 (2014).

[2] J. Rothe et al., *Geosciences* 9, 91 (2019).

[3] C. Degueldre et al., *Nuc. Instrum. Meth. in Phys. Res. B* 336, 116–122 (2014).

[4] E. Curti et al., *Environ. Sci.: Processes Impacts* 17, 1760–1768 (2015).

Biological reduction of selenate in the deep geological repository case (DGR): a spectroscopic and microscopic study

M.A. Ruiz-Fresneda,¹ M.V. Fernandez-Cantos,¹ J. Gómez-Bolívar,¹ P.L. Solari,² M.L. Merroun,¹

¹ Department of Microbiology, University of Granada, Granada, Spain,

² MARS Beamline, Synchrotron SOLEIL, L'Orme des Merisiers, Saint-Aubin, Gif-sur-Yvette 15 Cedex, France

Deep geological repository (DGR) multi-barrier systems are being studied as the best alternative for radioactive waste storage from an environmental point of view. Radioactive residues contain hazardous radioisotopes including actinides such as curium (Cm), americium (Am), or uranium (U), and other relevant elements such as selenium (Se). Se is a common component of the spent nuclear fuel present in these residues mainly as ⁷⁹Se isotope (half-life 3.7 x 10⁵ years) [1]. This element is widely distributed throughout the biosphere in different oxidation states: selenate (Se^{VI}) and selenite (Se^{IV}), which are soluble and toxic, and elemental Se (Se⁰) and selenide (Se^{-II}), which are insoluble and non-toxic forms. Microbial isolates from bentonite clay barriers, proposed for their use in DGRs, have been reported to efficiently reduce the solubility of Se hazardous forms. That is the case of the bacterium *Stenotrophomonas bentonitica*, which can biotransform Se^{IV} to Se⁰ forming amorphous Se (*a-Se*) nanospheres and crystalline (monoclinical (*m-Se*) and trigonal (*t-Se*)) Se nanostructures [2].

The present study describes the capacity of *S. bentonitica* cells in reducing Se^{VI} to Se⁰ nanorods through a combination of spectroscopic and microscopic techniques. Time-dependent synchrotron-based technique XAS (EXAFS/XANES) analysis (Figure 1) suggests a Se crystallization process, similar to that found for Se^{IV} as Se precursor, based on the biotransformation of *a-Se* into stable and less mobile *t-Se*, through *m-Se*. HAADF-STEM analysis showed the bacterium to produce intra and extracellular crystalline Se⁰ nanorods, made mainly of two different Se allotropes: *m-Se* and *t-Se*. However, no *a-Se* was detected with this technique. Other advances spectroscopic technologies such as X-ray diffraction (XRD) also confirmed the presence of crystalline *t-Se* of the bioreduction products. Differences in the structure and location of the Se reduction products when Se^{VI} is the initial source suggest a different biotransformation pathway than the one proposed for Se^{IV}. The zero-valent oxidation state, tubular shape, and crystallinity of the Se nanostructures produced suggest *S. bentonitica* as a potential bioremediation candidate in the context of DGR system and other contaminated environments, as well as novel and environmentally friendly Se nanorod fabrication method.

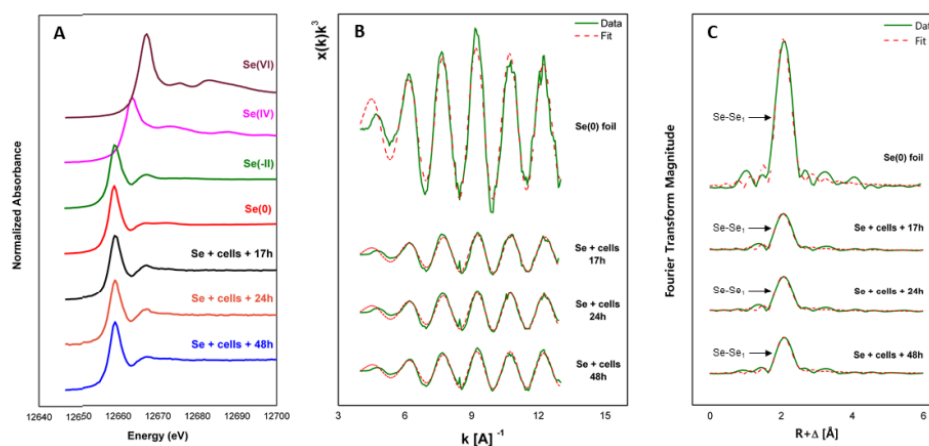


Figure 1. XANES (A), EXAFS (B), and their corresponding FT spectra (C) of Se reference compounds [Se(VI)-(Na₂SeO₄), Se(IV)-(Na₂SeO₃), Se(0)-(Se foil), and Se(-II)-(SeS₂)] and *S. bentonitica* samples incubated with 200 mM Se(VI) at different incubation times (17, 24, and 48 h).

[1] Ikonen, J. et al. (2016) Journal of Contaminant Hydrology. 192, 203-211.

[2] Ruiz-Fresneda, M.A. et al (2018). Environmental Science: Nano. 5(9), 2103-2116.

Covalency in UX_6^{n-} ($X = F, Cl, Br; n = 1, 2$) Complexes Probed Using Ligand- and Metal-Based XAS

Patrick W. Smith, Jacob A. Branson, Dominic R. Russo, Corwin H. Booth, Stefan G. Minasian

Chemical Sciences Division, Lawrence Berkeley National Laboratory, Berkeley, CA 94720, USA

Covalency in f-element systems has been the subject of significant investigation for many years. It is well-known that better energetic matching between atomic orbitals leads to enhanced orbital mixing in f-element systems; this so-called “energy-driven covalency” does not necessarily coincide with good *overlap* between these orbitals, which is necessary for significant covalent bond energy.[1] Previous work by researchers at Lawrence Berkeley and Los Alamos National Laboratories has used soft X-rays to probe ligand $1s$ to ψ^* transitions in a series of $AnCl_6^{2-}$ compounds, a technique known as “ligand K-edge XAS”. [2] This technique makes use of the relationship between the intensity of a pre-edge feature and the local atomic orbital character in the acceptor state, i.e. the extent to which ligand valence p-orbitals participate covalently in the bonding. Here, we have used both metal- and ligand-based XAS to probe covalency in a series of UX_6^{n-} complexes where the central uranium atom is kept constant while the nature of the ligand (F, Cl, Br) or oxidation state ($n = 1, 2$) is varied. This presentation will focus on the spectra obtained for bromide complexes, and compare results obtained not only of uranium, but also Ce and the group IV elements Ti, Zr, and Hf. Despite the larger core-hole lifetime at the Br K-edge (relative to Cl and F), fine structure is observed in the rising edge that is metal- and oxidation-state-dependent.

We have also leveraged U L_3 -edge XAS to characterize bonding in these systems. While core-hole broadening at this edge is large, the U L_3 -edge XANES of the U(V) complexes nonetheless display fine-structure reminiscent of the “double peaked” Ce L_3 -edge XANES of Ce(IV) complexes, where differences in intensity directly report upon f-covalency.[3] Moreover, we are developing methods to utilize the so-called “atomic XAFS” (AXAFS) to discern differences in charge distribution *around the uranium atom*. While these long-period oscillations are typically removed from the EXAFS with the post-edge background,[4] they nonetheless contain chemical information. In particular, they are sensitive to differences in the amount and distribution of valence electron density[5] and as such hold great potential for analysis of covalent bonding. To wit, AXAFS is known to be sensitive to distal substitution in Pt organometallic complexes.[6] By looking at a variety of halide ligands and multiple oxidation states of U, we have begun to develop an understanding of how AXAFS may report on bonding in actinide systems.

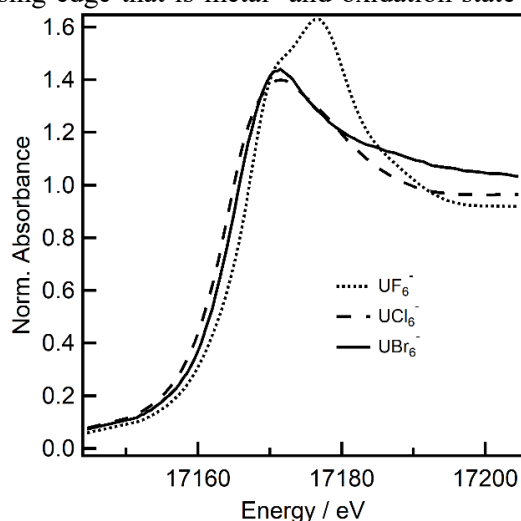


Figure: U L_3 XANES of the series UX_6^{n-} clearly showing a double-peak for $X = F$. The same structure is visible in second derivatives for $X = Br, Cl$. Measurements were made in transmission mode at SSRL BL 11-2.

- [1] Neidig, M. L.; Clark, D. L.; Martin, R. L. Covalency in F-Element Complexes. *Coord. Chem. Rev.* **2013**, *257*, 394–406.
- [2] Su, J.; *et al.* Energy-Degeneracy-Driven Covalency in Actinide Bonding. *J. Am. Chem. Soc.* **2018**, *140*, 17977–17984.
- [3] Sergentu, D. C.; Booth, C. H.; Autschbach, J. Probing Multiconfigurational States by Spectroscopy: The Cerium XAS L_3 -Edge Puzzle. *Chem. Eur. J.* **2021**, *27*, 7239–7251.
- [4] Bridges, F.; Booth, C. H.; Li, G. G. An Iterative Approach to “Atomic Background” Removal in XAFS Data Analysis. *Phys. B Phys. Condens. Matter* **1995**, *208–209* (C), 121–124.
- [5] Ramaker, D. E.; Mojet, B. L.; Koningsberger, D. C.; O’Grady, W. E. Understanding Atomic X-Ray Absorption Fine Structure in x-Ray Absorption Spectra. *J. Phys. Condens. Matter* **1998**, *10*, 8753–8770.
- [6] Tromp, M.; Slaght, M. Q.; Klein Gebbink, R. J. M.; Van Koten, G.; Ramaker, D. E.; Koningsberger, D. C. Atomic XAFS as a Probe of Electron Transfer within Organometallic Complexes: Data Analysis and Theoretical Calculations. *Phys. Chem. Chem. Phys.* **2004**, *6*, 4397–4406.

How to get to MARS?

P.L. Solari¹, M.O.J.Y. Hunault¹, D. Menut¹

¹ Synchrotron SOLEIL, L'Orme des Merisiers, Saint-Aubin, BP 48, 91192 Gif-sur-Yvette Cedex, France

MARS (Multi-Analyses on Radioactive Samples) beamline at the French synchrotron SOLEIL is devoted to advanced structural and chemical characterizations of radioactive matter (solid or liquid) using hard X-rays in the 3-35 keV range [1-5]. The beamline is opened to French as well as international users.

Since its opening in 2010, capabilities for synchrotron-based radionuclides and actinides sciences have been continuously expanded, driven by users' need.

Since 2019, the beamline is licensed to accept sample holders with radio-activities up to 18.5 GBq, including 2 GBq for gamma and neutron emitters, for experiments at ambient pressure and temperature (see table 1, boxes filled with gray light shading). Licensing to perform experiments at high pressures, high temperatures, low temperatures or with chemical reactions, for activities up to 200 times the French exemption limit has been granted in 2021 (see table 1). This complementary contribution will focus on the practical aspects to perform experiments on the beamline in particular for what concerns licensing as well as safety rules and procedures.

Tab. 1: Class of samples' maximum activities expressed by the European exemption limit Q ratio versus the Families of experimental conditions.

	F0: Ambient temperature & pressure	F1: High pressure (P < 100 GPa, T < 2000 K)	F2: Low temperature (T > 10 K)	F3: chemical reactions (T < 450 K)	F4: High temperature (T < 1800 K)
C0 (Q < 1)	OK	OK	OK	OK	OK
C1 (Q < 200)	OK	OK	OK	OK	OK
C2 (Q < 2x10 ⁴)	OK		foreseen	foreseen	foreseen
C3 (Q < 2x10 ⁶)	OK				foreseen

[1] B. Sitaud, et al., Journal of Nuclear Materials (2012) 425 (1-3), 238–243.

[2] I. Llorens, et al. Radiochimica Acta (2014) 102 (11), 957–972

[3] Dumas, T. et al. J Synchrotron Radiation (2022) 29, 30–36

[4] M.O.J.Y. Hunault, et al. Inorganic Chemistry (2019) 58, 6858–6865.

[5] Hunault, M. O. J. Y., et al. Crystals (2021) 11, 56

Uptake and reduction behavior of plutonium on Al-substituted hematite ($\alpha\text{-Fe}_2\text{O}_3$) and goethite ($\alpha\text{-FeOOH}$)

M. Vejar,¹ F. Zengotita,¹ A. Hixon¹

¹Department of Civil and Environmental Engineering and Earth Sciences, University of Notre Dame, USA

Plutonium (Pu) is a toxic radionuclide present in used nuclear fuel, reprocessing products, and at legacy contaminated sites [1]. To facilitate the continued use of commercial nuclear energy generation and address environmental contamination, it is essential to understand Pu fate and transport in subsurface environments, which is tied to the rich redox chemistry of Pu (i.e., generally, Pu(IV) is assumed to be immobile and Pu(V) is assumed to be mobile) [2, 3].

Iron oxide minerals (e.g., hematite ($\alpha\text{-Fe}_2\text{O}_3$) and goethite ($\alpha\text{-FeOOH}$)) are abundant in surface and subsurface environments and are common industrial corrosion products. Iron oxides are also an integral part of determining the ultimate performance of a generic geologic repository (e.g., granite, clay, salt) for used nuclear fuel and they influence contaminant fate and transport in the environment.

Metal substitution (i.e., the presence of impurities) in minerals occurs naturally due to geologic and anthropogenic processes. Iron oxides are some of the most sorption-reactive mineral phases and commonly contain up to 15% aluminum (Al) [4]. There is relatively little understanding of how naturally ubiquitous mineral complexity, such as metal substitution, impact contaminant sorption and redox processes. Thus, synthesizing metal-doped minerals is a controlled approach to increasing mineral complexity and measuring the concurrent change in physicochemical properties and their impact on Pu immobilization to better simulate and understand Pu behaviour in natural and engineered systems.

The ability to predict the mobility of plutonium in geologic and engineered environments requires geochemical understanding and modeling approaches that can describe the redox behavior of plutonium in the presence of complex mineral assemblages [5]. We hypothesize that estimates that fail to account for impurities in mineral assemblages result in inaccurate projections of Pu redox behavior and mobility in the environment.

To test this hypothesis, we combine the application of (i) macroscopic batch sorption experiments with synthetic Al-substituted minerals and (ii) synchrotron-based X-ray absorption spectroscopy (XAS) to develop a more comprehensive understanding of plutonium sorption and reduction as a function of mineral complexity. XAS reveals that Pu sorption to Al-substituted iron oxides leads to different coordination environments compared to sorption to minerals without metal substitution.

Determining the oxidation state distribution, bonding environment, and speciation of Pu associated with the solid phase will help us assess the impact(s) of Al substitution in iron oxide minerals on the uptake and surface-mediated reduction of Pu, and the resulting implications for fate and transport in natural and engineered environments.

[1] Romanchuk, A. Yu. et al. (2020) *Front. Chem.* 8. <https://doi.org/10.3389/fchem.2020.00630>.

[2] Kvashnina, K. O. et al. (2019) *Angew. Chem. Int. Ed.* 58 (49), 17558–17562. <https://doi.org/10.1002/anie.201911637>.

[3] Hixon, A. E. and Powell, B. A. (2018) *Environ. Sci.: Processes Impacts*, 20 (10), 1306–1322. <https://doi.org/10.1039/C7EM00369B>.

[4] Hu, P. et al. (2016) *Journal of Geophysical Research: Solid Earth*, 121 (6), 4180–4194. <https://doi.org/10.1002/2015JB012635>.

[5] Romanchuk, A. Yu. and Kalmykov, S. N. (2020) *Behavior of Radionuclides in the Environment I: Function of Particles in Aquatic System*; Springer: Singapore, pp 151–176. https://doi.org/10.1007/978-981-15-0679-6_6.

Bonding properties of uranium carbonate species in liquid and solid state in multiple oxidation states studies by U M₄-edge high resolution X-ray spectroscopy

C. Vollmer, H. Kaufmann, T. Neill, B. Schacherl, T. Prüssmann, H. Geckeis, T. Vitova

Karlsruhe Institute of Technology (KIT), Institute for Nuclear Waste Disposal (INE), P.O. Box3640, 76021 Karlsruhe, Germany

It is a long-standing discussion how the 5f electrons of the actinide (An) elements participate in chemical bonds. For investigating this and specifically the covalency of the An-ligand-bond [1, 2, 3], X-ray emission spectroscopy (XES) techniques, such as high-resolution x-ray absorption near edge structure (HR-XANES) [4] and valence band resonant inelastic x-ray scattering (VB-RIXS) [5], are advanced tools. In this study the changes in the electronic structure were investigated for uranium carbonate complexes with the oxidation states from IV to VI in solid and - for the first-time using the VB-RIXS technique – in liquid phase. A spectro-electrochemical cell for simultaneous measurement of XES and UV-Vis spectroscopy while applying a potential was successfully used to change in-situ the U oxidation state from VI to V while suppressing the disproportionation of U(V) [6].

U M₄ edge HR-XANES and VB-RIXS experiments were performed at the ACT station of the CAT-ACT beamline [7, 8]. The U coordination environment in solution was confirmed with U L₃-edge EXAFS at the INE-Beamline [9]; both beamlines are at the KIT Light Source, KIT, Germany [10].

A solution with 34 mM U in 1.5 M sodium carbonate at pH 12.5 was used to measure U M₄ edge HR-XANES and VB-RIXS for [U(VI)O₂(CO₃)₃]⁴⁻ species and after reduction to [U(V)O₂(CO₃)₃]⁵⁻ carbonate species. A solution sample of 31.7 mM [U(IV)(CO₃)₅]⁶⁻ at pH 8.3 as well as solid samples of Na₄[U(VI)O₂(CO₃)₃] and Ca[U(VI)O₂(CO₃)₃·10H₂O] were studied too.

A decrease in covalency of the O=U=O axial bond is detected using the HR-XANES spectra when reducing U(VI)-yl to U(V)-yl and U(V)-yl to U(IV). With a decreasing oxidation state of the uranium atom, the U 5f and 6p electron population of the occupied valence molecular orbitals also decreases as illustrated by the VB-RIXS spectra. This result suggests reduction of covalency for both axial and equatorial bonds. We will demonstrate that the U M₄ edge VB-RIXS technique is valuable for investigations of U 5f and 6p electron contributions in the occupied valence band of [U(VI)O₂(CO₃)₃]⁴⁻ in solution and Na₄[U(VI)O₂(CO₃)₃], Ca[U(VI)O₂(CO₃)₃·10H₂O] solids.

Acknowledgement

We thank the Institute for Beam Physics and Technology (IBPT) for the operation of the storage ring, the Karlsruhe Research Accelerator (KARA). This work is part of the ERC Consolidator grant project “THE ACTINIDE BOND” (grant agreement No. 101003292)

-
- [1] T. Vitova, et al., *Nat. Commun.* **2017**, **16053**.
 - [2] T. Vitova, et al., *Inorg.* **2020**, **8-22**.
 - [3] M. Zegke, et al., *Chem. Sci.* **2019**, **9740-9751**.
 - [4] F.d. Groot, *Chem. Rev.* **2001**, **1779-1808**.
 - [5] A. Kotani, S. Shin, *RMP* **2001**, **203-246**.
 - [6] I. Pidchenko, PhD Thesis *KIT Karlsruhe* **2016**, DOI: 10.5445/IR/1000054271.
 - [7] A. Zimina, et al., *Rev. Sci. Instrum.* **2017**, **113113**.
 - [8] B. Schacherl, et al., *J. Synchrotron Rad.* **2022**, **80-88**.
 - [9] J. Rothe, et al., *Rev. Sci. Instrum.* **2012**, **43105**.
 - [10] Y.-L. Mathis, et al., *J. Biol. Phys.* **2003**, **313-318**.

Investigating the complex interaction of technetium with magnetite nanoparticles

T. Zimmermann,¹ N. Mayordomo,¹ T. Stumpf,¹ A.C. Scheinost^{1,2}

¹ Institute of Resource Ecology, Helmholtz-Zentrum Dresden-Rossendorf, 01328 Dresden, Germany

² Rossendorf Beamline at ESRF (ROBL), 38000 Grenoble, France

Nanoparticles (NPs) are relevant in medicine, catalysis and environmental remediation. Among them, magnetite (Fe(II)Fe(III)₂O₄) NPs are especially interesting due to their redox and magnetic properties as well as their tunability of size and surface properties, which makes them suited for the removal of many redox-active pollutants. Tc is of great concern for the safety assessment of nuclear waste repositories, since ⁹⁹Tc is a fission product with a long half-life ($t_{1/2} = 2.1 \cdot 10^5$ years). Under oxidative conditions Tc forms an anionic species, pertechnetate (Tc(VII)O₄⁻), which is mobile due to its weak interactions with minerals. Under anaerobic conditions, pertechnetate is reduced by reducing agents to Tc(IV), which sorbs on minerals, forms insoluble oxides like TcO₂, or is structurally incorporated by stable natural minerals. [1]

Previous studies by Yalcintas et al. [2] suggested that Tc(VII) reduction by magnetite resulted in the precipitation and surface adsorption of TcO₂-like oligomers at pH 9, i.e. close to the pH of magnetite solubility minimum, while reduction at lower pH of 6-7 resulted in a partial incorporation of Tc(IV) in octahedral Fe sites of magnetite [3]. A working hypothesis was that the incorporation happens only at higher magnetite solubility, while the final retention mechanism remains enigmatic. Thus, our investigations are aimed to carry out a systematic approach covering a wide pH range (3-13), initial Tc concentration ([Tc] = μM-mM) and equilibration time ($t_{eq} = 1-210$ days).

The results show that magnetite removes at least 98 % dissolved Tc. To characterize the molecular geometry of the Tc vicinity, mainly X-ray absorption spectroscopy (XAS) has been used. XANES analysis reveals the predominance of Tc(IV) at all evaluated pH values, supporting that reductive Tc immobilization is the main retention mechanism. A detailed EXAFS analysis with different preparation methods (sorption, coprecipitation, Fe(II)-recrystallization) is currently underway to elucidate the molecular structure of the retained Tc species.

We thank the German Federal Ministry of Economic Affairs and Energy (BMWi) for funding the KRIMI project (02NUK056C).

[1] A.H. Meena, Y. Arai (2017) Environ. Chem. Lett., 15, 241.

[2] E. Yalcintas et al. (2016) Dalton Trans., 45, 17874.

[3] T. Kobayashi et al. (2013) Radiochimica Acta, 101, 323.